1051-H-11

Y3.N88:25/2294

COMPLETED
119

ornl

NUREG/CR-2294
ORNL/Sub-81/7755/1

OAK
RIDGE
NATIONAL
LABORATORY

UNION
CARBIDE

Development of a Standard Test for Measuring K_{Ia} With a Modified Compact Specimen

P. B. Crosley
E. J. Ripling

Work funded by
U.S. Nuclear Regulatory Commission
Office of Nuclear Regulatory Research
Under Interagency Agreements 40-551-75 and 40-552-75

OPERATED BY
UNION CARBIDE CORPORATION
FOR THE UNITED STATES
DEPARTMENT OF ENERGY

I

Printed in the United States of America. Available from
National Technical Information Service
U.S. Department of Commerce
5285 Port Royal Road, Springfield, Virginia 22161

Available from

GPO Sales Program
Division of Technical Information and Document Control
U.S. Nuclear Regulatory Commission
Washington, D.C. 20555

This report was prepared as an account of work sponsored by an agency of the United States Government. Neither the United States Government nor any agency thereof, nor any of their employees, makes any warranty, express or implied, or assumes any legal liability or responsibility for the accuracy, completeness, or usefulness of any information, apparatus, product, or process disclosed, or represents that its use would not infringe privately owned rights. Reference herein to any specific commercial product, process, or service by trade name, trademark, manufacturer, or otherwise, does not necessarily constitute or imply its endorsement, recommendation, or favoring by the United States Government or any agency thereof. The views and opinions of authors expressed herein do not necessarily state or reflect those of the United States Government or any agency thereof.

NUREG/CR- 2294
ORNL/Sub-81/7755/1
Dist. Category RF

DEVELOPMENT OF A STANDARD TEST FOR MEASURING K_{Ia} WITH A MODIFIED COMPACT SPECIMEN

P. B. Crosley and E. J. Ripling

Manuscript Completed February 1981

Date Published: August 1981

Work funded by
U.S. Nuclear Regulatory Commission
Office of Nuclear Regulatory Research
Under Interagency Agreements 40-551-75 and 40-552-75
NRC FIN No. B0119

Report prepared by
Materials Research Laboratory, Inc.
One Science Road
Glenwood, Illinois 60425

Under Subcontract No. 7755
MRL No. 535

Prepared for
OAK RIDGE NATIONAL LABORATORY
Oak Ridge, Tennessee 37830
operated by
UNION CARBIDE CORPORATION
for the
DEPARTMENT OF ENERGY

Contract No. W-7405-eng-26

Materials
Research
Laboratory,
Inc.

TABLE OF CONTENTS

	Page No.
List of Tables	iii
List of Illustrations	v
Foreword	ix
1. Introduction	1
References	2
2. Analysis of Co-op Program Data	3
2.1 Compliance Calibration of MRL and BCL Compact Crack Arrest Specimens	4
2.1.1 Introduction	4
2.1.2 MRL Specimen Compliance Calibration	5
2.1.3 BCL Specimen Compliance Calibration	7
2.2 Cooperative Crack Arrest Test Program Results	9
2.3 Analysis of Crack Arrest Program Test Results	10
2.3.1 Difference in Scatter Between K_{Ia} and K_{ID}	10
2.3.2 Origin of Scatter in K_{Ia}	13
2.3.2.1 Analysis of Variation Between Laboratories	13
2.3.2.2 Dependence of K_{Ia} on Specimen Location	15
2.3.2.3 Dependence of K_{Ia} on Crack Jump Distance	16
2.3.2.4 Origin of Scatter in K_{Ia}--Summary	17
References	18
3. Crack Arrest Toughness of Structural Steels	59
3.1 Test Program on A36 Steel	59

TABLE OF CONTENTS, Continued

	Page No.
3.1.1 Purpose of Tests	59
3.1.2 Material Characterization	60
3.1.2.1 Specification Values	60
3.1.2.2 DWT and CVN Tests	60
3.1.3 Test Procedure	61
3.1.4 Test Results	62
3.1.4.1 Tensile Tests	62
3.1.4.2 Toughness Tests	62
3.1.5 Specimen Size Requirements	64
3.1.5.1 Thickness Requirements	64
3.1.5.2 In-Plane Dimension Requirements	66
3.1.6 Conclusions Regarding the Use of A36 in the Round Robin Program	67
3.2 Test Program on A514 Steel	68
3.3 Use of Structural Steels in the Round Robin Program	68
References	69
4. Round Robin Program	87
4.1 Test Materials and Number of Tests	87
4.2 Participants	87
5. Conclusions and Recommendations	88

LIST OF TABLES

Table No.		Page No.
2-I	Experimental Calibration of MRL Compact Crack Arrest Specimen	18
2-II	Dimensionless Stress Intensity Factor as a Function of Dimensionless Crack Length	19
2-III	Experimental Compliance Calibration of BCL Crack Arrest Specimen	20
2-IV	Summary of Co-operative Test Program Data on AISI 1018 Steel	22
2-V	Summary of Co-operative Test Program Data, MRL Specimens of SA533, Grade B, Class 1 Steel Tested at Room Temperature	24
2-VI	Summary of Co-operative Test Program Data, BCL Specimens of SA533, Grade B, Class 1 Steel Tested at Room Temperature . .	26
2-VII	Summary of Co-operative Test Program Data, MRL Specimens of SA533, Grade B, Class 1 Steel Tested at 0°C	28
2-VIII	Summary of Co-operative Test Program Data, BCL Specimens of SA533, Grade B, Class 1 Steel Tested at 0°C	30
2-IX	Statistical Data on K_{Ia} and K_{ID} and their Dependence on K_Q	32
2-X	Comparison of Intra-Laboratory Standard Deviation with Expected Deviation Based on Total Program Scatter	33
3-I	Mechanical Properties and Chemical Analysis of A36 Steel	70
3-II	Through the Thickness Tensile Properties of 50.8 mm A36 Plate	71

LIST OF TABLES, Continued

Table No.		Page No.
3-III	Mechanical Properties of ASTM A514, Grade B and H	72
3-IV	Chemical Analysis of ASTM A514	73

LIST OF ILLUSTRATIONS

Fig. No.		Page No.
2-1	MRL Compact Crack Arrest Specimen	34
2-2	BCL Compact Crack Arrest Specimen	35
2-3	Newman's results for opening displacement, Δ, at 0.25W from load line for ASTM Standard E399 compact specimen and wedge-loaded (CLWL) specimen. MRL expression for K_{Ia} compact specimen shown for comparison .	36
2-4	Photograph of test set-up for calibrating MRL compact crack arrest specimen	37
2-5	Experimental compliance calibration of MRL compact crack arrest specimen	38
2-6	Curve fitted to experimental calibration for MRL compact crack arrest specimen compared with Newman's results	39
2-7	Dimensionless stress intensity factor as a function of dimensionless crack length for MRL compact crack arrest specimen . . .	40
2-8	Photograph of test set-up for measuring dependence of displacement at 0.25 W (Δ) on opening load for BCL CCA specimen	41
2-9	Photograph of test set-up for measuring the relationship of two displacements, Δ and y	42
2-10	Comparison of experimental compliance calibration of MRL and BCL compact crack arrest specimens and Newman results	43
2-11	Experimental compliance and Newman calculated values for BCL compact crack arrest specimen compared	44
2-12	Dimensionless stress intensity factor vs. dimensionless crack length for BCL compact crack arrest specimen	45

LIST OF ILLUSTRATIONS, Continued

Fig. No.		Page No.
2-13	Crack arrest toughness, K_{Ia}, plotted as a function of initiation toughness, K_Q. MRL specimens of AISI 1018 tested at room temperature	46
2-14	Dynamic fracture toughness, K_{ID}, plotted as a function of initiation toughness, K_Q. MRL specimens of AISI 1018 steel tested at room temperature	47
2-15	Crack arrest toughness, K_{Ia}, plotted as a function of initiation toughness, K_Q. MRL and BCL specimens of SA533, Grade B, Class 1 steel tested at room temperature	48
2-16	Dynamic fracture toughness, K_{ID}, plotted as a function of initiation toughness, K_Q. MRL and BCL specimens of SA533, Grade B Class 1 steel tested at room temperature . . .	49
2-17	Crack arrest toughness, K_{Ia}, plotted as a function of initiation toughness, K_Q. MRL and BCL specimens of SA533, Grade B, Class 1 steel tested at 0°C	50
2-18	Dynamic fracture toughness, K_{ID}, plotted as a function of initiation toughness, K_Q. MRL and BCL specimens of SA533, Grade B, Class 1 steel tested at 0°C	51
2-19	Comparison of the fractional rate of change in K_{Ia} and K_{ID} produced by a change in final crack position, x = a/W	52
2-20	Comparison of the variation in K_{Ia} and K_{ID} produced by same change in crack jump distance	53
2-21	Location of MRL specimens in parent plate	54
2-22	Location of specimens which gave high or low values of K_{Ia} outside of standard deviation	55

LIST OF ILLUSTRATIONS, Continued

Fig. No.		Page No.
2-23	Crack arrest toughness, K_{Ia}, plotted against arrest crack position, a/W, for MRL specimens of AISI 1018 steel tested at room temperature. Solid curves show expected dependence for values of K_Q one standard deviation above and below the average K_Q	56
2-24	Crack arrest toughness, K_{Ia}, plotted against arrested crack position, a/W, for MRL specimens of SA533, Grade B, Class 1 steel tested at room temperature. Solid curves show expected dependence for values of K_Q one standard deviation above and below the average K_Q	57
2-25	Crack arrest toughness, K_{Ia}, plotted against arrest crack position, a/W, for MRL specimens of SA533, Grade B, Class 1 steel tested at 0°C. Solid curves show expected dependence for values of K_Q one standard deviation above and below the average K_Q	58
3-1	CVN Impact and Lateral Expansion as a function of testing temperature for A36 steel [50.8 mm (2 in.) thick, L-T direction]. . . .	74
3-2	CVN Impact Energy and Lateral Expansion as a function of testing temperature for A36 steel [25.4 mm (1 in.) thick, L-T direction]. .	75
3-3	CVN Impact Energy and Lateral Expansion as a function of testing temperature for A36 steel [25.4 mm (1 in.) thick, T-L direction] .	76
3-4	Through-thickness variation of CVN toughness for 50.8 mm (2 in.) thick plate	77
3-5	Microstructure through 50.8 mm (2 in.) plate thickness. (a) Surface. (b) 6 mm (0.24 in.) from surface (scratch shows edge of side groove plane). (c) 23 mm (0.47 in.) from surface. (d) Center. (62X, nital etch).	78

LIST OF ILLUSTRATIONS, Continued

Fig. No.		Page No.
3-6	Test Specimen Dimensions: W = 169.3 mm (6.67 in.), H = 101.6 mm (4.00 in.), B = plate thickness, B_N = 0.75 B, W - a_o = 110.1 mm (4.33 in.), D = 25.4 mm (1.00 in.)	79
3-7	Tensile properties of A36 steel plates	80
3-8	Effect of test temperature on the crack arrest toughness of 50.8 mm (2 in.) thick A36 steel tested in the L-T direction	81
3-9	Fracture appearance of 50.8 (2 in.) thick specimen. A. Loading point. B. End of machined notch. C. End of crack jump, marked by heat tinting	82
3-10	Effect of test temperature on the crack arrest toughness of 25.4 mm (1 in.) thick A36 steel	83
3-11	Comparison of 25.4 mm (1 in.) and 50.8 mm (2 in.) plate toughness with toughness of 25.4 mm (1 in.) specimens cut from 50.8 mm (2 in.) plate, L-T direction	84
3-12	Ratio of uncracked ligament length to plastic zone size for plane stress and plane strain cracking	85

FOREWORD

The work reported here was performed by Materials Research Laboratory, Inc., under Subcontract No. 7775 to Oak Ridge National Laboratory (ORNL), under sponsorship of the U.S. Nuclear Regulatory Commission's (NRC) Heavy-Section Steel Technology (HSST) Program, which is directed by ORNL. The program is conducted as part of the ORNL Pressure Vessel Technology Program, of which G. D. Whitman is manager. The manager for the NRC is Milton Vagins.

This report is designated Heavy-Section Steel Technology Program Technical Report No. 59. Prior reports in this series are listed below.

1. S. Yukawa, Evaluation of Periodic Proof Testing and Warm Prestressing Procedures for Nuclear Reactor Vessels, HSSTP-TR-1, General Electric Company, Schenectady, NY (July 1, 1969).

2. L. W. Loechel, The Effect of Testing Variables on the Transition Temperature in Steel, MCR-69-189, Martin Marietta Corporation, Denver, CO (Nov. 20, 1969).

3. P. N. Randall, Gross Strain Measure of Fracture Toughness of Steels, HSSTP-TR-3, TRW Systems Group, Redondo Beach, CA (Nov. 1, 1969).

4. C. Visser, S. E. Gabrielse, and W. VanBuren, A Two-Dimensional Elastic-Plastic Analysis of Fracture Test Specimens, WCAP-7368, Westinghouse Electric Corporation, PWR Systems Division, Pittsburgh, PA (Oct. 1969).

5. T. R. Mager and F. O. Thomas, Evaluation by Linear Elastic Fracture Mechanics of Radiation Damage to Pressure Vessel Steels, WCAP-7328 (Rev.), Westinghouse Electric Corporation, PWR Systems Division, Pittsburgh, PA (Oct. 1969).

6. W. O. Shabbits, W. H. Pryle, and E. T. Wessel, Heavy-Section Fracture Toughness Properties of A533 Grade B Class 1 Steel Plate and Submerged Arc Weldment, WCAP-7414, Westinghouse Electric Corporation, PWR Systems Division, Pittsburgh, PA (Dec. 1969).

7. F. J. Loss, Dynamic Tear Test Investigations of the Fracture Toughness of Thick-Section Steel, NRL-7056, Naval Research Laboratory, Washington DC (May 14, 1970).

8. P. B. Crosley and E. J. Ripling, Crack Arrest Fracture Toughness of A533 Grade B Class 1 Pressure Vessel Steel, HSSTP-TR-8, Materials Research Laboratory, Inc., Glenwood, IL (March 1970).

9. T. R. Mager, Post-Irradiation Testing of 2T Compact Tension Specimens, WCAP-7561, Westinghouse Electric Corporation, PWR Systems Division, Pittsburgh, PA (Aug. 1970).

10. T. R. Mager, Fracture Toughness Characterization Study of A 533, Grade B, Class 1 Steel, WCAP-7578, Westinghouse Electric Corporation, PWR Systems Division, Pittsburgh, PA (Oct. 1970).

11. T. R. Mager, Notch Preparation in Compact Tension Specimens, WCAP-7579, Westinghouse Electric Corporation, PWR Systems Division, Pittsburgh, PA (Nov. 1970).

12. N. Levy and P. V. Marcal, Three-Dimensional Elastic-Plastic Stress and Strain Analysis for Fracture Mechanics, Phase I: Simple Flawed Specimens, HSSTP-TR-12, Brown University, Providence, RI (Dec. 1970).

13. W. O. Shabbits, Dynamic Fracture Toughness Properties of Heavy Section A533 Grade B Class 1 Steel Plate, WCAP-7623, Westinghouse Electric Corporation, PWR Systems Division, Pittsburgh, PA (Dec. 1970).

14. P. N. Randall, Gross Strain Crack Tolerance of A533-B Steel, HSSTP-TR-14, TRW Systems Group, Redondo Beach, CA (May 1, 1971).

15. H. T. Corten and R. H. Sailors, Relationship Between Material Fracture Toughness Using Fracture Mechanics and Transition Temperature Tests, T&AM Report 346, University of Illinois, Urbana, IL (Aug. 1, 1971).

16. T. R. Mager and V. J. McLoughlin, The Effect of an Environment of High Temperature Primary Grade Nuclear Reactor Water on the Fatigue Crack Growth Characteristics of A 533 Grade B Class 1 Plate and Weldment Material, WCAP-7776, Westinghouse Electric Corporation, PWR Systems Division, Pittsburgh, PA (Oct. 1971).

17. N. Levy and P. V. Marcal, Three-Dimensional Elastic-Plastic Stress and Strain Analysis for Fracture Mechanics, Phase II: Improved Modelling, HSSTP-TR-17, Brown University, Providence, RI (Nov. 1971).

18. S. C. Grigory, Tests of 6-in.-Thick Flawed Tensile Specimens, First Technical Summary Report, Longitudinal Specimens Numbers 1 through 7, HSSTP-TR-18, Southwest Research Institute, San Antonio, TX (June 1972).

19. P. N. Randall, Effects of Strain Gradients on the Gross Strain Crack Tolerance of A533-B Steel, HSSTP-TR-19, TRW Systems Group, Redondo Beach, CA (June 15, 1972).

20. S. C. Grigory, Tests of 6-Inch-Thick Flawed Tensile Specimens, Second Technical Summary Report, Transverse Specimens Numbers 8 through 10, Welded Specimens Numbers 11 through 13, HSSTP-TR-20, Southwest Research Institute, San Antonio, TX (June 1972).

21. L. A. James and J. A. Williams, Heavy Section Steel Technology Program Technical Report No. 21, The Effect of Temperature and Neutron Irradiation Upon the Fatigue-Crack Propagation Behavior of ASTM A533 Grade B, Class 1 Steel, HEDL-TME 72-132, Hanford Engineering Development Laboratory, Richland, WA (Sept. 1972).

22. S. C. Grigory, Tests of 6-Inch-Thick Flawed Tensile Specimens, Third Technical Summary Report, Longitudinal Specimens Numbers 14 through 16, Unflawed Specimen Number 17, HSSTP-TR-22, Southwest Research Institute, San Antonio, TX (Oct. 1972).

23. S. C. Grigory, Tests of 6-Inch-Thick Tensile Specimens, Fourth Technical Summary Report, Tests of 1-Inch-Thick Flawed Tensile Specimens for Size Effect Evaluation, HSSTP-TR-23, Southwest Research Institute, San Antonio, TX (June 1973).

24. S. P. Ying and S. C. Grigory, Tests of 6-Inch-Thick Tensile Specimens, Fifth Technical Summary Report, Acoustic Emission Monitoring of One-Inch and Six-Inch-Thick Tensile Specimens, HSSTP-TR-24, Southwest Research Institute, San Antonio, TX (Nov. 1972).

25. R. W. Derby, J. G. Merkle, G. C. Robinson, G. D. Whitman and F. J. Witt, Tests of 6-Inch-Thick Pressure Vessels. Series 1: Intermediate Test Vessels V-1 and V-2, ORNL-4895, Oak Ridge National Laboratory, Oak Ridge, TN (Feb. 1974).

26. W. J. Stelzman and R. G. Berggren, Radiation Strengthening and Embrittlement in Heavy Section Steel Plates and Welds, ORNL-4871, Oak Ridge National Laboratory, Oak Ridge, TN (June 1973).

27. P. B. Crosley and E. J. Ripling, Crack Arrest in an Increasing K-Field, HSSTP-TR-27, Materials Research Laboratory, Inc., Glenwood, IL (Jan. 1973).

28. P. V. Marcal, P. M. Stuart, and R. S. Bettes, Elastic Plastic Behavior of a Longitudinal and Semi-Elliptic Crack in a Thick Pressure Vessel, HSSTP-TR-28, Brown University, Providence, RI (June 1973).

29. W. J. Stelzman, Characterization of HSST Plate 02 (in preparation).

30. D. A. Canonico, Characterization of Heavy Section Weldments in Pressure Vessel Steels (in preparation).

31. J. A. Williams, The Irradiation and Temperature Dependence of Tensile and Fracture Properties of ASTM A533, Grade B, Class 1 Steel Plate and Weldment, HEDL-TME 73-75, Hanford Engineering Development Laboratory, Richland, WA (Aug. 1973).

32. J. M. Steichen and J. A. Williams, High Strain Rate Tensile Properties of Irradiated ASTM A533 Grade B Class 1 Pressure Vessel Steel, Hanford Engineering Development Laboratory, Richland, WA (July 1973).

33. P. C. Riccardella and J. L. Swedlow, A Combined Analytical-Experimental Fracture Study of the Two Leading Theories of Elastic-Plastic Fracture (J-Integral and Equivalent Energy), WCAP-8224, Westinghouse Electric Corporation, Pittsburgh, PA (Oct. 1973).

34. R. J. Podlasek and R. J. Eiber, Final Report on Investigation of Mode III Crack Extension in Reactor Piping, Battelle Columbus Laboratories, Columbus, OH (Dec. 14, 1973).

35. T. R. Mager, J. D. Landes, D. M. Moon and V. J. McLaughlin, Interim Report on the Effect of Low Frequencies on the Fatigue Crack Growth Characteristics of A533 Grade B Class 1 Plate in an Environment of High-Temperature Primary Grade Nuclear Reactor Water, WCAP-8256, Westinghouse Electric Corporation, Pittsburgh, PA (Dec. 1973).

36. J. A. Williams, The Irradiated Fracture Toughness of ASTM A533, Grade B, Class 1 Steel Measured with a Four Inch Thick Compact Tension Specimen, HEDL-TME 75-10, Hanford Engineering Development Laboratory, Richland, WA (Jan. 1975).

37. R. H. Bryan, J. G. Merkle, M. N. Raftenberg, G. C. Robinson and J. E. Smith, Test of 6-Inch-Thick Pressure Vessels. Series 2: Intermediate Test Vessels V-3, V-4, and V-6, ORNL-5059, Oak Ridge National Laboratory, Oak Ridge, TN (Nov. 1975).

38. T. R. Mager, S. E. Yanichko, and L. R. Singer, Fracture Toughness Characterization of HSST Intermediate Pressure Vessel Material, WCAP-8456, Westinghouse Electric Corporation, Pittsburgh, PA (Dec. 1974).

39. J. G. Merkle, G. D. Whitman, and R. H. Bryan, An Evaluation of the HSST Program Intermediate Pressure Vessel Tests in Terms of Light-Water-Reactor Pressure Vessel Safety, ORNL-TM-5090, Oak Ridge National Laboratory, Oak Ridge, TN (Nov. 1975).

40. J. G. Merkle, G. C. Robinson, P. P. Holz, J. E. Smith and R. H. Bryan, Test of 6-In.-Thick Pressure Vessels. Series 3: Intermediate Test Vessel V-7, ORNL/NUREG-1, Oak Ridge National Laboratory, Oak Ridge, TN (Aug. 1976).

41. J. A. Davidson, L. J. Ceschini, R. P. Shogan, and G. V. Rao, The Irradiated Dynamic Fracture Toughness of ASTM A533, Grade B, Class 1 Steel Plate and Submerged Arc Weldment, WCAP-8775, Westinghouse Electric Corporation, Pittsburgh, PA (Oct. 1976).

42. R. D. Cheverton, Pressure Vessel Fracture Studies Pertaining to a PWR LOCA-ECC Thermal Shock: Experiments TSE-1 and TSE-2, ORNL/NUREG/TM-31, Oak Ridge National Laboratory, Oak Ridge, TN (Sept. 1976).

43. J. G. Merkle, G. C. Robinson, P. P. Holz and J. E. Smith, Test of 6-in.-Thick Pressure Vessels. Series 4: Intermediate Test Vessels V-5 and V-9 with Inside Nozzle Corner Cracks, ORNL/NUREG-7, Oak Ridge National Laboratory, Oak Ridge, TN (Aug. 1977).

44. J. A. Williams, The Ductile Fracture Toughness of Heavy Section Steel Plate, Hanford Engineering Development Laboratory, Richland, WA, NUREG/CR-0859 (Sept. 1979).

45. R. H. Bryan, T. M. Cate, P. P. Holz, T. A. King, J. G. Merkle, G. C. Robinson, G. C. Smith, J. E. Smith and G. D. Whitman, Test of 6-in.-Thick Pressure Vessels. Series 3: Intermediate Test Vessel V-7A Under Sustained Loading, ORNL/NUREG-9, Oak Ridge National Laboratory, Oak Ridge, TN (Feb. 1978).

46. R. D. Cheverton and S. E. Bolt, Pressure Vessel Fracture Studies Pertaining to a PWR LOCA-ECC Thermal Shock: Experiments TSE-3 and TSE-4 and Update of TSE-1 and TSE-2 Analysis, ORNL/NUREG-22, Oak Ridge National Laboratory, Oak Ridge, TN (Dec. 1977).

47. D. A. Canonico, Significance of Reheat Cracks to the Integrity of Pressure Vessels for Light-Water Reactors, ORNL/NUREG-15, Oak Ridge National Laboratory, Oak Ridge, TN (July 1977).

48. G. C. Smith and P. P. Holz, Repair Weld Induced Residual Stresses in Thick-Walled Steel Pressure Vessels, NUREG/CR-0093 (ORNL/NUREG/TM-153), Oak Ridge National Laboratory, Oak Ridge, TN (June 1978).

49. P. P. Holz and S. W. Wismer, Half-Bead (Temper) Repair Welding for HSST Vessels, NUREG/CR-0113 (ORNL/NUREG/TM-177), Oak Ridge National Laboratory, Oak Ridge, TN (June 1978).

50. G. C. Smith, P. P. Holz and W. J. Stelzman, Crack Extension and Arrest Tests of Axially Flawed Steel Model Pressure Vessels, NUREG/CR-0126 (ORNL/NUREG/TM-196), Oak Ridge National Laboratory, Oak Ridge, TN (Oct. 1978).

51. R. H. Bryan, P. P. Holz, J. G. Merkle, G. C. Smith, J. E. Smith and W. J. Stelzman, Test of 6-in.-Thick Pressure Vessels. Series 3: Intermediate Test Vessel V-7B, NUREG/CR-0309 (ORNL/NUREG-38), Oak Ridge National Laboratory, Oak Ridge, TN (Oct. 1978).

52. R. D. Cheverton, S. K. Iskander and S. E. Bolt, Applicability of LEFM to the Analysis of PWR Vessels Under LOCA-ECC Thermal Shock Conditions, NUREG/CR-0107 (ORNL/NUREG-40), Oak Ridge National Laboratory, Oak Ridge, TN (Oct. 1978).

53. R. H. Bryan, D. A. Canonico, P. P. Holz, S. K. Iskander, J. G. Merkle, J. E. Smith and W. J. Stelzman, Test of 6-in.-Thick Pressure Vessels, Series 3: Intermediate Test Vessel V-8, NUREG/CR-0675 (ORNL/NUREG-58), Oak Ridge National Laboratory, Oak Ridge, TN (December 1979).

54. R. D. Cheverton and S. K. Iskander, Application of Static and Dynamic Crack Arrest Theory to TSE-4, NUREG/CR-0767 (ORNL/NUREG-57), Oak Ridge National Laboratory, Oak Ridge, TN (June 1979).

55. J. A. Williams, Tensile Properties of Irradiated and Unirradiated Welds of A533 Steel Plate and A508 Forgings, NUREG/CR-1158 (ORNL/Sub-79/50917/2), Hanford Engineering Development Laboratory, Richland, WA (July 1979).

56. K. W. Carlson and J. A. Williams, The Effect of Crack Length and Side Groove on the Ductile Fracture Toughness Properties of ASTM A533 Steel, NUREG/CR-1171 (ORNL/Sub-79/50917/3), Hanford Engineering Development Laboratory, Richland, WA (Oct. 1979).

57. P. P. Holz, Flaw Preparations for HSST Program Vessel Fracture Mechanics Testing; Mechanical-Cyclic Pumping and Electron-Beam Weld-Hydrogen Charge Cracking Schemes, NUREG/CR-1274 (ORNL/NUREG/TM-369), Oak Ridge National Laboratory, Oak Ridge, TN (May 1980).

58. S. K. Iskander, Two Finite Element Techniques for Computing Mode I Stress Intensity Factors in Two- or Three-Dimensional Problems, NUREG/CR-1499 (ORNL/NUREG/CSD/TM-14), Computer Sciences Div., Union Carbide Corporation, Nuclear Division (Feb. 1981).

1. Introduction

Two methods have been advanced for defining the plane strain crack arrest fracture toughness of metals. One, proposed by the Battelle Columbus Laboratories, defines toughness in terms of a quantity, K_{ID}, which is derived from a dynamic analysis that BCL purports to describe the complete event of a run-arrest segment of crack extension[1-1]. The other, proposed by the Materials Research Laboratory, defines a value, K_{Ia}, which is based on a static analysis of the crack tip stresses at the end of the event[1-2]. So long as this controversy persisted, it was not possible to write a test method for measuring the property, in spite of the fact that the ASME Boiler and Pressure Vessel Code, Sections III and XI, require the use of crack arrest toughness data. Recently, two large test programs were undertaken to help resolve the controversy, and both generated data that support the K_{Ia} approach. In the first case, a Cooperative Test Program on Crack Arrest was conducted under the sponsorship of ASTM. Contrary to the prediction made by the BCL dynamic analysis, K_{Ia} did not show a systematic dependence on K_Q, the value of K needed to initiate cracking; instead, it emerged as a reproducible material property. On the other hand, K_{ID} did depend systematically on K_Q.

In the second test program, cracks were placed on the inside of thick walled steel cylinders, which were subjected to a severe thermal shock. Calculations were made of the amount the crack would extend due to the thermal shock, using both K_{Ia} and K_{ID} as the material property. The calculated and experimental values of crack jump length were in agreement when K_{Ia} was used, but were not in agreement when K_{ID} was used[1-3, 1-4].

On the basis of these results, a consensus was reached that work should now be started to develop a standard ASTM test method, based on the MRL procedure. This report describes the work done to initiate the program.

REFERENCES

1-1 P. C. Gehlen, R. G. Hoagland, and C. H. Popelar, "A Method of Extracting Dynamic Fracture Toughness from CT Tests," Int. Jour. of Fracture, Vol. 15, No. 1, February 1979, pp. 69-84.

1-2 P. B. Crosley and E. J. Ripling, "A Compact Specimen for Plane Strain Crack Arrest Toughness Testing, Jour. Testing and Evaluation, Vol. 8, No. 1, ASTM, 1980.

1-3 R. D. Cheverton and S. E. Bolt, "Pressure Vessel Fracture Studies Pertaining to a PWR LOCA-ECC Thermal Shock: Experiments TSE3 and TSE4 and Update of TSE1 and TSE2 Analysis," ORNL/NUREG-22, December 1977.

1-4 R. D. Cheverton, "Quick Look Report for HSST Thermal Shock Experiment TSE5," TSP-1006 August 14, 1979.
R. D. Cheverton, "HSST Thermal Shock Program Quick Look Report for TSE-5A," TSP-1007, October 9, 1980.

For an ASTM standard test method to have wide acceptance in the technical community, it must define the types of materials to which it is applicable, as well as defining the acceptable limits on a host of different test parameters. Further, for ASTM to evaluate the method, a Round Robin Test Program must be conducted as well. Work done over this contract period was concerned with each of these phases of writing a test method: tests were conducted to determine whether or not the test method could be extended to include the structural steels as well as the pressure vessel steels. The available K_{Ia} data were examined to see what testing parameter limits can be gleaned from the published literature, and steps were taken to initiate the Round Robin program.

2. Analysis of Co-op Program Data

The co-op program, already undertaken, involved thirty laboratories, each of which was supposed to test ten specimens, six of MRL design and four of BCL design. Almost all of the projected tests were, in fact, run, and the result was a large body of test data, which could serve as input in developing the standard test method. A major effort on this project, therefore, was analysis of the co-op program test data.

Neither of the two specimens used in the co-op program were experimentally compliance calibrated, and because of this, there was some questioning of the data. Consequently, experimental calibrations of both the MRL and the BCL specimens were carried out on this project. The former was necessary, in any case, in order to have an accurate calibration for the standard test method.

Using the more reliable experimentally based calibrations for the two specimen types, all of the K_{Ia} and K_{ID} were recomputed, and a summary of all the data obtained on the co-op test program is included in this report.

The co-op data were also analyzed to see if the scatter in K_{Ia}, which exceeded ± ten percent, could be traced to identifiable sources.

Questions of the laboratory-to-laboratory variation in K_{Ia}, of its dependence on the location of specimens in the test plate, and whether or not crack jump distance influenced the value of K_{Ia} were investigated. The aim was to use the findings in modifying or clarifying the developing standard test procedure.

2.1 Compliance Calibration of MRL and BCL Compact Crack Arrest Specimens

2.1.1 Introduction

Both MRL and BCL supplied specimens, each of their own design, to the Co-operative Test Program participants. The MRL specimen had the dimensions shown in Fig. 2-1 with the exception that the slot had the same width, N, from the loading hole to the edge of the specimen, as it had from the hole to the crack initiation notch. The BCL specimen had the dimensions shown in Fig. 2-2.

The expressions supplied for calculating K for these specimens were based on analytical compliance calibrations developed by MRL and BCL, each for their own test method (2-1). Neither of the expressions was verified experimentally, and a need for doing this became apparent in the course of the Co-operative Program. The MRL test method used displacement measurements made at 0.25W from the loading hole, and assumed that there was no effect of loading hole pattern. Newman (2-2) had shown by means of a boundary collocation method that, for short crack lengths, displacements at 0.25W, Δ, were significantly affected by the loading hole pattern. The compliances for specimens using pin-hole loading, and crack-line, wedge-loading, according to Newman, are compared with the MRL expression supplied to the Co-operative Program participants in Fig. 2-3.

The BCL test method measured displacement, y, on the split pins. The influence of hole pattern for displacements measured at the load line are small. Nevertheless, some measurements made by BCL directly on the specimen load-line, rather than on the split pin, suggested

that the measurements made on the latter were not identical with load-point displacements.

Because of these uncertainties in the K expressions supplied to the Co-op Program participants, both the MRL and BCL specimens were experimentally compliance calibrated. This was done by relating the opening load to the displacement at the location where the participants were asked to measure it.

2.1.2 MRL Specimen Compliance Calibration

The experimental compliance calibrations were made with specimens like the one shown in Fig. 2-1. This configuration is identical to the K_{Ia} specimens which were tested in the Co-operative Crack Arrest Program. The only difference was that a portion of the machined slot was wider (N_i versus N in Fig. 2-1) to permit installation of the loading device. The calibration specimens did not, of course, have a machine notched, brittle, weld crack starter; but the notch depth and configuration duplicated the final machined condition of the actual specimens. One calibration specimen was made from 7075 aluminum alloy for which Young's modulus was taken to be 69×10^3 MPa, and a second was made from SA533 Grade B Class 1 steel for which Young's modulus was taken to be 200×10^3 MPa.

In order to apply a load to the calibration specimens in such a manner that the load could be measured, two yokes were used. The yokes had cylindrical bearing surfaces which contacted the specimen loading hole just as the wedge-bushing loading device does in a K_{Ia} test. The assembly was installed in a test machine where load was measured with an in-line load cell. A photograph of the test set-up is shown in Fig. 2-4.

The opening displacement at 0.25W from the load line was measured exactly as it is measured in a K_{Ia} test. An aluminum target block and an aluminum transducer holder block were bolted to the front edge of the specimen so as to locate the center-line of the transducer at the

desired measurement location. Prior to testing and at times during the testing, the transducer was calibrated in a micrometer stand over the same range of openings that would be sampled in the test. Plots of load versus opening displacement were made on an X-Y recorder.

Compliance calibration involved obtaining load versus opening displacement traces on the specimen in the original condition and with saw cuts of different depths corresponding to different crack lengths. The sawing was done on a band saw which produced an 0.8 mm kerf. It was assumed that this amount of material removal would not give results significantly different from a real crack where no material is lost. The sawing was done in intervals of approximately 6 mm; the actual "crack" length at each stage was obtained by measure (W - a) with a traveling microscope. Measurements on the two sides of the specimen generally agreed with 0.4 mm, the average of the two measurements was used to obtain the crack length, a.

The experimental results are given in Table 2-1. The results are plotted in Fig. 2-5 in terms of the quantity $EB\Delta\ (1 - x)^2/P$. Also shown is a least squares parabolic fit to the data which corresponds to

$$EB\Delta/P = (9.85 - 0.17x + 11.0x^2)/(1 - x)^2 \qquad (2\text{-}1)$$

Comparison of this with the Newman results is as follows:

a/W	EBΔ/P (Newman, CLWL)	EBΔ/P (Eq. 2-1)
0.30	19.90	(22.0)
0.35	25.12	26.36
0.40	31.58	32.06
0.45	39.73	39.67
0.50	50.33	50.06
0.55	64.59	64.61
0.60	84.63	85.68
0.65	114.3	117.4
0.70	161.0	168.0
0.75	140.8	154.6
0.80	392.4	418.9

The curve fitted to the experimental data is compared with Newman's analytical results in Fig. 2-6. The difference is not large. The experimental results were obtained on the actual compact K_{Ia} specimen configuration which has side grooves and a fairly wide starter notch and these features were not incorporated in the Newman analysis.

Newman has also presented a relation between K and P for a crack-line loaded compact specimen using a boundary collocation analysis (2-2). His data points were fit to the following polynomial by Rosenfield (2-4).

$$KB\sqrt{W}/P = \frac{2.2434}{(1-x)^{3/2}}\left[1.7164 - 0.9x + x^2\right] \qquad (2\text{-}2)$$

Combining eqs. (2-1) and (2-2) gives the dependence of the dimensionless stress intensity factor on dimensionless crack length:

$$\frac{K\sqrt{W}}{E\Delta}\left(\frac{B_N}{B}\right)^{\frac{1}{2}} = \frac{2.2434\,(1.7164 - 0.9x + x^2)\,\sqrt{1-x}}{(9.85 - 0.17x + 11.0\,x^2)} \qquad (2\text{-}3)$$

A tabulation of this function is given in Table 2-II, and it is plotted in Fig. 2-7.

This expression is the best available representation of the behavior of the MRL compact crack arrest specimen, and will be used for all future calculations of K_Q and K_{Ia} for this specimen.

2.1.3 BCL Specimen Compliance Calibration

The dimensions of the BCL specimen used for experimental compliance calibration, like the MRL specimen, had dimensions identical with the specimens used on the Co-operative Test Program, Fig. 2-2. The specimen differed from the ones tested in that it was monolithic, rather than being made of two pieces welded together. Only one specimen was calibrated, and it was made of SA533 Grade B Class 1 steel for which it was assumed that $E = 200 \times 10^3$ MPa.

Calibrating the BCL specimen was more difficult than calibrating the MRL ones. To duplicate the displacement, y, measured by the

co-op program participants, the measurement had to be made on the two split pin halves which are driven apart by the wedge. This prevents simultaneous measurements of y and opening load, P, so that the calibration had to be carried out in two steps. The dependence of the displacement at 0.25W, Δ, on P was measured first, using a test set-up that was essentially identical with that used for the MRL specimen calibration, Fig. 2-8. The second step then related the two displacements y and Δ, by using two gages, one at 0.25W, and a second across the two halves of the split pin, as shown in Fig. 2-9. The dependence of split-pin motion on load was obtained by combining these two sets of readings.

As was the case with the MRL specimens, the first pair of measurements were made for the initial crack length, which in this case was a = 0.32W, after which the specimen was sawed to simulate crack extension, again leaving an 0.8 mm kerf. The saw cut intervals were about 12 mm long, and crack lengths were measured in the same fashion as described above for the MRL specimens. The first set of measurements were identical with those made on the MRL specimens so that the compliance values obtained on the larger BCL specimen could be compared with those obtained on the MRL specimen, and by the Newman analysis. As shown in Fig. 2-10, the differences between the two specimens and the Newman analysis are small.

Unlike the first set of curves, the second set, Δ vs. y, always had some curvature, and there was as much as five percent uncertainty in defining their slope. For all crack positions, at least four compliance lines were drawn (with both specimen types) so that some of the uncertainty in the Δ vs. y curves might have been averaged out. The experimentally measured compliance and Newman's calculated values are compared in Fig. 2-11. A polynomial describing this experimental curve was combined with eq. (2-2) to arrive at the expression of K vs. a for the BCL Compact Crack Arrest Specimen:

$$\frac{K\sqrt{W}}{Ey}\left(\frac{B_N}{B}\right)^{\frac{1}{2}} = 0.9133 - 2.936x + 4.23x^2 - 2.25x^3 \qquad (2\text{-}4)$$

This expression is compared with the one supplied to the Co-operative Program participants in Fig. 2-12. The largest difference between the two expressions is about 10 percent.

2.2 Cooperative Crack Arrest Test Program Results

Tables 2-IV to 2-VIII summarize the Cooperative Test Program Results. The tabulated values of K_Q and K_{Ia} were calculated from expressions based on the experimental compliance calibration described in the previous section of this report. For the MRL specimen K_Q and K_{Ia} were calculated from eq. 2-3; for the BCL specimen eq. 2-4 was used. The K_{ID} values were calculated from the K_Q values using expressions provided by Battelle.* These were, for the MRL specimen,

$$\frac{K_{ID}}{K_Q} = 1.64 - \left(1.23\,\frac{\Delta a}{W} + 0.41\right)^{\frac{1}{2}} \qquad (2\text{-}5)$$

and for the BCL (duplex) specimen

$$\frac{K_{ID}}{K_Q} = 1.018 - \left(0.471\,\frac{\Delta a}{W} - 0.0848\right)^{\frac{1}{2}} \qquad (2\text{-}6)$$

where Δa is the crack jump distance; that is, the difference between the crack length at arrest and the length of the machined notch. These same data are plotted in Figs. 2-13 to 2-18. Here, K_{Ia} and K_{ID}, the two crack arrest parameters, are plotted against K_Q, the formally calculated value of K corresponding to the onset of crack extension. For reasons that have been discussed elsewhere (2-5), K_Q rather than crack jump distance or final crack position is an appropriate independent variable to use in a comparative assessment of the two crack arrest toughness parameters.

Tests on the AISI 1018 steel were conducted only with the MRL type specimen. Each individual test, of course, could be used to obtain values of both K_{Ia} and K_{ID}, which are plotted in Figs. 2-13 and 2-14,

* The expressions are numerical representations of information supplied in graphical form to Co-operative Test Program participants for use in calculating K_{ID}.

respectively. Fifty-five tests defined K_{Ia} = 86.7 ± 12.5 MPa·m$^{\frac{1}{2}}$, and there was no systematic dependence of K_{Ia} on K_Q. The same tests defined K_{ID} = 108.3 ± 11.8 MPa·m$^{\frac{1}{2}}$. The variation in K_{ID}, thus, was somewhat less than the variation in K_{Ia}. For the K_{ID}, however, there is also a marked dependence on K_Q; the standard deviation of K_{ID} about a least squares straight line fit to K_{ID} versus K_Q was only 6.5 MPa·m$^{\frac{1}{2}}$, compared to a standard deviation of 11.8 MPa·m$^{\frac{1}{2}}$ about the mean K_{ID}.

Similar results were obtained on tests run on SA 533 Grade B Class 1 steel at room temperature and at 0°C. In these tests both MRL specimens and BCL specimens were run, and, except in tests where there were instrumentation problems, individual tests of both types of specimen yielded both K_{Ia} and K_{ID} results. In Figs. 2-15 and 2-16 results of room temperature tests from both specimen types are plotted together, K_{Ia} in Fig. 2-15 and K_{ID} in Fig. 2-16. The same presentation is used in Figs. 2-17 and 2-18, which show the results of the 0°C tests. The appearance of the graphs and the statistical summary given in Table 2-IX support the following: The tests defined K_{Ia} with a standard deviation somewhat greater than 10 percent. There was no systematic variation of K_{Ia} with K_Q, and the two specimen types give essentially the same values. The overall percentage variation in K_{ID} was not greatly different from that in K_{Ia}, but there was a systematic dependence of K_{ID} on K_Q. There was also some difference in K_{ID} values between the two specimen types. This difference may be primarily associated with the fact that the two specimens generally sampled different ranges of K_Q.

2.3 Analysis of Crack Arrest Program Test Results

2.3.1 Difference in Scatter Between K_{Ia} and K_{ID}

Variations in the measured values of K_{Ia} and K_{ID} presented in the previous section may be associated with two phenomena: (1) a systematic dependence of K_{Ia} or K_{ID} on K_Q, and (2) a variation of K_{Ia} or K_{ID} arising from toughness differences between specimens and from measurement uncertainties. The first type of variation was found to

affect only the K_{ID} measurements, and not K_{Ia}. The second, of course, is a factor in both K_{Ia} and K_{ID} measurements. As the overall scatter in K_{ID} was about the same as that in K_{Ia}, while the latter showed no systematic dependence on K_Q, there must be a larger scatter in K_{Ia} than in K_{ID} at a given value of K_Q. This was, of course, the case, as can be seen by inspecting Figs. 2-13 to 2-18, or by comparing the deviation about linear regression fits to K_{Ia} and K_{ID} as a function of K_Q. The purpose here is to investigate the origin of this larger scatter in K_{Ia}.

Sources of variation in K_{Ia} or K_{ID} include:

1. errors in evaluating K_Q (i.e., measuring initial displacement and slot length),
2. errors in evaluating K_{Ia} or K_{ID} (i.e., in measuring arrested crack length and, in the case of K_{Ia}, the arrest displacement),
3. specimen-to-specimen variation of crack arrest behavior--in two specimens in which crack initiation occurs at the same K_Q, the crack, in fact, runs different distances before it arrests.

A given specimen can be used to calculate both K_{Ia} and K_{ID}, and hence both parameters should be equally affected by the first two sources of variation. Comparison of scatter in K_{Ia} and K_{ID}, then, boils down to a consideration of the sensitivity of K_{Ia} and K_{ID} to variations in crack jump distance at a given K_Q. This is strictly a matter of analyzing the calculational procedures by which K_{Ia} and K_{ID}, respectively, are obtained from the same basic laboratory measurements. Such an analysis is carried out here.

The K expression for the MRL specimen can be written

$$\frac{K\sqrt{W}}{E\Delta}\left(\frac{B_N}{B}\right)^{\frac{1}{2}} = h\,(x)$$

where x = a/W and where the function h(x) and the other symbols are as given in eq. 2-3. The above equation is used in calculating both K_Q and K_{Ia} by using the appropriate values of displacement (Δ_o and Δ_f) and of crack length (a_o and a_f). The ratio K_{Ia}/K_Q is

$$\frac{K_{Ia}}{K_Q} = \frac{\Delta_f}{\Delta_o} \frac{h\,(a_f/W)}{h\,(a_o/W)} \qquad (2\text{-}7)$$

A parameter S_{Ia} which reflects the sensitivity of K_{Ia} to variations in a_f for fixed K_Q can be defined as follows:

$$S_{Ia} = -\frac{W}{K_Q} \frac{dK_{Ia}}{da} \qquad (2\text{-}8)$$

In practice the ratio Δ_f/Δ_o does not greatly exceed unity; and for the purposes of this analysis the assumption that $\Delta_f/\Delta_o = 1$ is made. Then,

$$S_{Ia} = -\frac{h'\,(a_f/W)}{h\,(a_o/W)} \qquad (2\text{-}9)$$

In the BCL procedure, the value of K_{ID} is deduced from the initiation toughness, K_Q, and the crack jump prior to arrest, Δa. Specifically,

$$\frac{K_{ID}}{K_Q} = g\left(\frac{\Delta a}{W}\right) \qquad (2\text{-}10)$$

where the function g (a/W) for the MRL (ordinary expression) is given in eq. 2-5. A parameter, S_{ID}, for measuring the sensitivity of K_{ID} to variations in Δa under the assumption of constant K_Q can be defined as follows:

$$S_{ID} = -\frac{W}{K_Q} \frac{dK_{ID}}{da} \qquad (2\text{-}11)$$

which, in terms of g(x) is given by

$$S_{ID}\Big|_{a_f/W} = -\frac{dg}{dx}\Big|_{x=\frac{a_f - a_o}{W}} \qquad (2\text{-}12)$$

where a_o is the initial slot length and a_f is the crack length at arrest.

For the MRL specimens tested in the Cooperative Test Program on Crack Arrest Toughness Measurement, the initial slot length corresponded to $a_o/W = 0.35$. Based on this condition, eqs. (2-9) and (2-12) were used to calculate S_{Ia} and S_{ID}, respectively, as functions of a_f/W. The results are plotted in Fig. 2-19. Over the range of $0.55 \leq a_f/W \leq 0.75$, which embraces the final crack front position in most tests, the ratio of S_{Ia} to S_{ID} is about 1.7 to 1.8. Thus, at a given value of K_Q, the scatter in K_{Ia} is expected to be 1.7 to 1.8 times the scatter in K_{ID}. This is a mathematical consequence of the way in which the two parameters, K_{Ia} and K_{ID}, are calculated, and says nothing about which is the more appropriate measure of a material's crack arrest toughness.

A graphical demonstration of why K_{Ia} shows more scatter--for a given K_Q--than does K_{ID}, is shown in Fig. 2-20. Here the BCL expression, eq. (2-5), relating K_{ID}/K_Q to $\Delta a/W$ has been translated to reflect an initial slot length corresponding to $a_o/W = 0.35$. On the same plot is a curve of K_{Ia}/K_Q obtained from eq. (2-7), again, with the assumption $\Delta_f/\Delta_o = 1$. It can be seen that for a given range in a/W, there is a larger range in K_{Ia} than in K_{ID}. This construction is equivalent to the analysis in terms of the parameters S_{Ia} and S_{ID}; these parameters are simply the magnitudes of the slopes of the respective curves in Fig. 2-20.

2.3.2 Origin of Scatter in K_{Ia}

2.3.2.1 Analysis of Variation Between Laboratories

An analysis was carried out to assess whether or not a significant amount of the variation in K_{Ia} could be attributed to differences between the various laboratories at which tests in the Cooperative Crack Arrest Test Program were run. The method and results are described here.

There were five different categories of test depending on the material tested (AISI 1018 steel or A533-B-1 steel), the test temperature (room temperature of 0°C), and the specimen type (MRL or NRL). The data analysis was applied to each test category, separately. The data used in the analysis consisted only of test results available in pairs from individual laboratories: in cases where a laboratory reported only one test result or more than two test results, the data from that laboratory were ignored. The number of pairs of test results in the different test categories, each pair coming from a different laboratory, is shown in Table 2-X. The average difference between the two values in each pair, that is, the average intra-laboratory difference, is also shown in Table 2-X. The data analysis consisted of comparing this average intra-laboratory difference against an expected difference.

The expected difference was calculated as follows: The pool of data in a given test category was grouped into pairs by a random selection process, and the average difference between the two values in each pair was calculated. This procedure was carried out 1000 times whereupon a mean value and standard deviation of the average difference was computed. This result is shown in Table 2-X as the expected difference.

In four of the five test categories, as can be seen in Table 2-X, the expected difference based on random pairing of the data exceeded the actual average intra-laboratory difference. In three of these four categories the difference was equal to just about one standard deviation in the expected difference; in the fourth (A533-B, 0°C, MRL specimen) the difference was substantially greater. The results suggest that if differences from laboratory to laboratory were eliminated, the K_{Ia} data collected in the Cooperative Crack Arrest Program would

show less variation; however, the effect would be limited. The values in Table 2-X suggest that the standard deviation might be reduced by about 15 percent.

2.3.2.2 Dependence of K_{Ia} on Specimen Location

A possible source of scatter in the K_{Ia} results would be a pattern of toughness variation with specimen location in the parent plate. This possibility was investigated considering only the MRL specimens which were machined as shown in Fig. 2-21. Each series of specimen numbers, (101-111, 201-211, 401-411, and 501-511) corresponds to a row of adjacent specimen blocks. Rows 100 and 200 and rows 400 and 500 represent adjacent specimens, but between rows 200 and 400 was a volume of material used in making BCL specimens. For each specimen number in Fig. 2-21 there were three specimens identified with the letter suffix A, B, or C. Specimens B were located on the mid-plane of the original plate, specimens A and C were located, respectively, above and below the mid-plane.

Figure 2-22 shows the location of the specimens for which K_{Ia} differed from the mean K_{Ia} by more than one standard deviation. Figure 2-22a shows the location of specimens which gave low values of K_{Ia}, values equal to or less than 78 and 96 $MPa \cdot \sqrt{m}$ fpr tests at 0°C and room temperature, respectively. In Fig. 2-22b, specimens corresponding to K_{Ia} greater than or equal to 99 and 124 $MPa \cdot \sqrt{m}$ at the same respective temperatures are indicated. While there is some tendency for specimens yielding high or low K_{Ia} values to be somewhat clustered, a uniform trend of K_{Ia} dependence on plate location is not apparent.

2.3.2.3 Dependence of K_{Ia} on Crack Jump Distance

All of the MRL specimens tested on the Cooperative Crack Arrest Test Program were the same nominal size and had the same initial slot length. The crack jump distance, therefore can be specified in terms of the normalized crack length, a/W, at the crack arrest position. In this section of the report, the symbol a/W refers to the arrested crack. As mentioned earlier and discussed elsewhere[2-5], the quantity, a/W, is not an independent variable in a population of K_{Ia} tests. Random variation in K_{Ia} (or any other crack arrest parameter) will show up as a systematic dependence on a/W. The reason for this is simply that in a sample of specimens with different arrest toughnesses, the crack will tend to run greater distances in specimens with lower crack arrest toughness. In investigating expected behavior, the scatter both in K_{Ia} and in the initiation toughness, K_Q, must be considered. If there were a range of K_Q values in a group of specimens yielding identical K_{Ia} values, then, of course, the K_{Ia} would be strictly independent of a/W. If, at the opposite extreme, there were a single value of K_Q for a group of tests yielding a range of K_{Ia} results, then K_{Ia} would show a distinct dependence on a/W--K_{Ia} would decrease systematically with increasing a/W. In real situations, such as represented by tests run in the cooperative test program, both K_Q and K_{Ia} will vary. The expected behavior, then, is a trend of decreasing K_{Ia} as a function of crack jump distance (or final crack front position). Figures 2-23 to 2-25 show K_{Ia} plotted against a_f/W for three categories of tests with MRL specimens. In each case, a downward trend of K_{Ia} with a_f/W is apparent. Also plotted on the same figures are curves of expected values of K_{Ia} as a function of a_f/W for specific values of K_Q. The specific values of K_Q that were chosen were one standard deviation above and below the average value of K_Q in each test category. It can be seen that the K_{Ia} data are in good agreement with the expected behavior.

The major reason for plotting K_{Ia} as a function of a/W as in Figs. 2-23 to 2-25 was not to demonstrate that the expected trend was in fact observed, but rather to look for any trends at very low or very high values of a/W that would indicate a limitation on the tolerable crack jump range that should be permitted in K_{Ia} testing. The data as plotted in Figs. 2-23 to 2-25 do not, however, suggest any limitations--the whole range of a/W sampled in the tests seems to give reasonable results.

2.3.2.4 Origin of Scatter in K_{Ia}--Summary

The K_{Ia} measurements made on the ASTM Cooperative Test Program on Crack Arrest showed a standard deviation of about ± twelve percent for each material/test temperature combination. This was a larger scatter than was anticipated, and the data were analyzed to see if any of it could be attributed to some features of the test procedure, so that undesirable practices could be modified or eliminated. The analysis of the scatter, however, failed to indict any particular aspect of the test procedure. Laboratory to laboratory differences did not account for a significant part of the K_{Ia} variation. There was no evidence that extremes of very short or very long crack jumps affected the K_{Ia} results. Position through the thickness of the SA 533 Grade B Class 1 plate had no effect, and regions of the plate showing unusually high or low values of K_{Ia} were generally not clearly defined and/or closely localized. At this stage the conclusion has to be that the observed scatter in K_{Ia} is an honest reflection of toughness variations in the materials.

REFERENCES

2-1. Barnes, C. R., et al., "Preliminary Compilation of the Test Data and Supplementary Information on the ASTM E24.01.06 Dynamic Initiation--Crack Arrest Task Group, Co-operative Test Program in Crack Arrest Toughness Measurement."

2-2. Newman, J. C., Jr., "Crack-Opening Displacements in the Center-Crack, Compact, and Crack-Line-Wedge-Loaded Specimens," NASA TN D-8268, National Aeronautics and Space Administration, Washington, DC, July, 1976.

2-3. Newman, J. C., Jr., "Stress Analysis of the Compact Specimen Including the Effects of Pin-loading," ASTM STP 560, 1974, p. 105.

2-4. Rosenfield, A. R. Private communication.

2-5. Crosley, P. B. and Ripling, E. J., "Significance of Crack Arrest Toughness (K_{ia}) Testing," Crack Arrest Methodology and Applications, ASTM STP 711, G. T. Hahn and M. F. Kanninen, Eds., American Society for Testing and Materials, 1980, pp. 321-337.

Materials Research Laboratory, Inc.

Table 2-I

EXPERIMENTAL CALIBRATION OF
MRL COMPACT CRACK ARREST SPECIMEN
(See Fig. A-1 for dimensions)

	W - a ($m \times 10^{-1}$)	Δ/P (m/GN)	a/W	EBΔ/P	EBΔ $(1 - x)^2$/P
Aluminum Alloy E = 69 x 10^3 MPa W = 169 mm, B = 50.8 mm	1.101	7.48	0.349	26.2	11.09
	1.042	8.59	0.385	30.1	11.39
	0.975	10.28	0.424	36.0	11.92
	0.907	12.33	0.464	43.2	12.40
	0.845	14.67	0.501	51.4	12.80
	0.785	17.50	0.537	61.3	13.16
	0.723	21.61	0.573	75.7	13.80
	0.658	26.44	0.611	92.6	14.00
	0.598	33.75	0.647	118.2	14.74
	0.525	45.62	0.690	159.8	15.38
	0.470	57.27	0.722	201.0	15.46
	0.406	79.08	0.760	277.0	15.92
	0.345	115.90	0.796	406.0	16.82
	0.281	183.30	0.834	642.0	17.67
Steel (A533-B-1) (E - 200 x 10^3 MPa) W = 169 mm, B = 50.8 mm	1.121	2.48	0.338	25.2	11.03
	1.057	2.72	0.376	27.7	10.77
	1.013	3.18	0.402	32.3	11.55
	0.946	3.77	0.442	38.3	11.94
	0.883	4.48	0.478	45.5	12.37
	0.835	5.15	0.507	52.3	12.72
	0.780	6.10	0.540	61.9	13.13
	0.726	7.30	0.571	72.4	13.30
	0.663	8.79	0.608	89.3	13.70
	0.601	11.05	0.645	112.2	14.12
	0.543	13.89	0.680	141.1	14.48
	0.473	19.01	0.721	193.1	15.05
	0.418	25.01	0.753	254.0	15.48
	0.359	35.29	0.788	358.0	16.15
	0.305	51.05	0.820	519.0	16.83
	0.238	89.82	0.859	912.0	18.02
	0.168	191.90	0.901	1949.0	19.21

Table 2-II

DIMENSIONLESS STRESS INTENSITY FACTOR, $\frac{K\sqrt{W}}{E\Delta}\left(\frac{B_N}{B}\right)^{\frac{1}{2}}$

AS A FUNCTION OF DIMENSIONLESS CRACK LENGTH, a/W

a/w	$\frac{K\sqrt{W}}{E\Delta}\left(\frac{B_N}{B}\right)^{\frac{1}{2}}$	a/W	$\frac{K\sqrt{W}}{E\Delta}\left(\frac{B_N}{B}\right)^{\frac{1}{2}}$
0.30	0.267	0.61	0.156
0.31	0.263	0.62	0.153
0.32	0.259	0.63	0.150
0.33	0.255	0.64	0.146
0.34	0.251	0.65	0.143
0.35	0.247	0.66	0.140
0.36	0.244	0.67	0.137
0.37	0.240	0.68	0.134
0.38	0.236	0.69	0.131
0.39	0.232	0.70	0.128
0.40	0.228	0.71	0.125
0.41	0.225	0.72	0.122
0.42	0.221	0.73	0.119
0.43	0.217	0.74	0.116
0.44	0.214	0.75	0.113
0.45	0.210	0.76	0.110
0.46	0.206	0.77	0.107
0.47	0.203	0.78	0.104
0.48	0.199	0.79	0.101
0.49	0.196	0.80	0.098
0.50	0.192	0.81	0.095
0.51	0.189	0.82	0.092
0.52	0.185	0.83	0.089
0.53	0.182	0.84	0.086
0.54	0.179	0.85	0.082
0.55	0.175	0.86	0.079
0.56	0.172	0.87	0.076
0.57	0.169	0.88	0.072
0.58	0.165	0.89	0.069
0.59	0.162	0.90	0.065
0.60	0.159		

Materials
Research
Laboratory,
Inc.

Table 2-III

EXPERIMENTAL COMPLIANCE CALIBRATION OF BCL
CRACK ARREST SPECIMEN
(See Fig. A-2 for dimensions)

a/W	$\frac{\Delta}{P}$ (m/GN)	y/Δ	$\frac{y}{P}$ (m/GN)	$\frac{EB\Delta}{P}$	$\frac{EB\Delta(1-x)^2}{P}$	$\frac{EBy}{P}$	$\frac{EBy(1-x)^2}{P}$
0.318	2.04	0.87	1.78	20.8	9.675	18.04	8.39
0.379	2.70	0.90	2.43	27.8	10.57	24.65	9.51
0.430	3.50	0.90	3.15	35.5	11.53	31.96	10.38
0.495	4.66	0.88	4.10	47.3	12.06	41.64	10.62
0.553	6.31	0.86	5.43	64.1	12.81	55.10	11.01
0.614	9.08	0.86	7.81	92.2	13.74	79.29	11.81
0.676	13.48	0.83	11.20	137.1	14.39	113.74	11.91
0.739	22.38	0.83	18.58	227.4	15.49	188.73	12.86
0.796	38.31	0.85	32.57	389.2	16.20	330.83	13.77
0.855	87.48	0.85	74.34	888.6	18.68	755.16	15.88

Δ = displacement at 0.25W
y = displacement at load-line, measured on pins
W = 169 mm
B = 50.8 mm
E = 200×10^3 MPa

Materials' Research Laboratory, Inc.

Table 2-IV

SUMMARY OF CO-OPERATIVE TEST PROGRAM DATA ON AISI 1018 STEEL

Lab. No.	Spec. No.	Temp. C	a/W	K_Q MPa-$m^{\frac{1}{2}}$	K_D MPa-$m^{\frac{1}{2}}$	K_a MPa-$m^{\frac{1}{2}}$
1	6341/41	22	0.592	134	107	99
1	6341/77	22	0.598	140	111	100
2	6341/21	26	0.750	169	116	80
2	6341/31	25	0.651	165	124	100
3	6341/07	23	0.664	158	118	91
3	6341/42	23	0.678	145	107	84
4	6341/03	22	0.548	106	88	82
4	6341/19	22	0.618	142	110	93
6	6341/68	22	0.877	184	112	57
6	6341/92	22	0.709	139	100	74
7	6341/47	21	0.542	114	95	86
7	6341/55	21	0.531	109	92	85
8	6341/08	28	0.563	138	113	101
8	6341/38	28	0.625	150	116	94
9	6341/27	20	0.697	154	111	90
9	6341/36	20	0.738	160	111	79
10	6341/56	23	0.749	146	101	69
10	6341/15	23	0.597	124	98	83
11	6341/66	25	0.579	136	109	94
11	6341/78	18	0.578	131	106	96
12	6341/02	20	0.613	169	132	101
12	6341/43	20	0.643	170	129	92
13	6341/44	21	0.791	175	116	76
13	6341/64	22	0.772	149	100	67
14	6341/98	24.5	0.862	188	116	68
14	6341/46	23.8	0.900	163	97	52
15	6341/28	20	0.638	146	112	99
15	6341/65	20	0.805	179	117	72
16	6341/11	20.5	0.626	145	112	95
16	6341/74	22.8	0.636	149	114	96
17	6341/52	25	0.732	184	129	93

Table 2-IV, Continued

Lab. No.	Spec. No.	Temp. C	a/W	K_Q MPa-$m^{\frac{1}{2}}$	K_D MPa-$m^{\frac{1}{2}}$	K_a MPa-$m^{\frac{1}{2}}$
18	6341/29	18	0.577	132	107	98
18	6341/45	16	0.667	140	104	90
19	6341/91	23	0.706	161	115	83
19	6341/54	23	0.828	187	119	68
20	6341/16	24	0.546	111	92	89
20	6341/33	24	0.591	123	98	85
21	6341/18	24.5	0.602	145	115	95
21	6341/76	24.5	0.579	146	117	98
22	6341/14	22	0.606	133	104	89
22	6341/04	23	0.580	139	112	105
23	6341/62	23	0.626	135	104	92
23	6341/57	23	0.570	71	58	51
24	6341/34	25	0.675	150	111	89
24	6341/96	25	0.564	123	101	88
26	6341/22	22	0.613	150	117	97
26	6341/06	22	0.596	127	101	87
27	6341/32	25	0.490	110	96	86
27	6341/97	26	0.606	147	115	98
28	6341/13	23	0.659	156	117	101
28	6341/51	23	0.558	114	94	72
29	6341/17	23	0.558	133	109	95
29	6341/35	23	0.633	139	106	90
30	6341/09	23	0.707	152	109	82
30	6341/12	23	0.629	152	117	93

Materials Research Laboratory, Inc.

Table 2-V

SUMMARY OF CO-OPERATIVE TEST PROGRAM DATA
MRL Specimens of SA533, Grade B, Class 1 Steel
Tested at Room Temperature

Lab. No.	Spec. No.	Temp. C	a/W	K_Q MPa-$m^{\frac{1}{2}}$	K_D MPa-$m^{\frac{1}{2}}$	K_a MPa-$m^{\frac{1}{2}}$
1	102C	22	0.623	166	128	109
1	103C	22	0.696	154	111	95
2	206A	25	0.692	214	155	114
2	502B	25	0.632	162	124	102
3	204A	22	0.696	186	135	100
3	204B	23	0.447	157	143	135
4	203B	22	0.568	192	156	139
4	207C	22	0.722	194	137	103
6	104A	22	0.569	169	138	119
6	502A	22	0.600	148	117	101
7	209B	20	0.663	192	143	112
7	201C	20	0.615	175	136	112
8	411B	30	0.723	193	136	98
8	202A	30	0.687	202	148	108
9	509A	20	0.671	178	132	102
9	510A	20	0.627	151	116	95
10	205A	23	0.603	204	161	133
10	101A	23	0.463	167	150	140
11	511C	19	0.622	164	127	103
11	108B	19	0.466	157	140	132
12	106A	20	0.693	198	144	108
12	406A	20	0.625	153	119	96
13	105C	21.5	0.723	207	146	106
13	501C	21.5	0.555	172	142	126
14	507C	24.4	0.484	155	136	126
14	409C	23	0.792	166	109	77
14	104C	23.5	0.685	178	130	104
14	508A	23.5	0.722	172	121	94
15	102A	20	0.729	192	135	99
15	401A	20	0.638	191	146	121
16	109C	23	0.716	190	135	101
16	404C	21.2	0.706	215	154	124

Table 2-V, Continued

Lab. No.	Spec. No.	Temp. C	a/w	K_Q MPa-$m^{\frac{1}{2}}$	K_D MPa-$m^{\frac{1}{2}}$	K_a MPa-$m^{\frac{1}{2}}$
17	106B	25	0.586	172	138	118
17	510B	25	0.622	142	110	91
18	110A	17	0.751	182	125	95
18	103B	17	0.697	169	122	100
19	107B	23	0.646	176	133	109
19	109B	23	0.665	185	138	108
20	111B	24	0.439	138	126	117
20	208A	24	0.611	206	161	134
21	201A	24	0.628	179	138	108
21	406B	24	0.515	158	134	121
22	105B	23.3	0.628	160	123	104
22	101B	22.8	0.552	158	130	116
23	511B	23	0.646	163	124	104
23	403C	23	0.458	138	124	116
24	211B	24	0.631	259	199	176
24	204C	24	0.724	171	120	95
26	107A	22	0.626	185	143	119
26	401B	20	0.649	179	135	104
27	409B	26	0.481	135	119	114
27	511A	26	0.637	149	114	86
28	202B	23	0.376	139	135	133
28	411C	22	0.735	182	127	99
29	205B	23	0.648	178	134	109
29	504B	23	0.711	197	140	106
30	203A	23	0.615	183	143	116
30	211A	23	0.537	146	122	110
30	502C	23	0.762	246	168	113
28	509B	23	0.535	146	122	110

Table 2-VI

SUMMARY OF CO-OPERATIVE TEST PROGRAM DATA
BCL Specimens of SA533, Grade B, Class 1 Steel
Tested at Room Temperature

Lab. No.	Spec. No.	Temp. C	a/w	K_Q MPa-$m^{\frac{1}{2}}$	K_D MPa-$m^{\frac{1}{2}}$	K_a MPa-$m^{\frac{1}{2}}$
1	RD7	22	0.738	185	127	95
2	RH77	25	0.693	168	122	99
2	RD49	25	0.689	178	130	104
3	RH90	22	0.730	230	161	108
3	RH78	23	0.704	205	147	103
4	RC101	22	0.701	232	166	124
5	RG127	7	0.727	206	144	103
5	RC94	9	0.642	198	152	117
6	RD34	22	0.694	177	129	105
6	RD42	22	0.775	158	106	77
7	RD23	21	0.639	209	161	118
7	RD33	21	0.671	190	140	110
8	RC109	16	0.614	92	74	0
9	RD20	12	0.727	196	137	94
9	RG130	24	0.680	187	137	98
10	RH61	23	0.712	219	157	112
10	RD29	22	0.753	225	153	102
11	RC99	19	0.726	185	129	0
12	RG134	20	0.588	185	153	121
13	RD31	25	0.708	206	148	106
13	RG144	25	0.772	228	152	98
14	RD39	22.8	0.717	222	157	109
14	RH62	23	0.735	231	160	113
15	RC96	20	0.632	185	144	103
16	RD13	21.7	0.736	226	156	105
16	RD8	20.7	0.770	232	155	99
17	RD41	20	0.782	195	129	92
17	RG138	20	0.793	220	144	86

Table 2-VI, Continued

Lab. No.	Spec. No.	Temp. C	a/w	K_Q MPa-$m^{\frac{1}{2}}$	K_D MPa-$m^{\frac{1}{2}}$	K_a MPa-$m^{\frac{1}{2}}$
18	RC95	18	0.691	200	146	106
18	RC111	19	0.652	203	154	113
19	RH73	23	0.728	171	120	83
19	RH87	23	0.719	243	171	118
20	RH75	23	0.764	163	109	86
20	RD25	23	0.721	152	107	92
21	RD12	24	0.736	232	159	102
21	RC98	24	0.537	211	191	0
22	RC124	22.8	0.569	183	155	116
22	RC3	22.8	0.753	204	139	92
24	RD43	25	0.546	199	178	135
24	RG136	24.4	0.758	228	160	113
26	RD5	20	0.681	191	140	104
26	RD28	20	0.739	216	149	110
27	RH64	25	0.670	228	169	133
28	RD58	16	0.715	211	150	100
29	RH68	23	0.749	164	111	77
29	RD22	23	0.535	138	123	91
30	RC100	23	0.694	216	159	111
30	RD14	23	0.689	234	170	119

Materials
Research
Laboratory,
Inc.

Table 2-VII

SUMMARY OF CO-OPERATIVE TEST PROGRAM DATA
MRL Specimens of SA533, Grade B, Class 1 Steel
Tested at 0°C

Lab. No.	Spec. No.	Temp. C	a/W	K_Q MPa-$m^{\frac{1}{2}}$	K_D MPa-$m^{\frac{1}{2}}$	K_a MPa-$m^{\frac{1}{2}}$
1	402A	0	0.704	170	122	103
1	503B	0	0.638	121	93	81
2	207B	0	0.668	164	121	95
3	206B	0	0.676	159	117	90
3	407A	0	0.708	148	106	79
4	505C	0	0.653	131	99	86
4	407C	0	0.624	145	112	98
6	203C	0	0.771	169	114	78
6	507A	0	0.733	141	99	79
7	504A	0	0.715	152	108	79
7	410C	0	0.731	164	115	86
8	205B	0	0.653	157	118	93
8	205C	0	0.745	170	118	83
9	111A	0	0.708	136	97	74
9	408A	0	0.615	134	104	94
10	210C	0	0.699	165	119	87
10	410B	0	0.634	148	113	90
11	104B	0	0.636	138	105	89
12	503A	0	0.651	155	117	93
12	110B	0	0.733	174	122	87
13	405A	5	0.716	165	117	89
13	410A	-1	0.804	155	102	65
15	505A	0	0.655	130	98	79
15	505B	0	0.656	139	105	85
16	509C	-0.1	0.699	173	125	97
16	408B	-10.3	0.687	164	120	94
17	111C	0	0.616	144	112	96
17	408c	0	0.648	145	110	88
18	403A	0	0.754	150	103	75
18	206C	0	0.702	151	108	82

Table 2-VII, Continued

Lab. No.	Spec. No.	Temp. C	a/W	K_Q MPa-$m^{\frac{1}{2}}$	K_D MPA-$m^{\frac{1}{2}}$	K_a MPa-$m^{\frac{1}{2}}$
19	405C	0	0.612	147	115	92
19	508B	0	0.666	148	110	87
20	507B	-18	0.732	144	108	76
20	101C	-18	0.684	132	96	73
21	103A	0	0.535	131	110	98
21	404B	0	0.665	153	113	98
22	209C	0	0.671	173	128	102
22	402C	0	0.588	129	103	87
23	211C	0	0.661	130	97	82
23	208B	0	0.731	148	104	79
24	503C	0	0.817	186	120	82
26	106C	0	0.762	194	132	92
26	109A	0	0.507	112	96	93
27	201B	0	0.505	99	85	84
27	110C	0	0.557	133	109	107
29	210B	0	0.664	191	142	116
29	209A	0	0.701	194	140	110
30	501B	0	0.668	159	118	93
30	108C	0	0.726	180	127	91

Materials Research Laboratory, Inc.

Table 2-VIII

SUMMARY OF CO-OPERATIVE TEST PROGRAM DATA
BCL Specimens of SA533, Grade B, Class a Steel
Tested at 0°C

Lab. No.	Spec. No.	Temp. C	a/W	K_Q MPa-$m^{\frac{1}{2}}$	K_D MPa-$m^{\frac{1}{2}}$	K_a MPA-$m^{\frac{1}{2}}$
2	RD16	0	0.781	173	115	80
2	RD30	0	0.775	196	131	97
4	RH65	0	0.860	216	132	64
4	RG133	0	0.817	216	137	84
5	RG139	0	0.784	204	134	83
5	RC120	0	0.739	208	144	114
6	RC92	0	0.761	186	126	94
6	RH66	0	0.713	174	124	91
7	RH57	0	0.802	201	129	75
7	RH72	0	0.803	189	122	68
8	RC119	0	0.631	216	166	0
9	RC93	0	0.787	208	137	81
9	RC115	0	0.806	209	135	76
10	RH82	0	0.750	231	158	105
10	RD11	0	0.713	219	156	108
11	RH48	0	0.800	190	123	73
11	RC126	0	0.789	204	134	82
12	RG128	0	0.811	201	129	73
12	RG132	0	0.728	201	140	95
13	RH84	4	0.818	205	131	75
13	RC103	5	0.761	200	135	89
14	RD19	-1	0.813	219	141	79
15	RG140	0	0.780	204	135	84
15	RG135	0	0.840	213	133	66
16	RD47	0.5	0.826	209	132	69
16	RC116	0.5	0.781	207	137	107
17	RG131	0	0.731	212	147	104
17	RC118	0	0.795	210	136	83
18	RG129	0	0.806	199	128	76
18	RG137	0	0.841	208	129	66

Table 2-VIII, Continued

Lab. No.	Spec. No.	Temp. C	a/W	K_Q MPa-$m^{\frac{1}{2}}$	K_D MPA-$m^{\frac{1}{2}}$	K_a MPa-$m^{\frac{1}{2}}$
19	RD18	0	0.758	201	136	90
19	RH76	0	0.785	198	131	83
20	RH51	-18	0.837	152	96	62
20	RD6	-18	0.869	187	114	62
21	RH52	0	0.770	199	134	85
21	RH83	0	0.823	204	131	72
22	RD32	0	0.760	207	140	92
22	RD9	0	0.763	198	134	84
24	RD38	0	0.758	210	143	95
24	RH46	0	0.781	210	140	90
26	RH67	0	0.795	209	136	85
26	RC112	0	0.767	179	120	77
27	RD45	0	0.833	215	134	82
27	RD37	0	0.897	213	126	47
28	RH59	0	0.768	170	114	72
28	RD27	1	0.795	196	128	77
29	RD35	0	0.770	166	110	75
29	RD21	0	0.823	157	98	59
30	RH71	0	0.829	220	139	72
30	RH69	0	0.746	223	153	101

Table 2-IX

STATISTICAL DATA ON K_{Ia} AND K_{ID} AND THEIR DEPENDENCE ON K_Q

Test Material	Test Temp.	Specimen Type	K_{Ia} (MPa $\sqrt{m}$)	K_{ID} (MPa $\sqrt{m}$)
AISI 1018	R. T.	MRL	(a) 86.7 ± 12.5	108.3 ± 11.8
			(b) $90.4 - 0.026\ K_Q \pm 12.5$	$45.7 + 0.434\ K_Q \pm 6.5$
SA533-B-1	R. T.	MRL	(a) 110.0 ± 13.4	133.9 ± 13.2
			(b) $99.2 + 0.062\ K_Q \pm 13.3$	$55.3 + 0.451\ K_Q \pm 8.4$
	R. T.	BLC	(a) 104.5 ± 12.9	144.4 ± 21.4
			(b) $50.6 + 0.267\ K_Q \pm 11.0$	$19.9 + 0.625\ K_Q \pm 11.0$
	R. T.	MRL and BCL	(a) 107.5 ± 13.6	136.9 ± 17.3
			(b) $93.5 + 0.076\ K_Q \pm 13.4$	$40.3 + 0.531\ K_Q \pm 10.2$
SA533-B-1	0°C	MRL	(a) 88.5 ± 9.9	111.7 ± 11.7
			(b) $64.2 + 0.160\ K_Q \pm 9.4$	$32.0 + 0.52 + K_Q \pm 4.7$
	0°	BCL	(a) 81.7 ± 13.9	132.3 ± 13.0
			(b) $24.5 + 0.285\ K_Q \pm 13.1$	$-4.0 + 0.679\ K_Q \pm 6.3$
	0°C	MRL and BCL	(a) 85.1 ± 12.5	122.1 ± 16.1
			(b) $87.1 - 0.0115\ K_Q \pm 12.5$	$36.9 + 0.482\ K_Q \pm 6.2$

(a) Mean value and standard deviation.

(b) Linear fit and deviation from fitted line.

Table 2-X

COMPARISON OF INTRA-LABORATORY STANDARD DEVIATION
WITH EXPECTED DEVIATION BASED ON TOTAL PROGRAM SCATTER

Material	Test Temp.	Specimen Type	No. of Pairs of K_{Ia} Measurements	Avg. Intra-Laboratory Difference $MPa\text{-}m^{\frac{1}{2}}$	Expected Difference $MPa\text{-}m^{\frac{1}{2}}$
1018	RT	MRL	26	11.5	13.8 ± 2.2
A533B	RT	MRL	22	16.2	14.9 ± 2.4
A533B	RT	BCL	19	11.6	14.1 ± 2.5
A533B	0°C	MRL	22	8.7	11.6 ± 1.8
A533B	0°C	BCL	23	14.0	16.1 ± 2.4

ORNL-DWG 81-15285

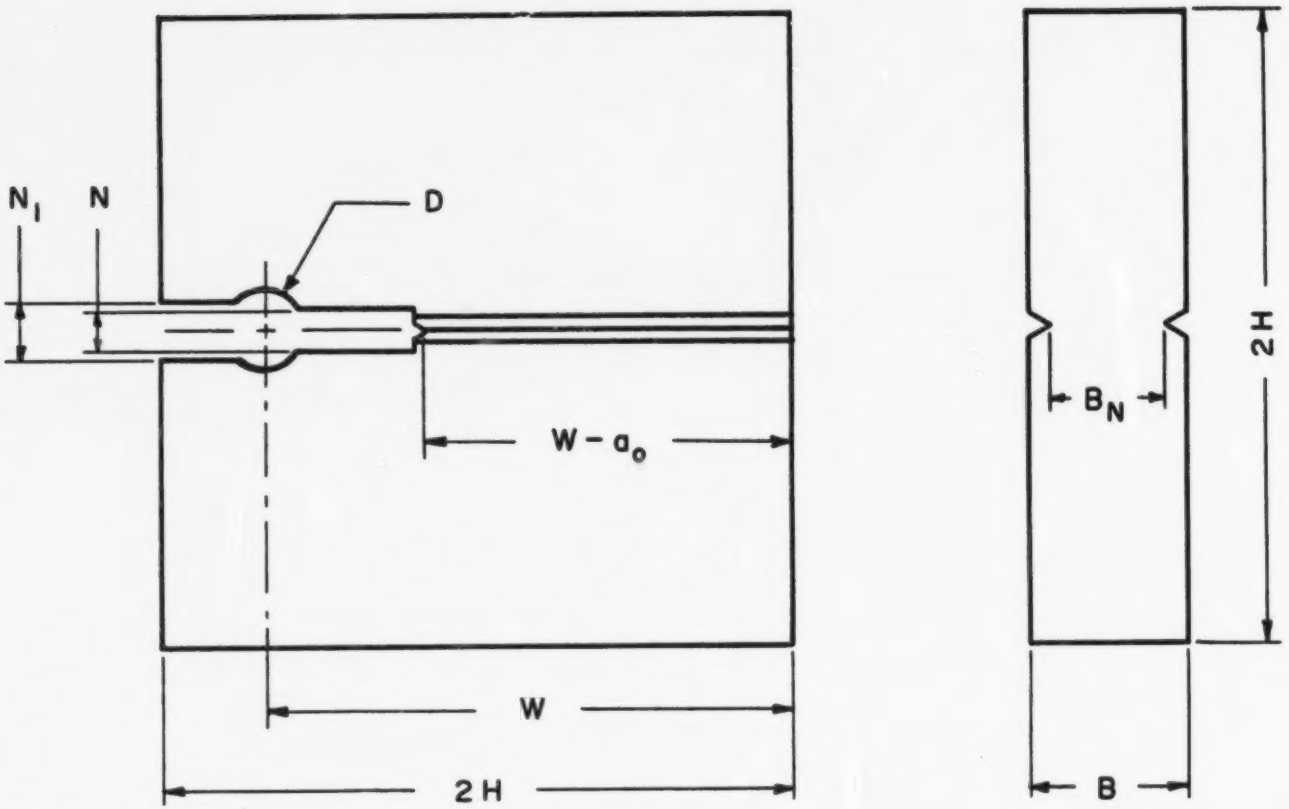

Fig. 2-1 MRL Compact Crack Arrest Specimen.
W = 169.3 mm, H = 101.6 mm, B = 50.8 mm, B_N = 0.75 B, W - a_o = 110.1 mm,
D = 25.4 mm, N = 12.7 mm, N_1 = 19.1 mm.

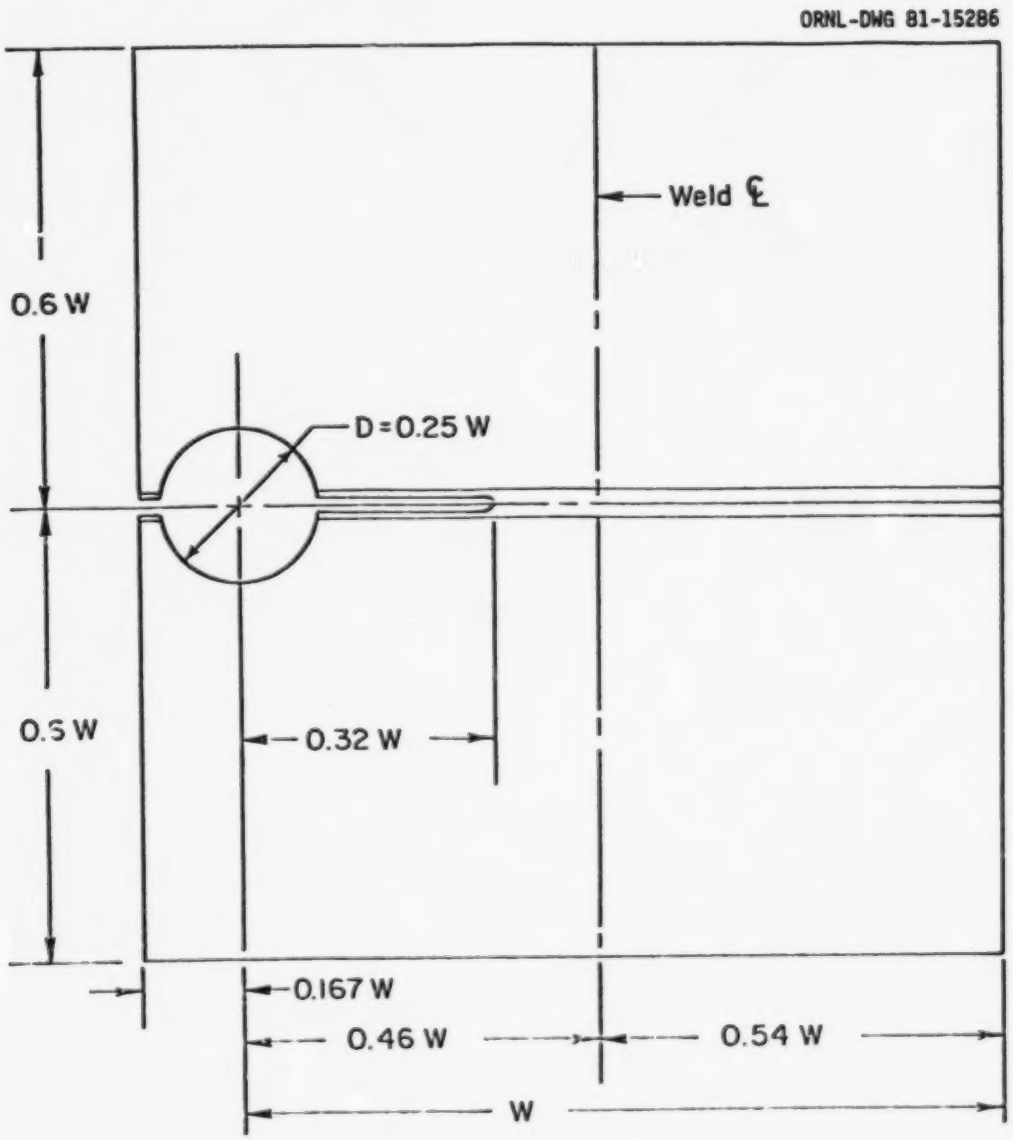

Fig. 2-2 BCL Compact Crack Arrest Specimen.
W = 208 mm, B = 50.8 mm, B_N = 0.75 B.

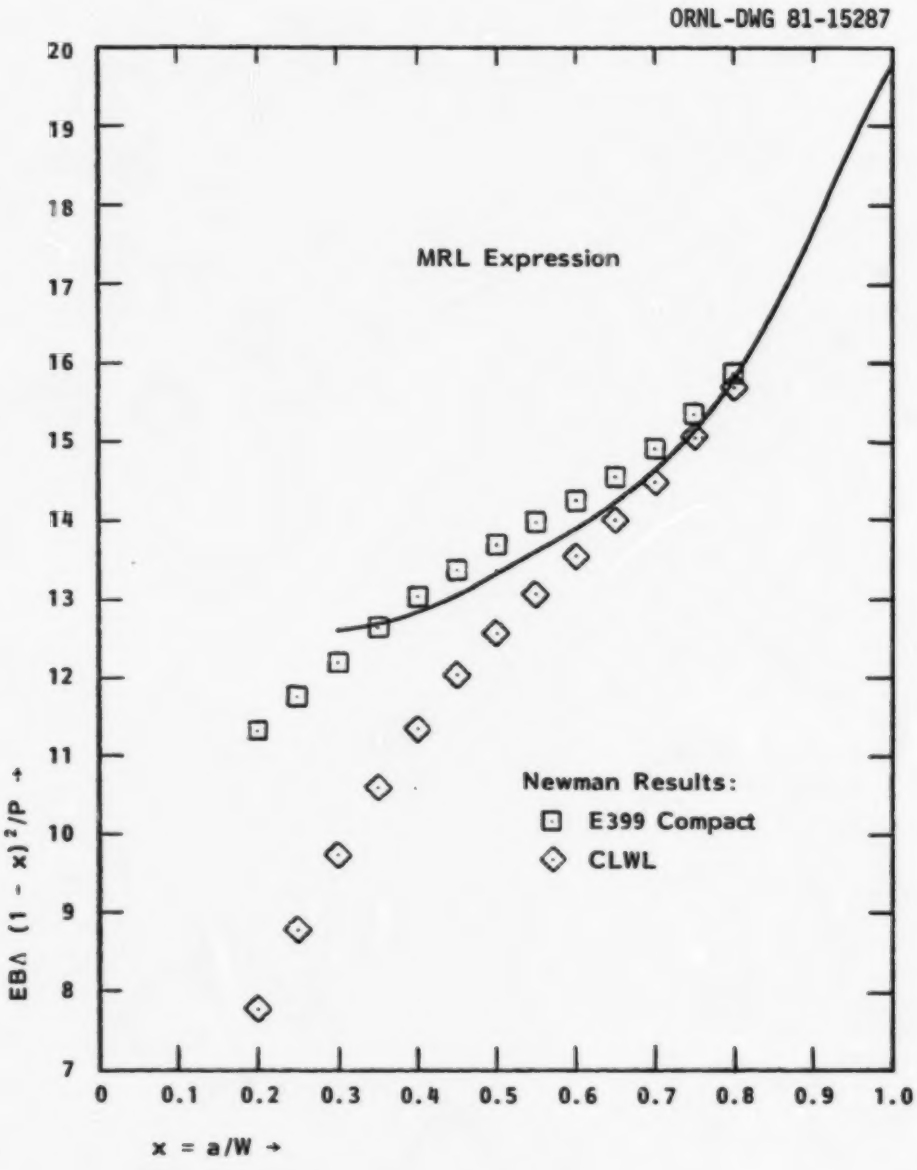

Fig. 2-3 Newman's results for opening displacement, Δ, at 0.25W from load line for ASTM Standard E399 compact specimen and wedge-loaded (CLWL) specimen. MRL expression for K_{Ia} compact specimen shown for comparison.

ORNL-PHOTO 4715-81

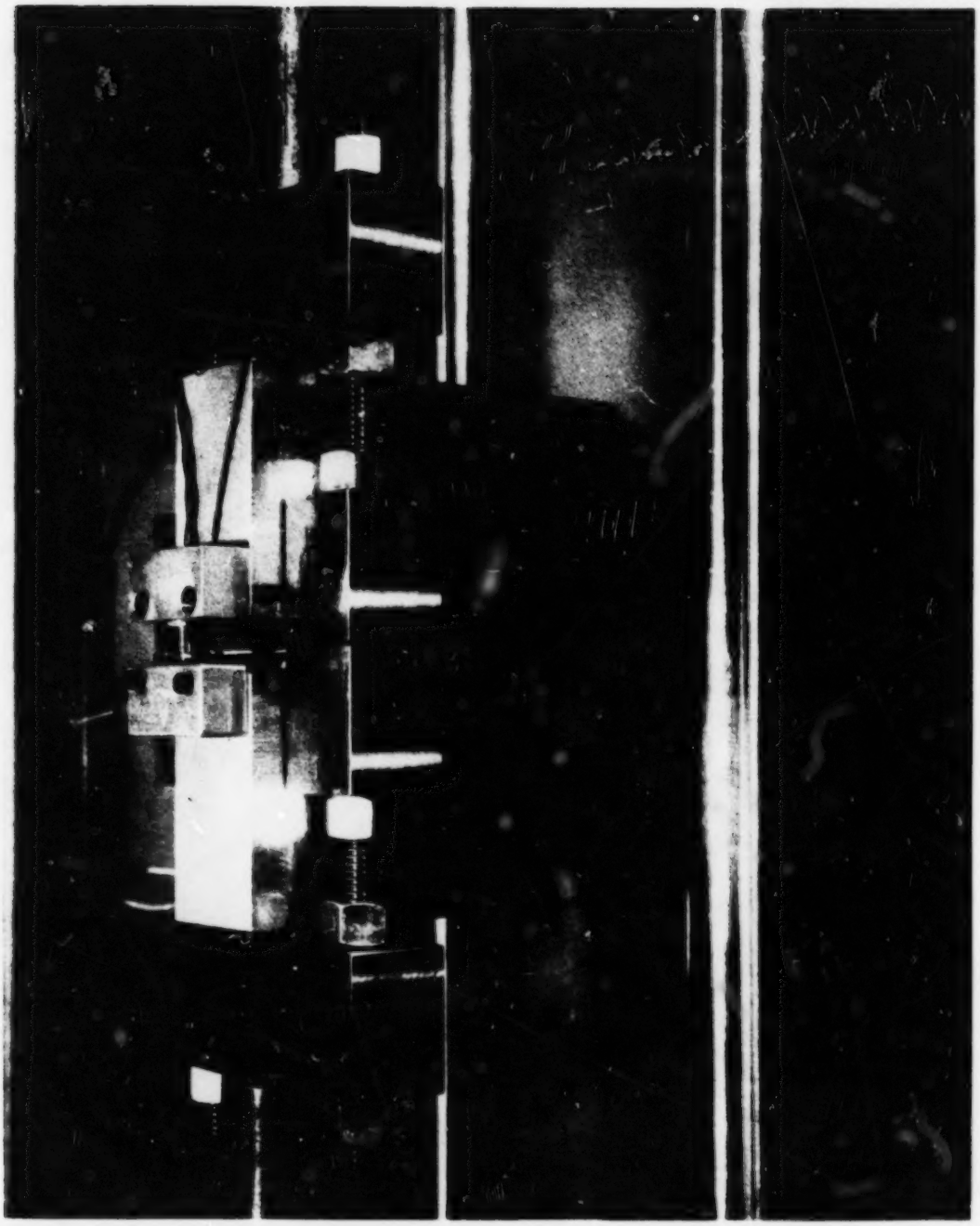

Fig. 2-4 Photograph of test set-up for calibrating MRL compact crack arrest specimen.

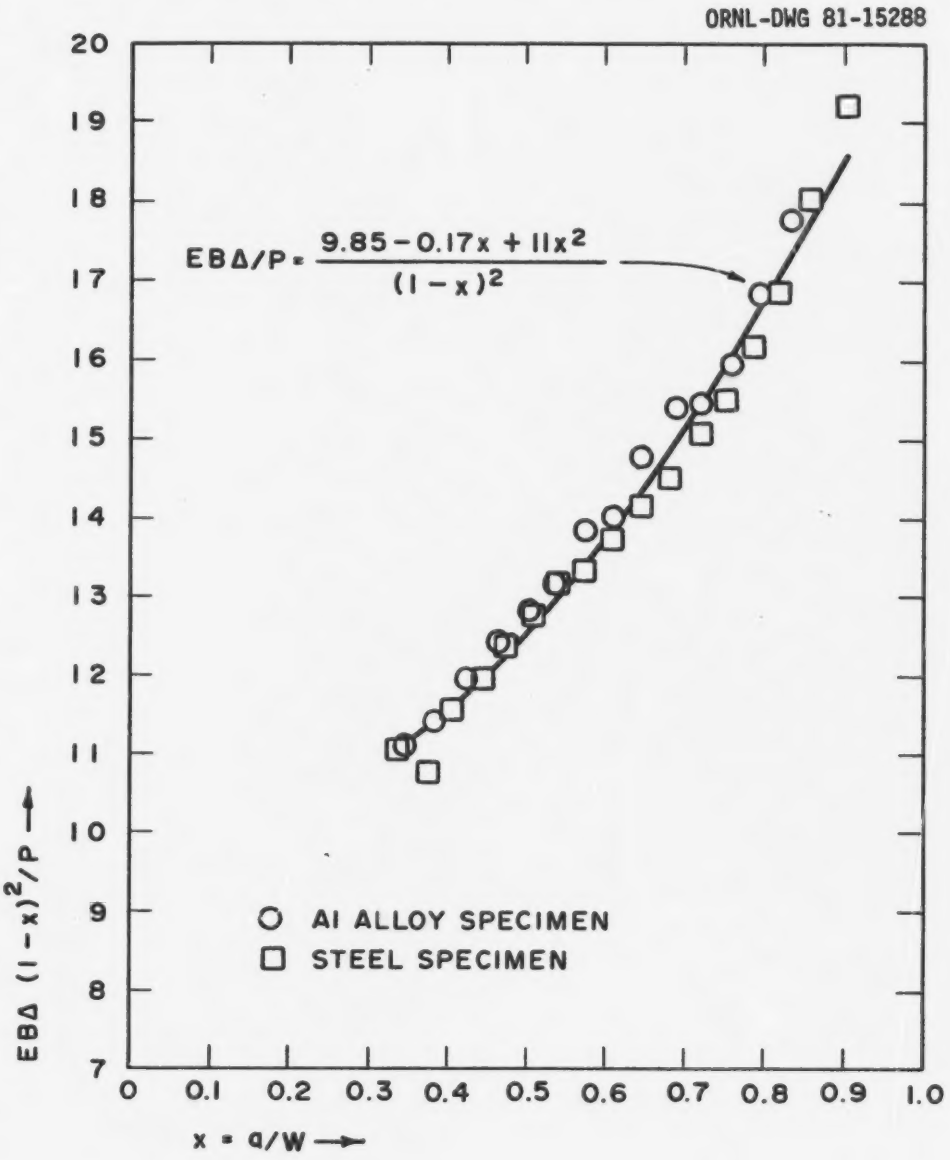

Fig. 2-5 Experimental compliance calibration of MRL Compact Crack Arrest Specimen.

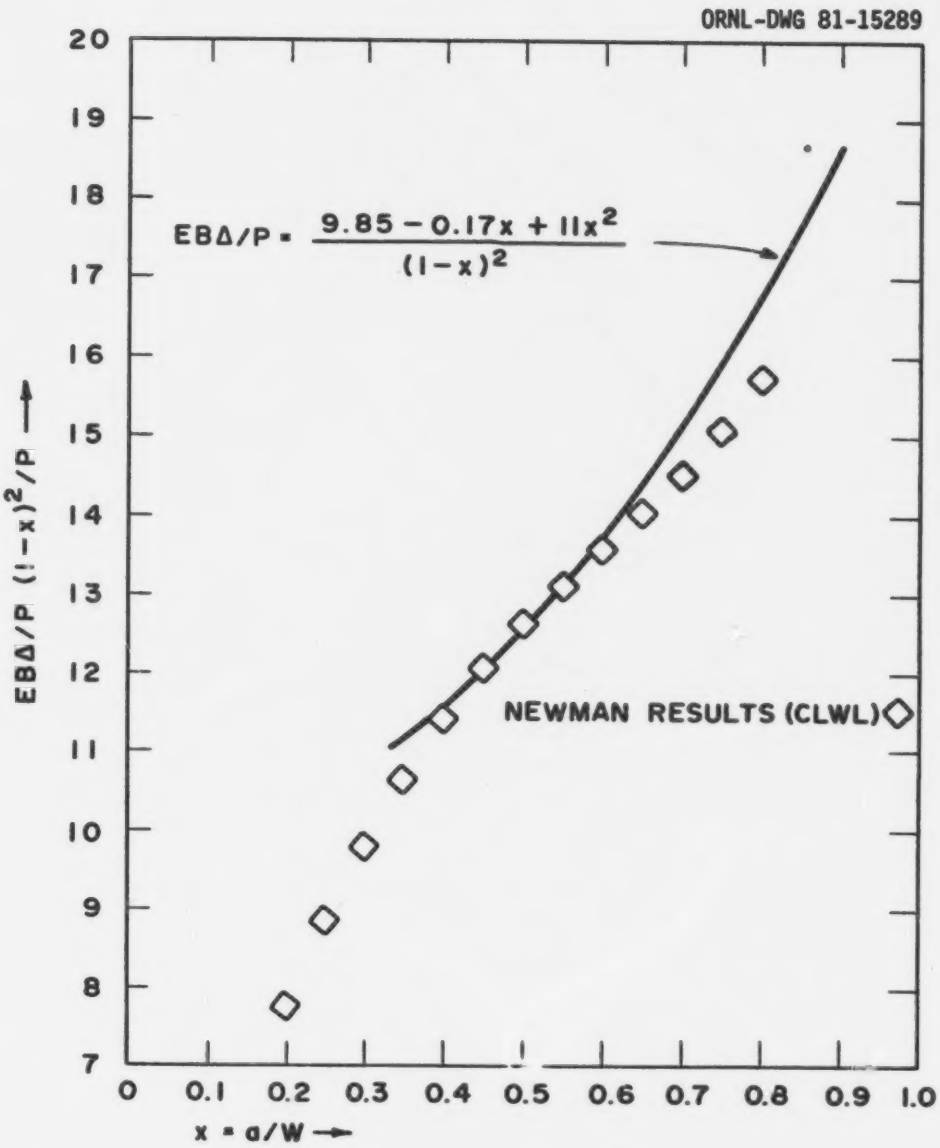

Fig. 2-6 Curve fitted to experimental calibration for MRL compact crack arrest specimen compared with Newman's results.

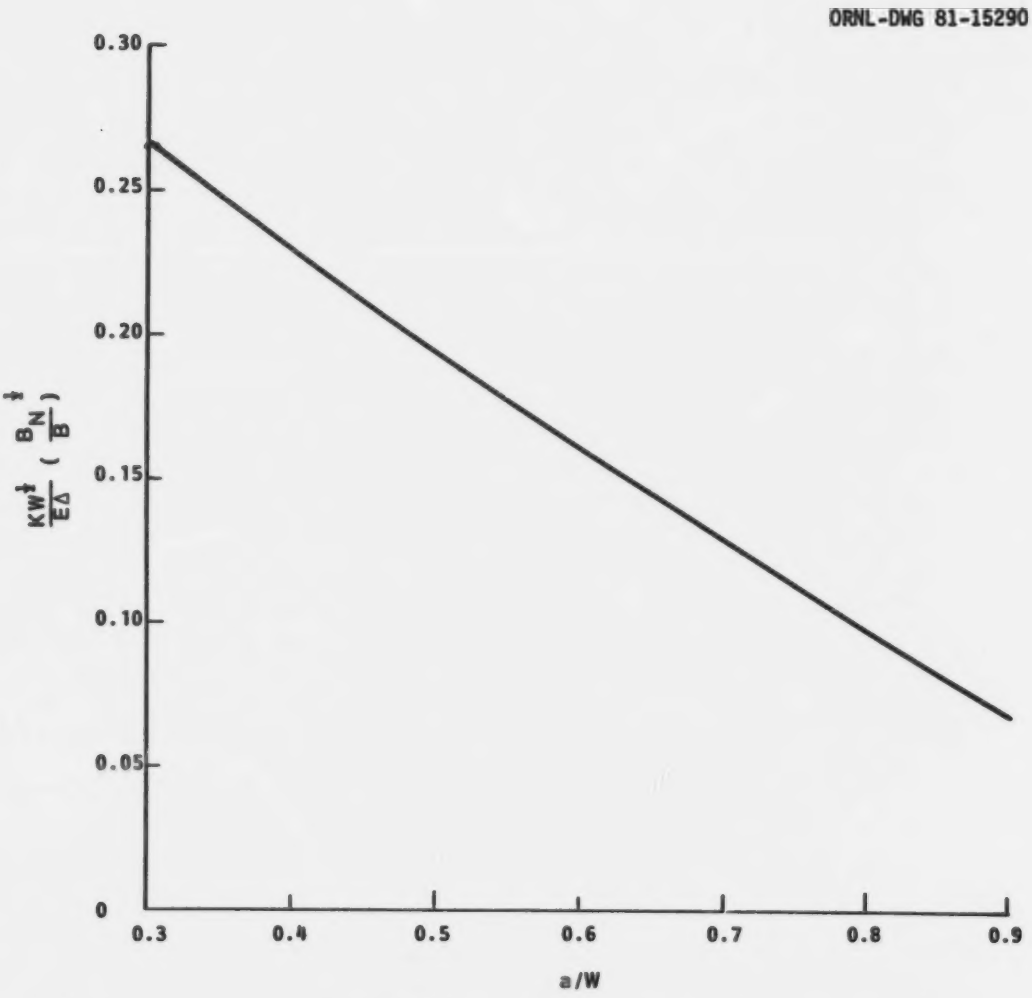

Fig. 2-7 Dimensionless stress intensity factor as a function of dimensionless crack length for MRL compact crack arrest specimen.

ORNL-PHOTO 4716-81

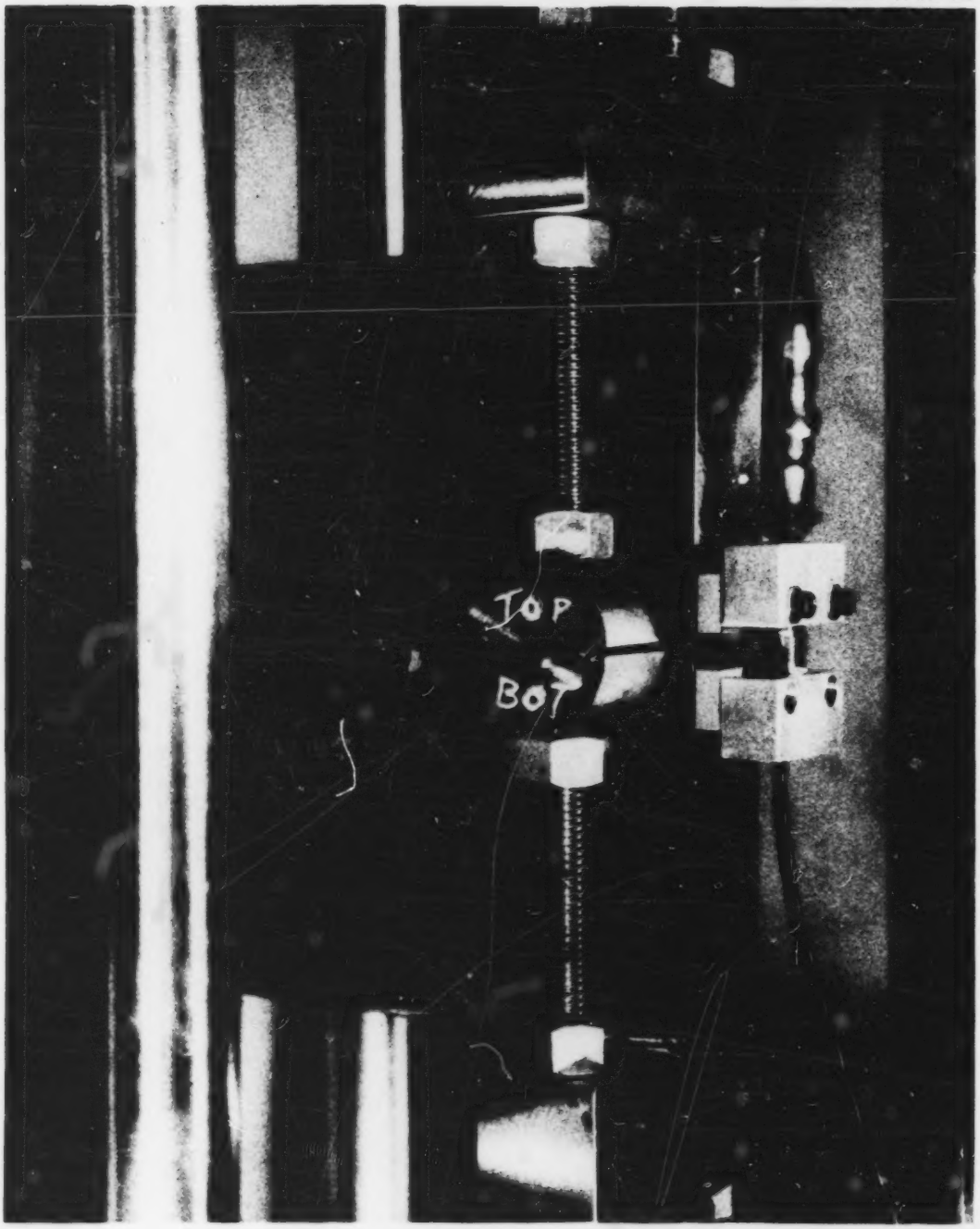

Fig. 2-8 Photograph of test set-up for measuring dependence of displacement at 0.25W (Δ) on opening load for BCL CCA specimen.

ORNL-PHOTO 4717-81

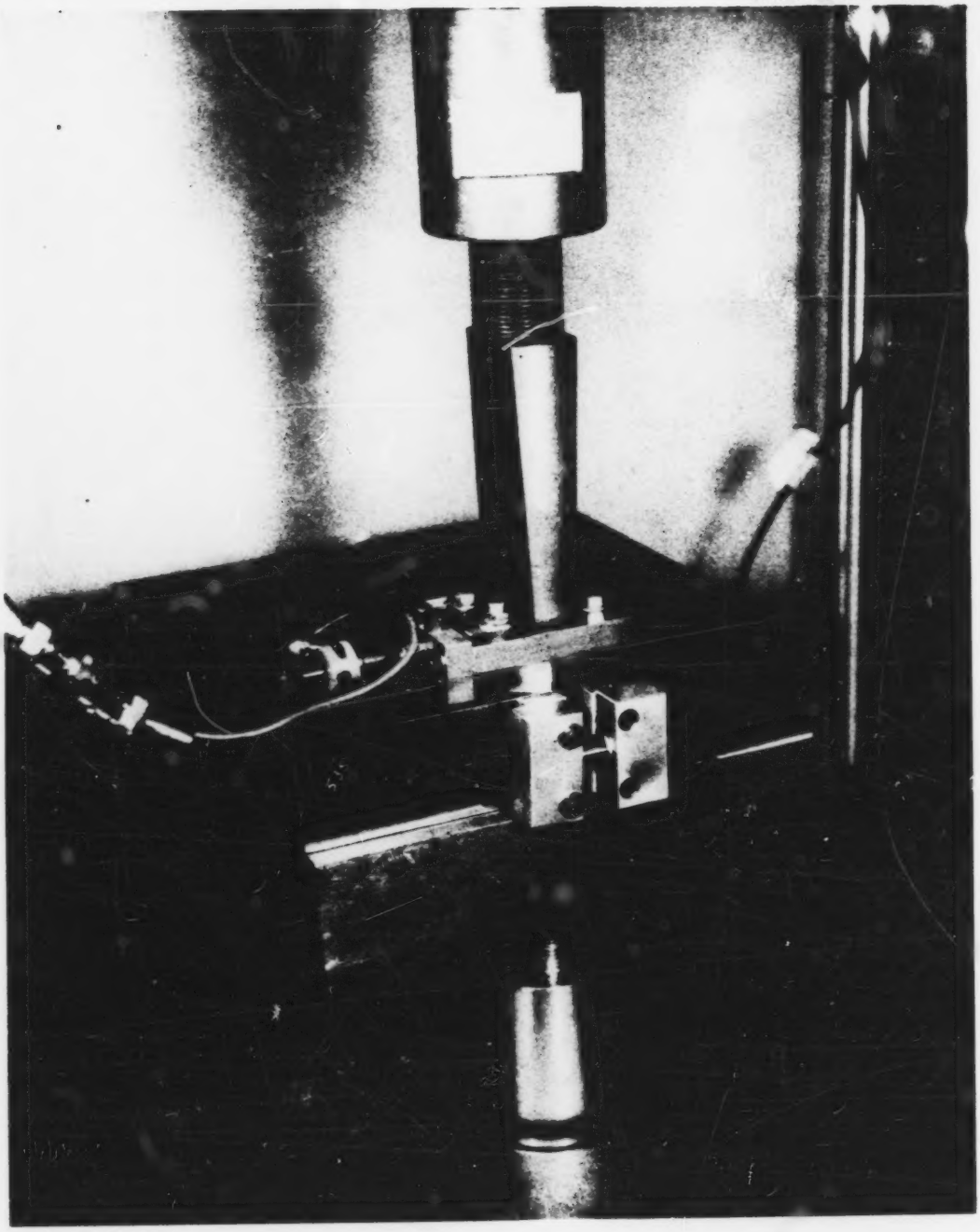

Fig. 2-9 Photograph of test set-up for measuring the relationship of two displacements, Δ and y.

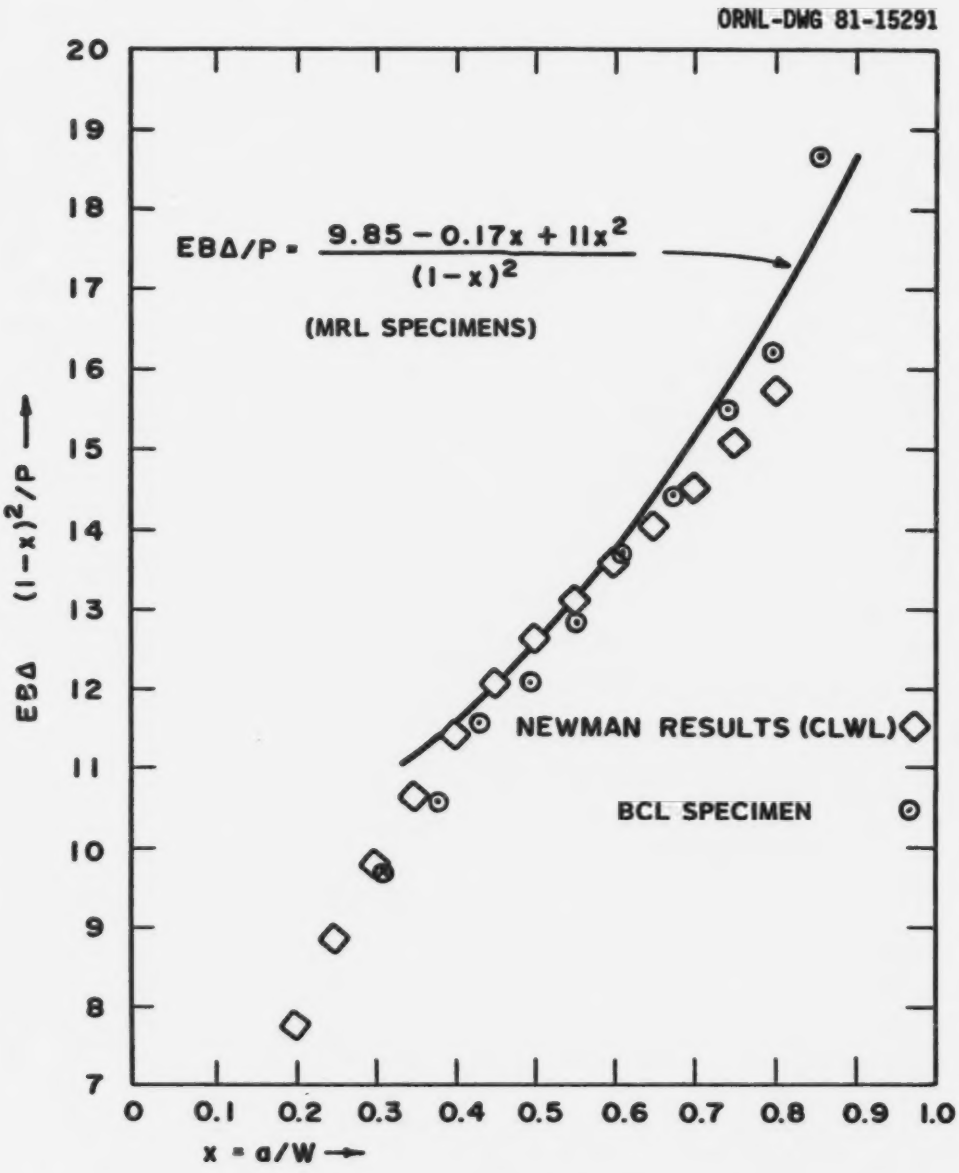

Fig. 2-10 Comparison of experimental compliance calibration of MRL and BCL compact crack arrest specimens and Newman results.

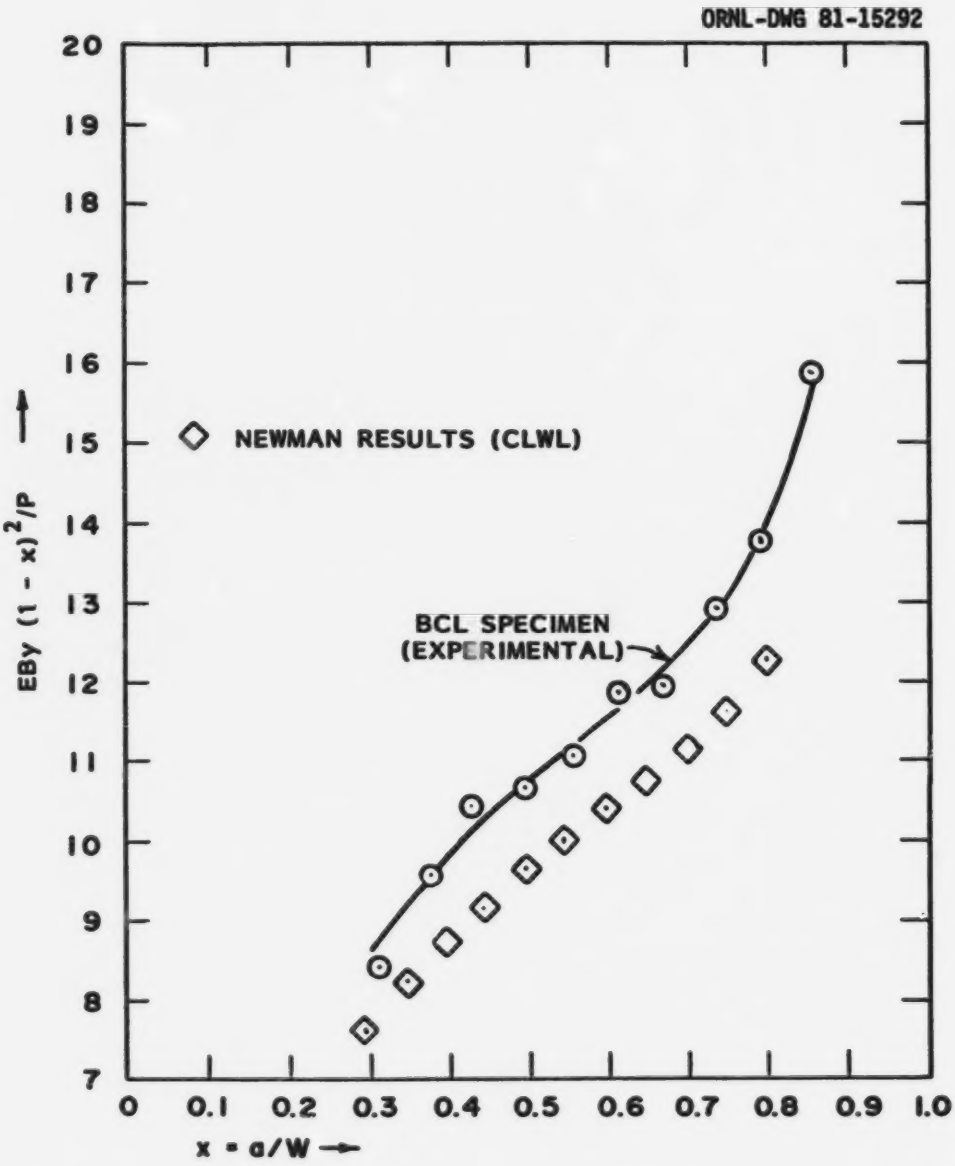

Fig. 2-11 Experimental compliance and Newman calculated values for BCL compact crack arrest specimen compared.

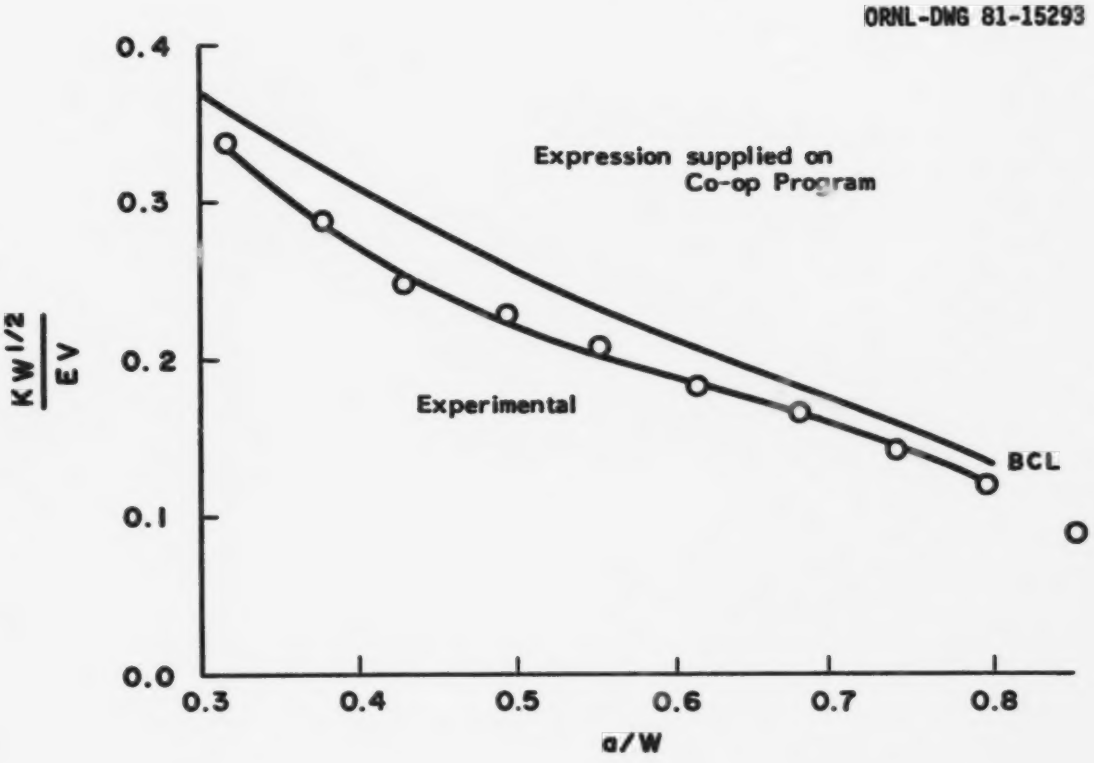

Fig. 2-12 Dimensionless stress intensity factor vs. dimensionless crack length for BCL compact crack arrest specimen.

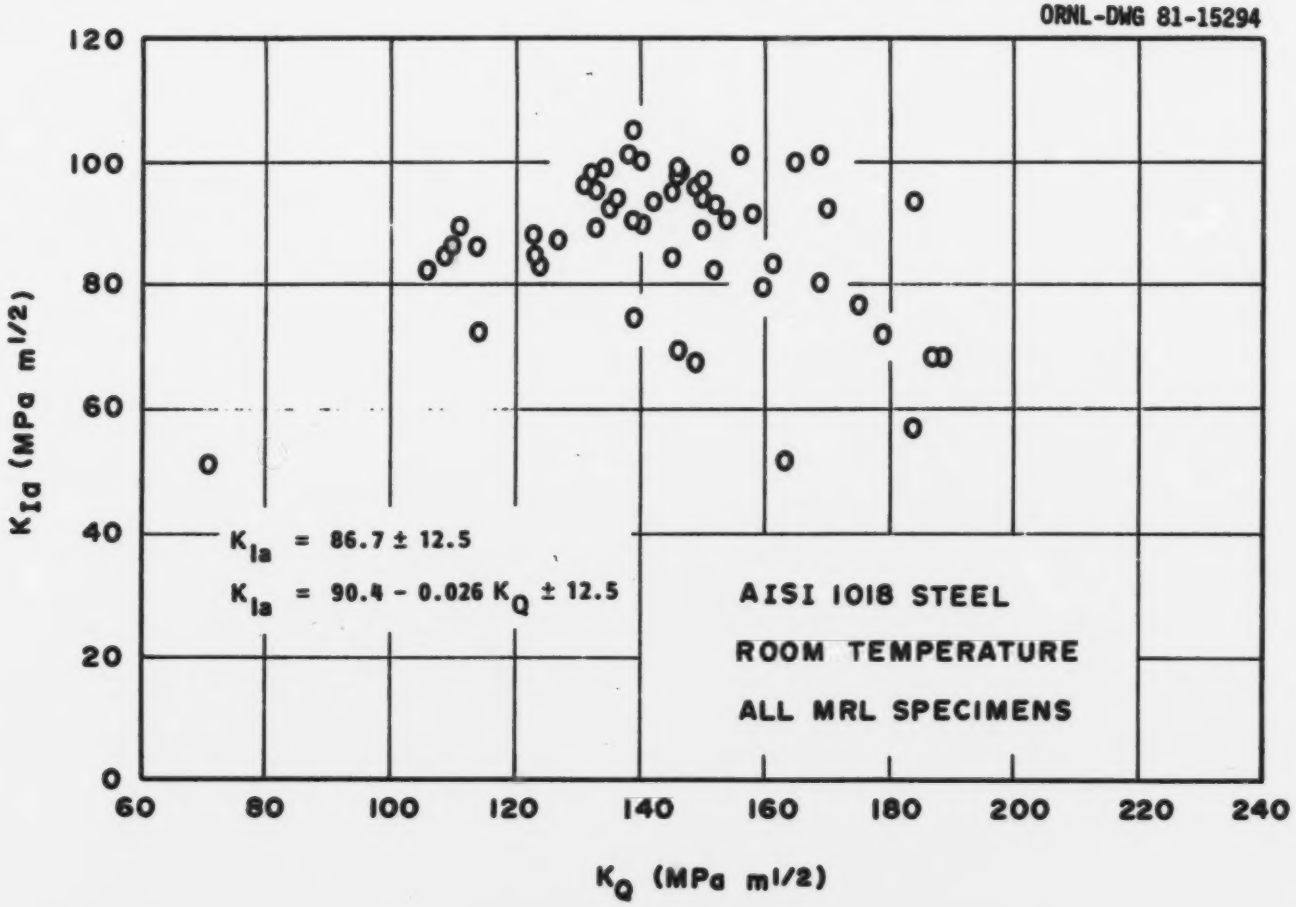

Fig. 2-13 Crack arrest toughness, K_{Ia}, plotted as a function of initiation toughness, K_Q. MRL specimens of AISI 1018 tested at room temperature.

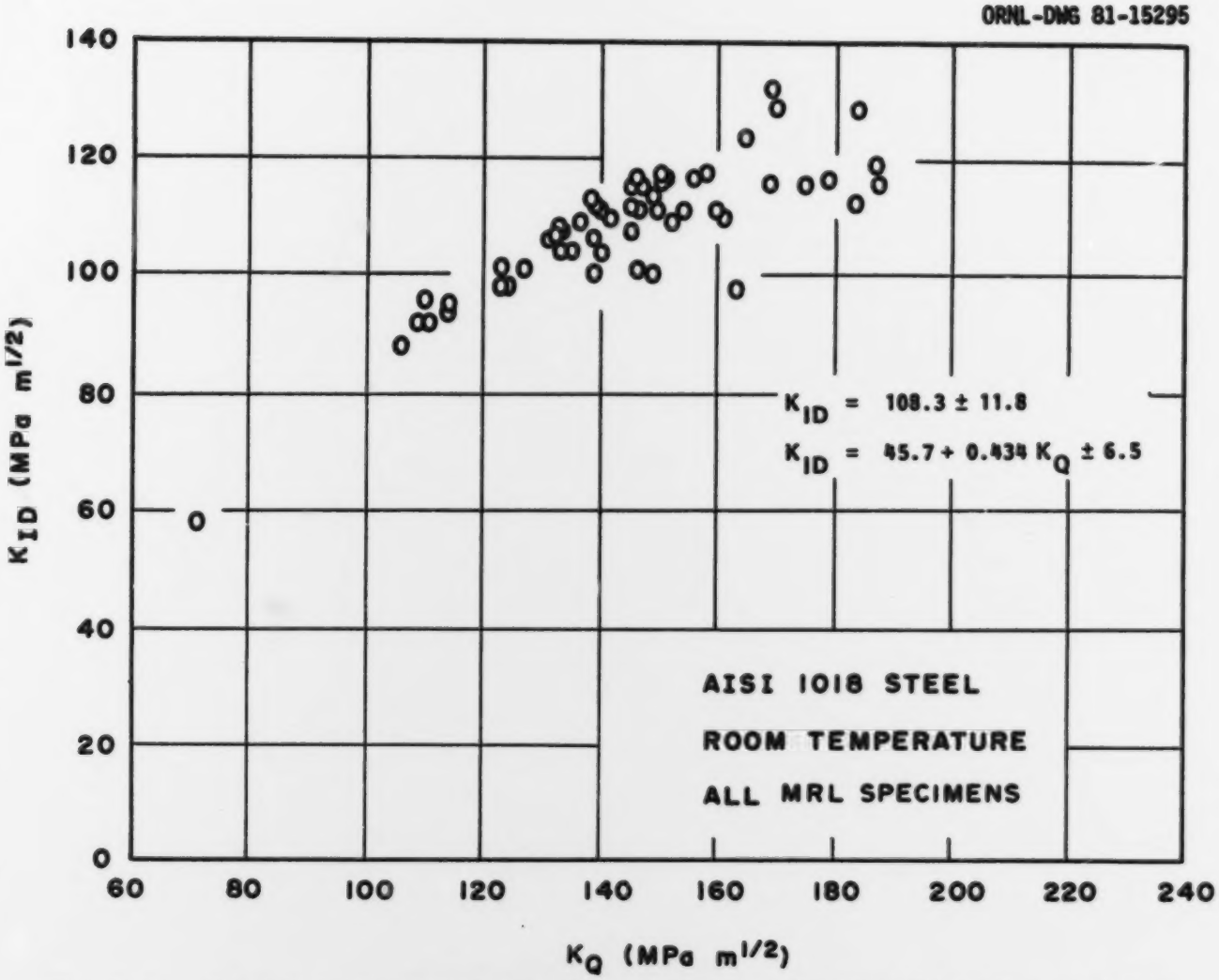

Fig. 2-14 Dynamic fracture toughness, K_{ID}, plotted as a function of initiation toughness, K_Q. MRL specimens of AISI 1018 steel tested at room temperature.

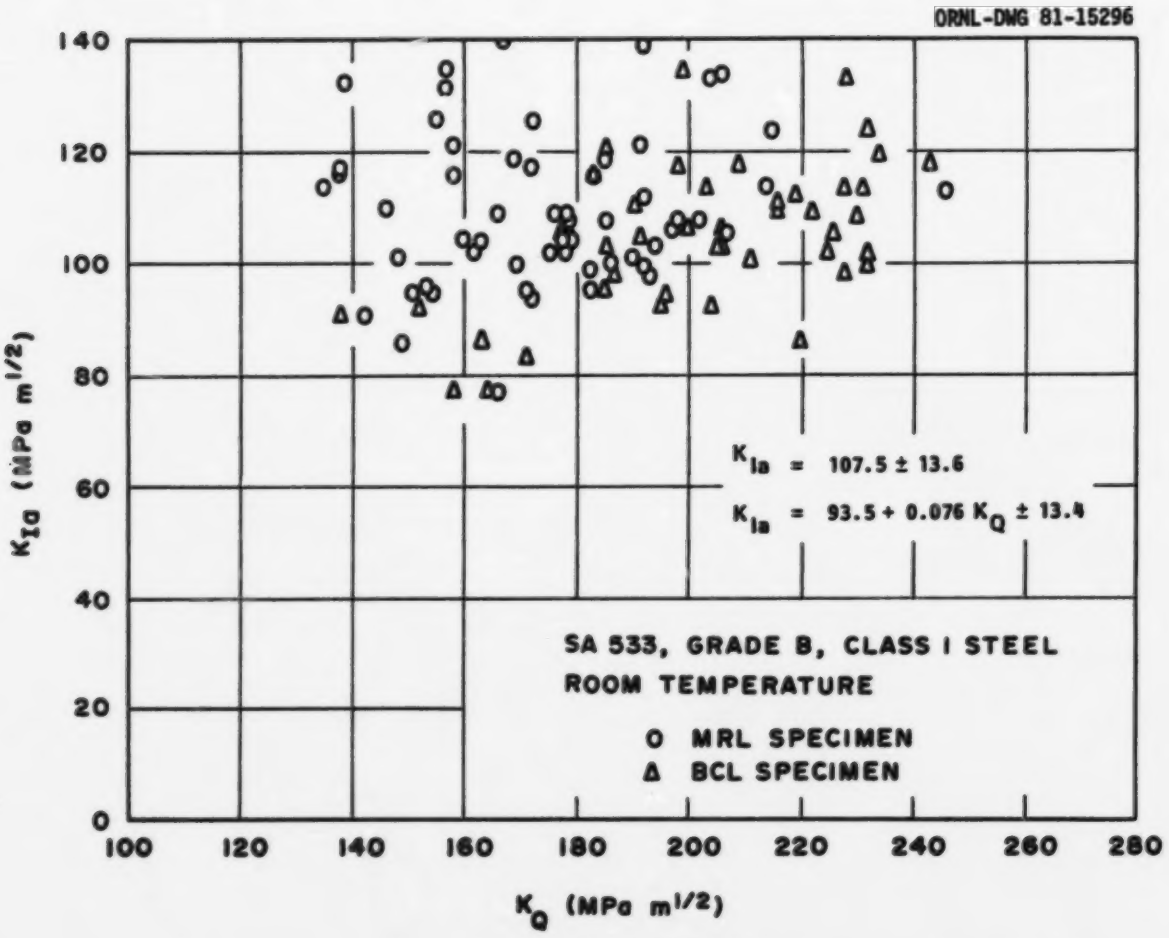

Fig. 2-15 Crack arrest toughness, K_{Ia}, plotted as a function of initiation toughness, K_Q. MRL and BCL specimens of SA533, Grade B, Class 1 steel tested at room temperature.

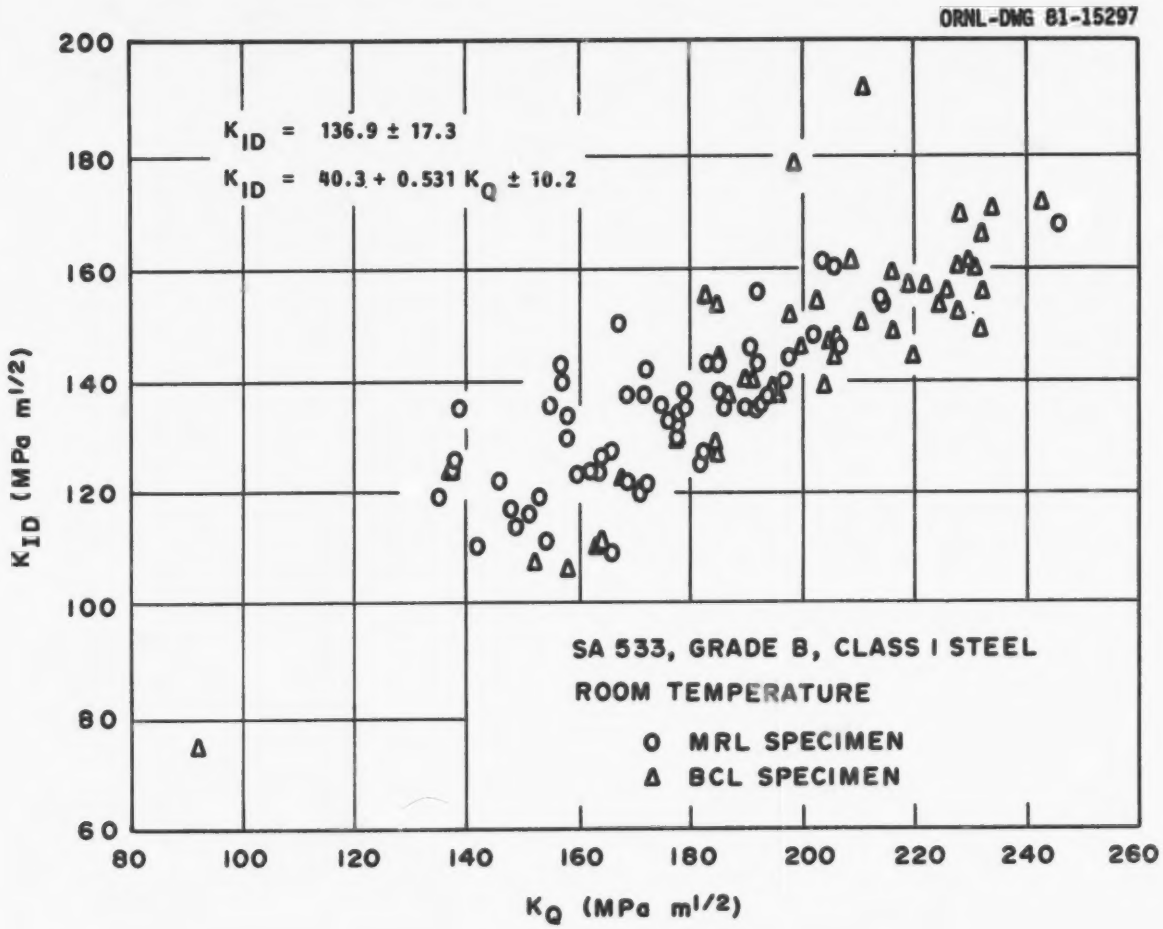

Fig. 2-16 Dynamic fracture toughness, K_{ID}, plotted as a function of initiation toughness, K_Q. MRL and BCL specimens of SA533, Grade B, Class 1 steel tested at room temperature.

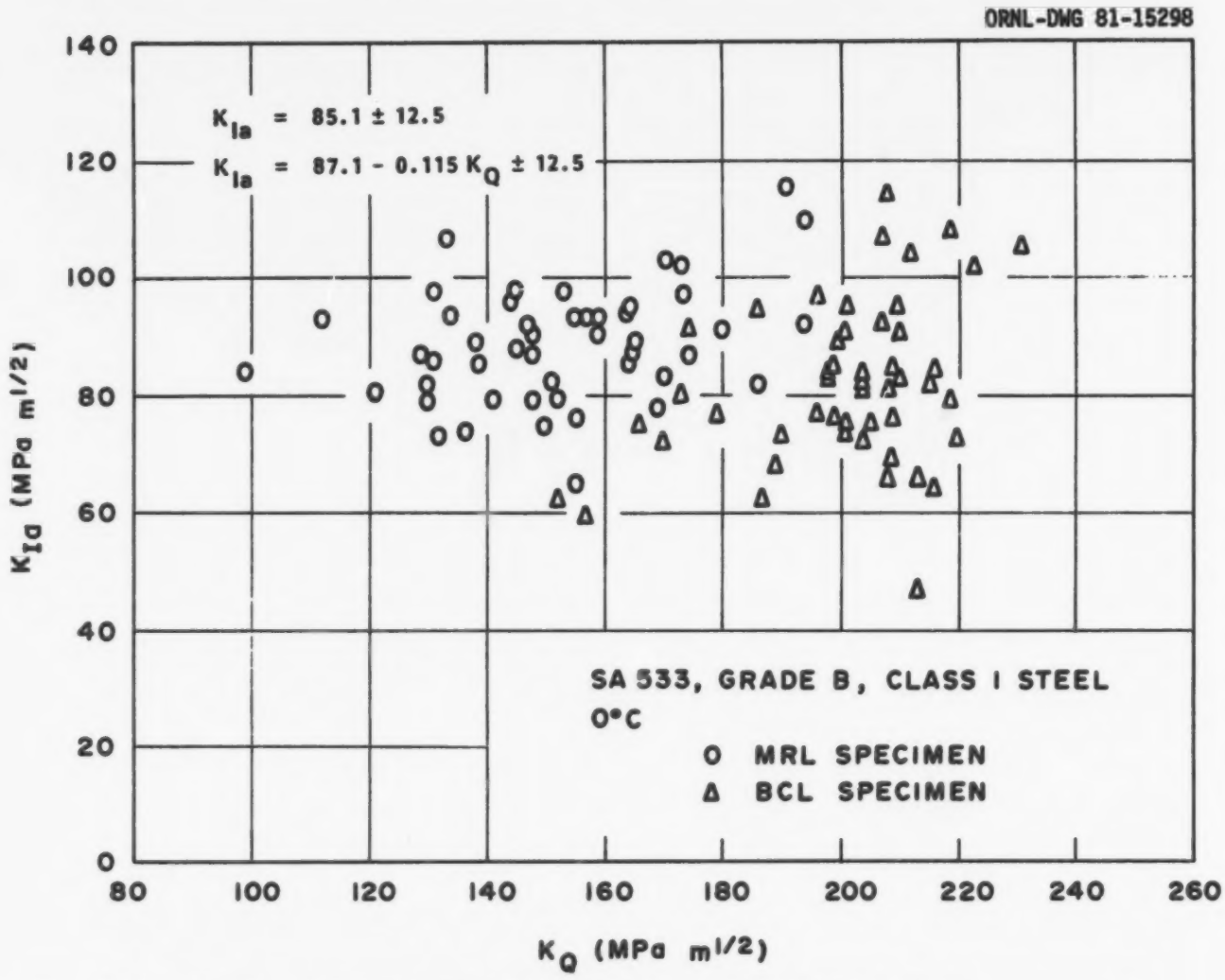

Fig. 2-17 Crack arrest toughness, K_{Ia}, plotted as a function of initiation toughness, K_Q. MRL and BCL specimens of SA533, Grade B, Class 1 steel tested at 0°C.

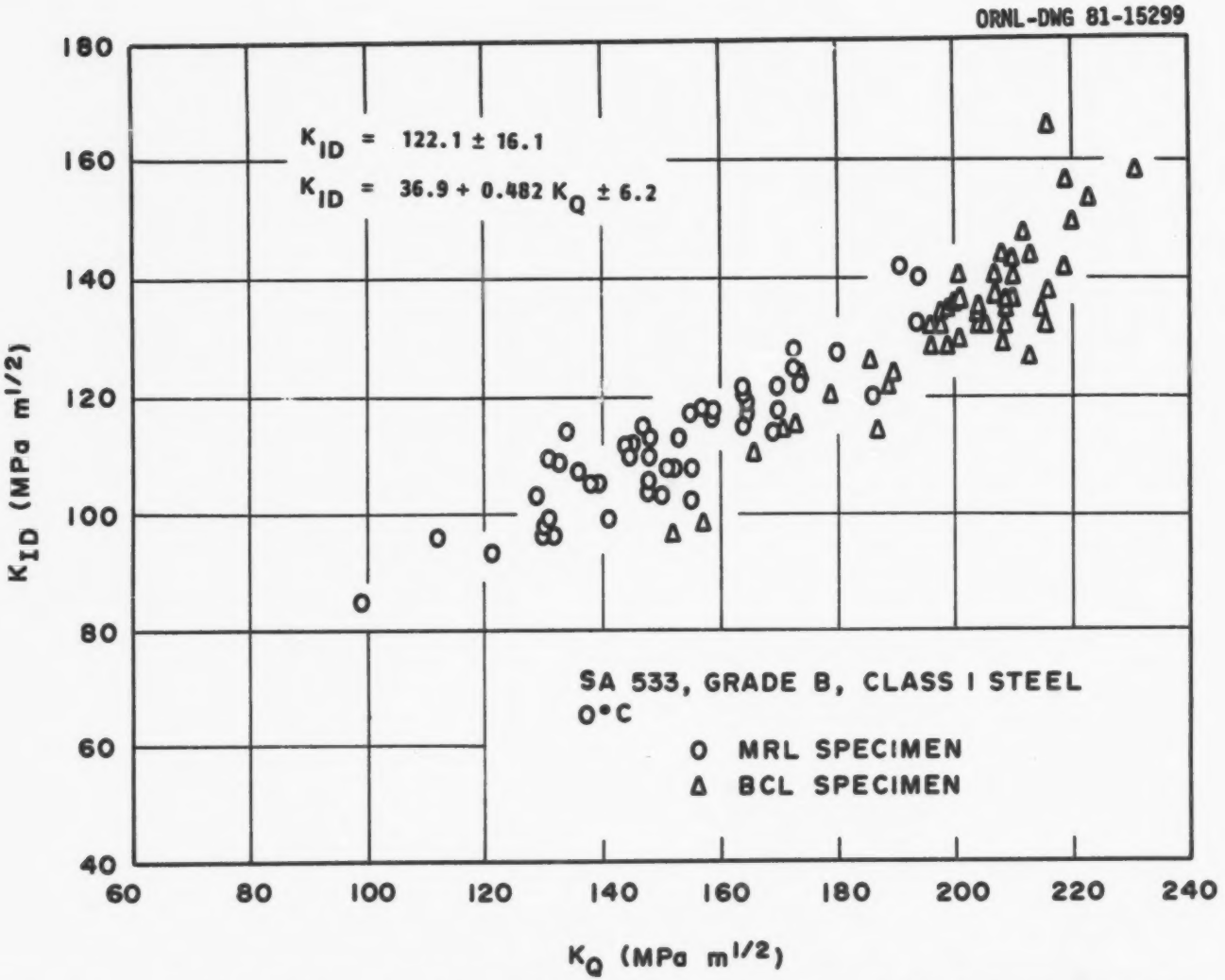

Fig. 2-18 Dynamic fracture toughness, K_{ID}, plotted as a function of initiation toughness, K_Q. MRL and BCL specimens of SA533, Grade B, Class 1 steel tested at 0°C.

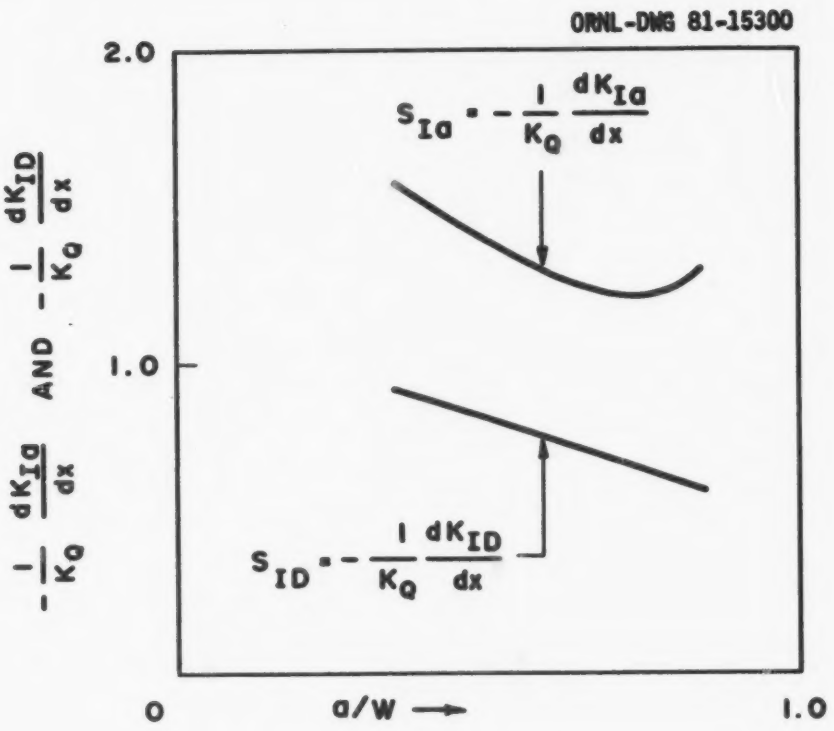

Fig. 2-19 Comparison of the fractional rate of change in K_{Ia} and K_{ID} produced by a change in final crack position, $x \triangleq a/W$.

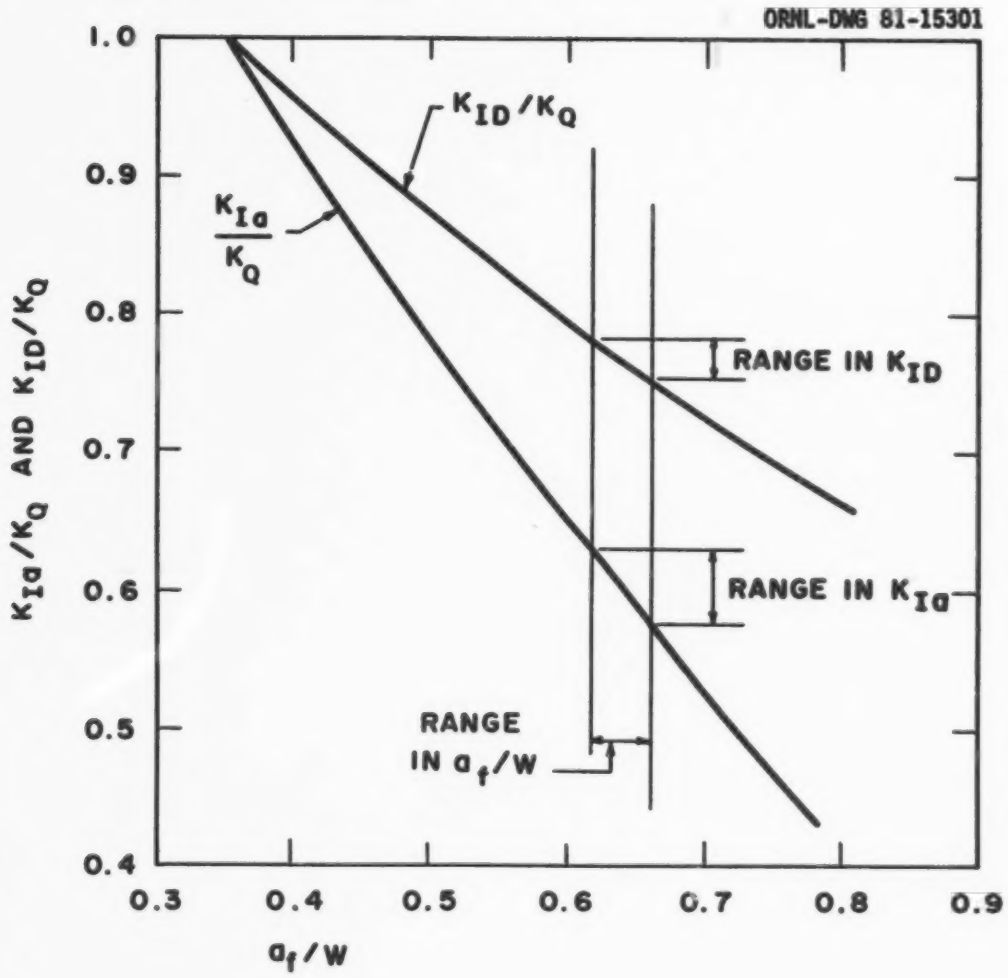

Fig. 2-20 Comparison of the variation in K_{Ia} and K_{ID} produced by same change in crack jump distance.

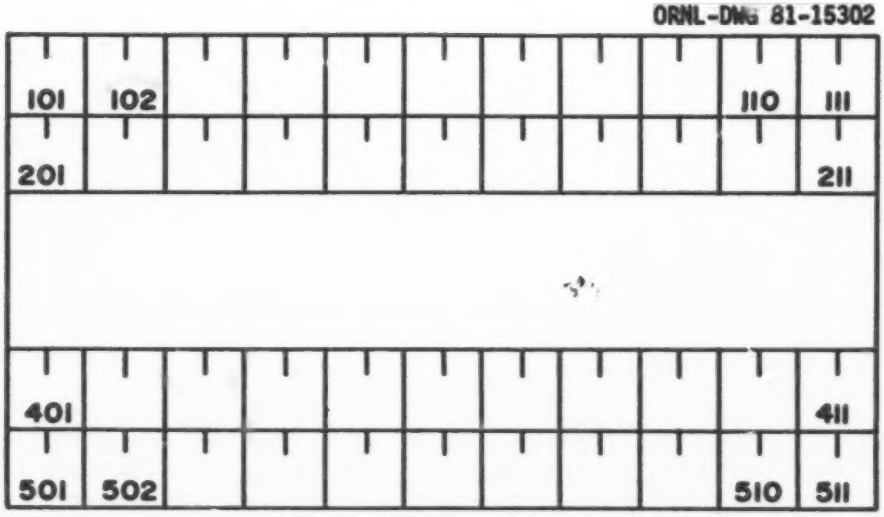

Fig. 2-21 Location of MRL specimens in parent plate.

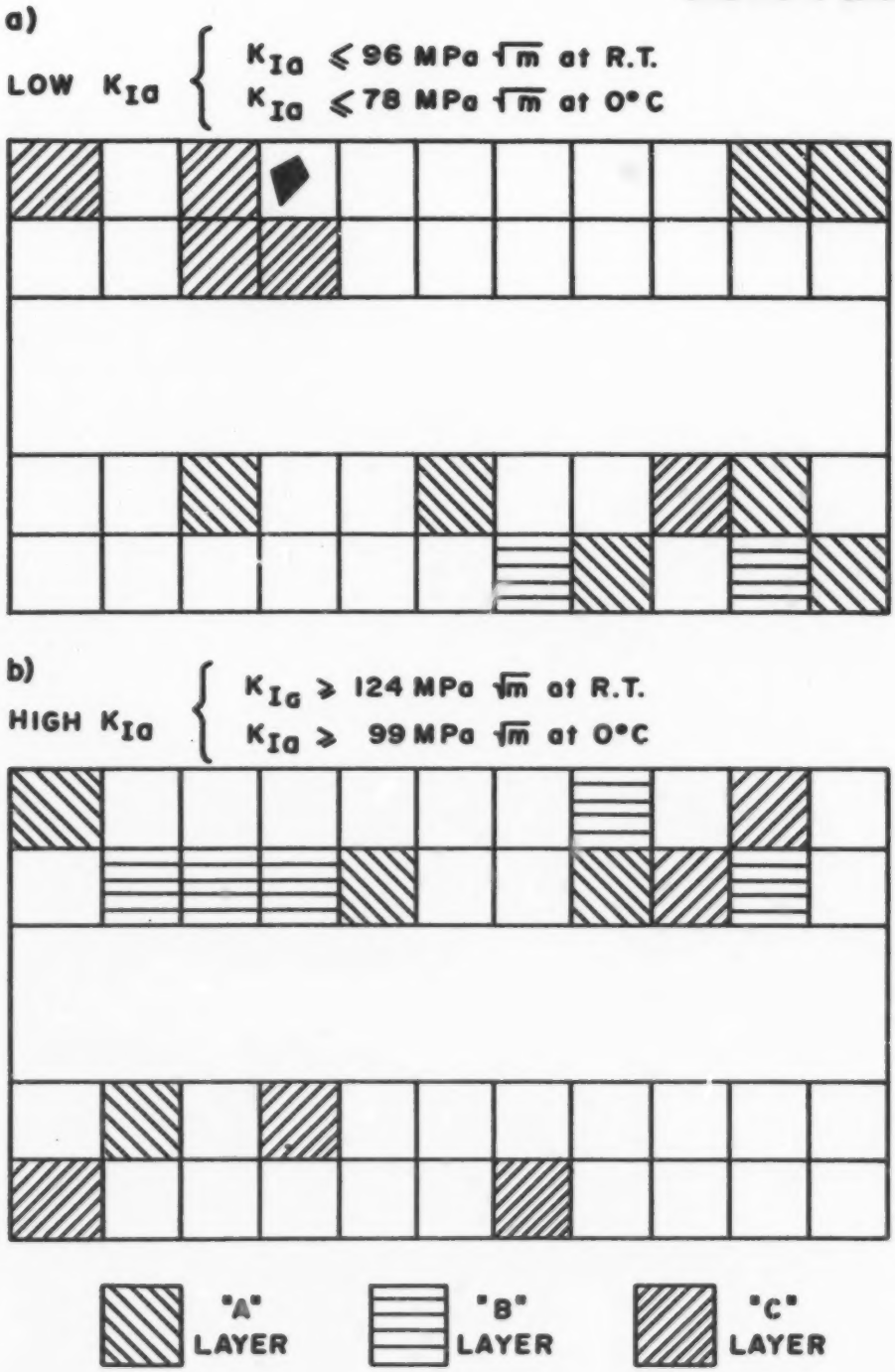

Fig. 2-22 Location of specimens which gave high or low values of K_{Ia} outside of standard deviation.

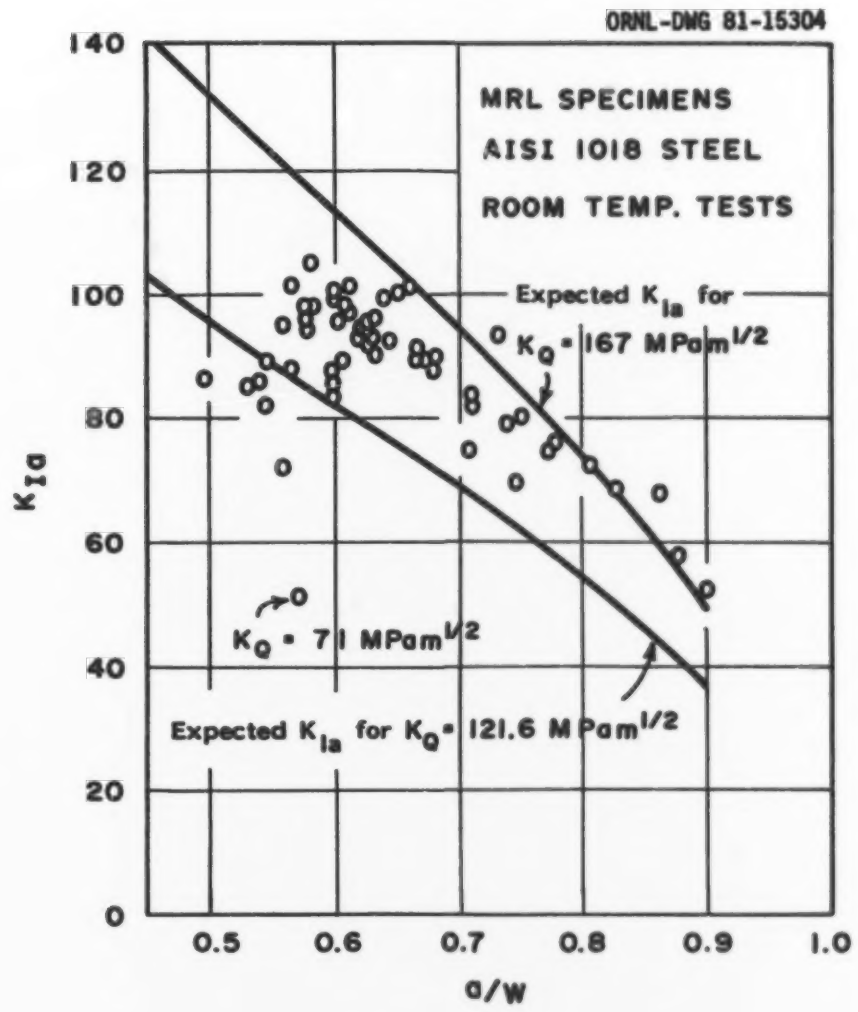

Fig. 2-23 Crack arrest toughness, K_{Ia}, plotted against arrested crack position, a/W, for MRL specimens of AISI 1018 steel tested at room temperature. Solid curves show expected dependence for values of K_Q one standard deviation above and below the average K_Q.

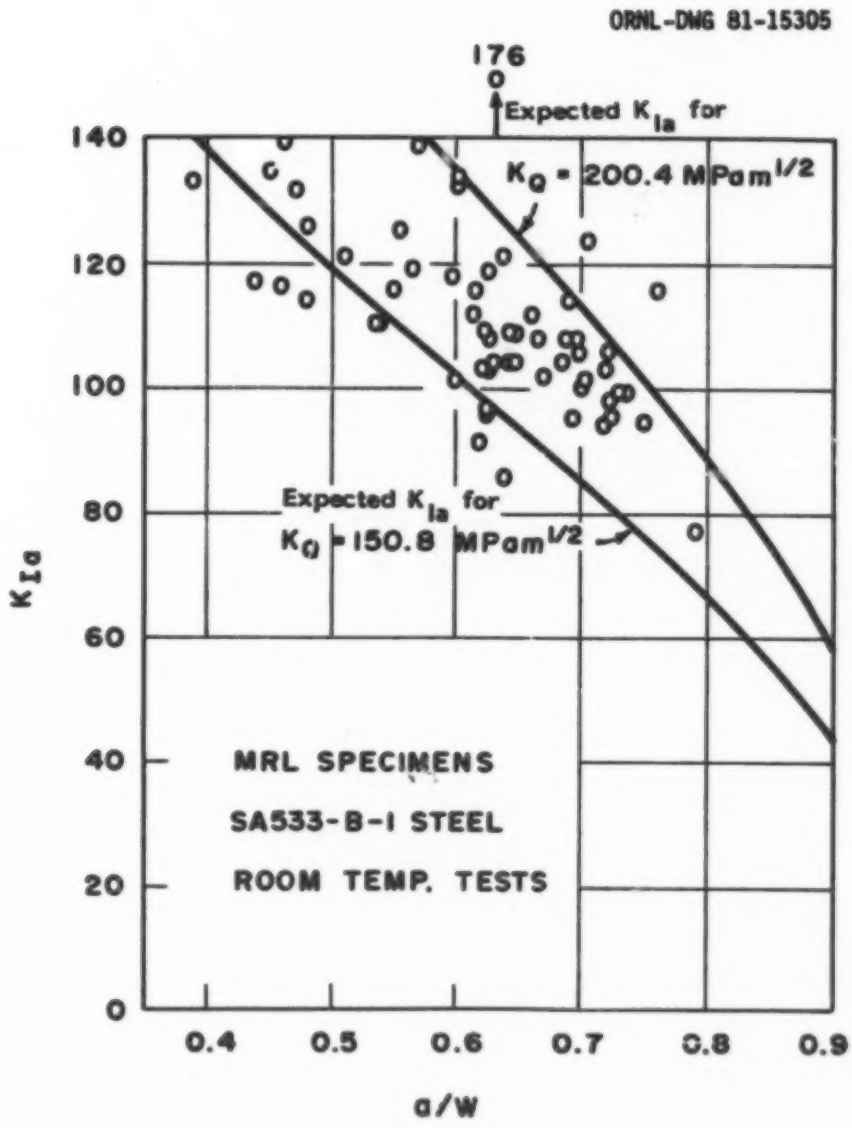

Fig. 2-24 Crack arrest toughness, K_{Ia}, plotted against arrested crack position, a/W, for MRL specimens of SA533, Grade B, Class 1 steel tested at room temperature. Solid curves show expected dependence for values of K_Q one standard deviation above and below the average K_Q.

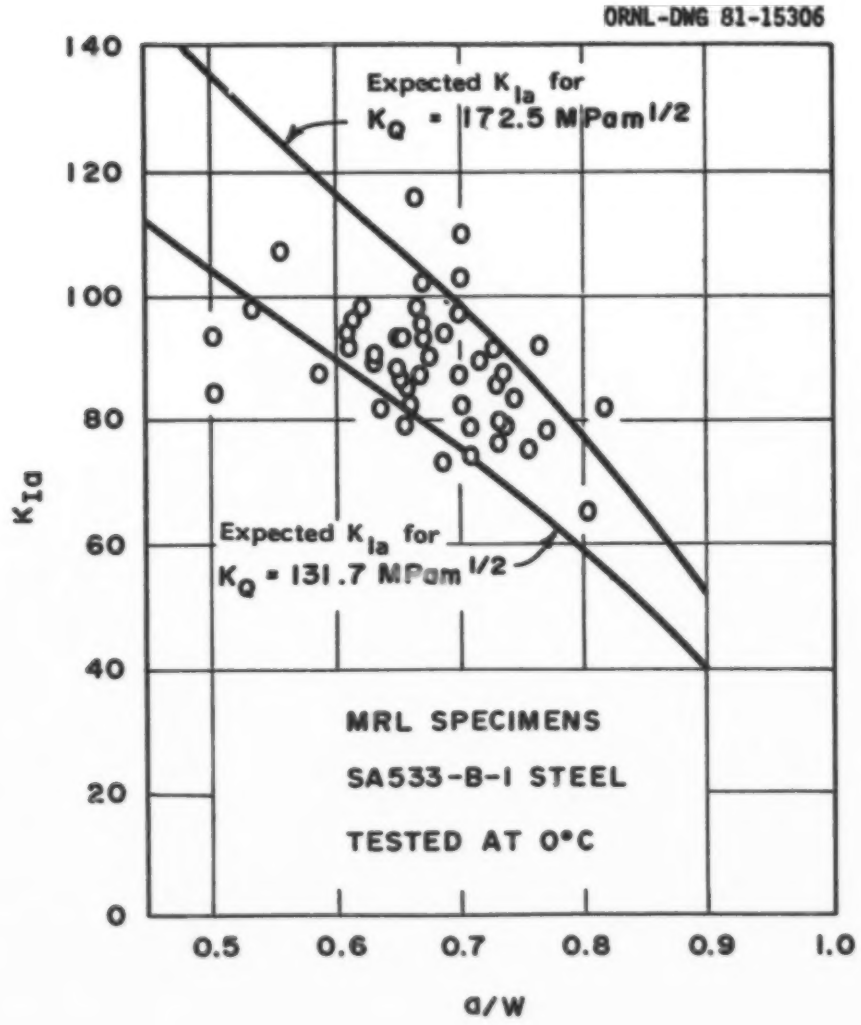

Fig. 2-25 Crack arrest toughness, K_{Ia}, plotted against arrested crack position, a/W, for MRL specimens of SA533, Grade B, Class 1 steel tested at 0°C. Solid curves show expected dependence for values of K_Q one standard deviation above and below the average K_Q.

3. Crack Arrest Toughness of Structural Steels

The Task Group appointed by ASTM to develop the crack arrest toughness test method proposed that the structural steels, A36 and A514, be tested in the Round Robin program in addition to the A533 Grade B, Class 1 steel, which was tested on the co-op program (see Section 4.1). This recommendation was made because one requirement for an ASTM test method is a definition of the type of materials to which the method is applicable. The two steels, A36 and A514, were selected because they have microstructures and strength levels that are different from A533B-1. Over the course of this contract period, A 36 was studied in some detail, while only a few tests were made on A514.

3.1 Test Program on A36 Steel

3.1.1 Purpose of Tests

The tests undertaken on the A36 steel were designed to answer three questions:

1. Is the K_{Ia} test applicable to this low strength pearlitic steel?

2. Does the crack arrest toughness of this steel scatter too much to use it in a Round Robin test program?

3. Can this steel be used to establish plane strain size requirements? Since A36 can be purchased in a range of thicknesses, it should be less expensive to use this steel for evaluating size requirements than A533B-1. (It was to save slabbing costs that AISI 1018 steel, rather than a pressure vessel steel, was used to develop the presently used K_{Ia} test.) Two thicknesses of A36 were used in the study: 50.8 mm (2 inch) and 25.4 (1 inch). The idea was to test these at the highest temperature at which a "pop" occurred. It was assumed that at this temperature the thinner plate would be tougher than the thick one. Tensile properties and K_a would then be measured at continuously lower temperatures until K_a was the same for the two plate thicknesses. The ratio of K_a to yield strength at this temperature might help in selecting the conditions that separate plane strain from mixed mode cracking.

3.1.2 Material Characterization

3.1.2.1 Specification Values

Two plates of steel, one 25.4 (1 in.) and the other 50.8 mm (2 in.) thick, both certified to be A36, were purchased from a local warehouse. The mechanical properties, chemical analyses supplied by the mill, and the ASTM specification for these values are shown in Table 3-I. Similar measurements were made at the quarter point of the plates, and these values are also given in the table.

3.1.2.2 DWT and CVN Tests

NDT was measured according to ASTM Test Method E208, and was found to be -7C (+20F) for both plates.

A relatively large number of CVN tests were made on the test plates to get some idea of the uniformity of its toughness, in order to anticipate the expected scatter in K_a*. The purchased plates were 2.44 x 0.46 m (8 x 1.5 ft.) and CVN specimens were cut from near the plate ends and center. The blanks for the thinner plates were taken at the two thickness quarter-points, which essentially evaluated the full plate thickness. For the thicker plate, both the quarter-points and center were used, in order to evaluate the full plate thickness. The thicker plate was tested only in the L-T direction, Fig. 3-1, while the thinner one was tested in both the L-T and T-L directions, Figs. 3-2 and 3-3.

In spite of the fact that the NDT temperatures for the two plates were the same, the CVN temperature curve for the thicker plate is shifted to a temperature about 20C (35F) higher than the curve for the thinner plate, when both were tested in the L-T direction.

The toughness scatter in the thicker plate also appears to be greater than that in the thinner one, and this was found to result from a

---

* The symbol K_a rather than K_{Ia} is used to represent crack arrest toughness throughout this report, unless the data is shown to be collected under conditions of plane strain.

systematic difference in toughness through the thickness of the 50.8 mm (2 in.) plate. The latter is shown by the data in Fig. 3-4, where CVN data collected on specimens cut near the plate surface and center are shown for three testing temperatures. At the two higher temperatures, where the toughness was high, specimens taken near the center of the plate were noticeably tougher than those taken near the surface. At the lower temperature, this difference was not as pronounced, probably because the CVN test is not sensitive to differences at these low levels of toughness. The occurrence of a tougher center than surface in a plate is unusual so that the chemical composition, tensile properties, and microstructure were also examined through the thickness. There was no systematic difference in C, Mn, Si, P or S as a function of position. There was a slight difference in yield strength, however, Table 3-II, but not in tensile strength nor ductility. The microstructure did vary with thickness, Fig. 3-5; the surface being finer grained than the center. The latter variation is not uncommon in plate, but this "normal" microstructure is not consistent with the "abnormal" toughness profile.

3.1.3 Test Procedure

Crack arrest fracture toughness tests were made by using the modified compact specimens shown in Fig. 3-6, and the test procedure described in reference (3-1). The compliance calibration given in this article was found to be incorrect so that a more recent, experimentally derived, K expression was used (See Section 2.1.2).

$$\frac{K\sqrt{W}}{E\Delta}\left(\frac{B_N}{B}\right)^{\frac{1}{2}} = \frac{2.2434\,(1.7164 - 0.9x + x^2)\sqrt{1-x}}{(9.85 - 0.17x + 11.0\,x^2)} \qquad (3\text{-}11)$$

where

- W = distance from center of loading hole to end of specimen
- E = Young's modulus
- Δ = displacement measured at 0.25W
- B_N = net specimen thickness on side-groove plane

B = gross specimen thickness

x = a/W

a = crack length

As stated earlier, one purpose of this study was to determine specimen size requirements for K_{Ia} testing. Two dimensions are critical for this purpose:

1. The uncracked ligament length (W - a), at the time of arrest, must be large compared with the crack tip plastic zone to preserve the applicability of linear elastic analysis.
2. The specimen must be sufficiently thick to develop a condition of plane strain at the moving crack tip.

3.1.4 Test Results

3.1.4.1 Tensile Tests

Tensile tests were conducted at 52C (125F) on the thicker plate, and at 20, -25 and -5C (70, -13 and -58F) for both plates on specimens cut from the quarter-plane in the L-T direction, and at the latter three temperatures for the thinner plate in the T-L direction. From the results shown in Fig. 3-7, it is apparent that although the tensile strength of the thicker plate is somewhat higher than that of the thinner one, in general the tensile properties of the two plates are similar.

3.1.4.2 Toughness Tests

Crack arrest fracture toughness tests were conducted on both plates with full thickness specimens from -50C (-58F) to room temperature, and at temperatures slightly above for the thick plate. The dependence of K_a on testing temperature for the latter is shown in Fig. 3-8. The toughness increased in a smooth, continuous fashion over the complete testing range, and over this range K_a increased by a factor of about three, which means that the critical flaw size increased almost ten fold.

(The dashed line on Fig. 3-8 corresponds to plasticity corrected K_a values which are discussed later.)

The maximum temperature at which K_a data could be collected was limited by the onset of ductile tearing. At temperatures about 60C (110F) or more above NDT, only ductile tearing occurred. Immediately below this temperature there was a range of about 15C (27F) over which some specimens cracked in cleavage and others by tearing, but in no case did a crack start in cleavage and arrest by tearing. Arrest occurred in these specimens, not because of a change in fracture mode, but because of a decrease in driving force, K.

One other feature of the fracture appearance of these specimens is worth noting: the arrested crack front was curved rather than straight, the crack length being longer near the plate surface than at its center, Fig. 3-9. It was shown earlier that the CVN impact energy was also lower near the plate surface than at the center (see Fig. 3-4) so that the crack front appearance shown in Fig. 3-9 must be a reflection of the toughness variation through the plate thickness.

The thinner plate, as shown in Fig. 3-10, acted much like the thicker one in that K_a again increased in a smooth continuous fashion over the testing range. The most noticeable difference in the two plates was that the thinner one cracked in cleavage only up to room temperature, while the thicker one continued to show cleavage to a considerably higher temperature. This dependence of the cleavage-tearing transition on plate thickness is consistent with observations made by Pellini, et al.[3-2], but the difference of 18C (32F) is larger than they would suggest for a 2:1 change in thickness.

Although there is some scatter in the data, the dependence of K_a on test temperature for the two test directions can be adequately represented by a single curve, suggesting that K_a is insensitive to crack direction.

3.1.5 Specimen Size Requirements

3.1.5.1 Thickness Requirements

When the toughness curves collected on the two plates are compared, it is seen that the data obtained on the thinner plate lies above that collected on the thicker one, and the distance between the two increases as the test temperature increases. This suggests, of course, that at the low temperatures where the curves are close together, both plates are under a condition of constraint that produces plane strain cracking, and as the temperature is increased, the constraint requirement became more and more violated, causing the two curves to separate. To eliminate the possibility that the difference between the two curves is strictly a material difference, rather than caused by a thickness difference, tests were made on 25.4 mm (1 in.) thick specimens cut from the 50.8 mm (2 in.) plate. Since the CVN data indicated that the plate was tougher near the surface than near the center, the specimens were cut from both of these locations, Fig. 3-11. At room temperature, at least, the center specimen data fell close to the curve obtained on the thinner plate while the thinner near-surface specimen data fell closer to the curve obtained on the thicker plate. Nevertheless, since the average of the center and surface data for the thinner specimens lies above the thick specimen data, it must be concluded that the thin specimen data, at least, did not represent plane strain values. At the two lower test temperatures, where the center specimen data lie above the thin plate data, plane strain cracking may be occurring.

In order to define thickness requirements, it is convenient to introduce a dimensionless parameter

$$\beta = \frac{1}{B}\left(\frac{K}{\sigma_{ys}}\right)^2 \qquad (3\text{-}2)$$

For evaluating the plane strain crack initiation toughness, K_{Ic}, according to ASTM Standard Test Method E-399, it is necessary that $\beta \leq 0.4$. The size requirements for K_{Ia} testing are expected to be less severe than they are for K_{Ic} testing. The reason for this is apparent from Eq. (3-2). For

K_{Ic} testing, σ_{ys} is the static yield strength; for K_{Ia} testing, σ_{ys} is the dynamic yield strength at the crack tip produced by the running crack as it decelerates toward zero velocity. Obviously, for rate sensitive materials, the latter will be higher than the former.

An estimate of β for plane strain crack arrest toughness testing can be made by using the specimen data collected to evaluate K_{Ia} for thick-walled, thermal shock tests. The cracks in these specimens are assumed to have extended in plane strain since the small specimen data were able to define the behavior of the thick-walled large structure. The specimens used in these tests were 50.8 mm (2 in.) thick, and the metal had a static yield strength of 475 MPa (69 ksi) and a K_{Ia} value of 107 MPa-$m^{\frac{1}{2}}$ (96 ksi-$in^{\frac{1}{2}}$).

If the static yield strength were used for calculating β for these tests, it would have a value $\beta_s = 1$. Using the static value is probably not reasonable, however, because the relative increase in flow stress would be higher for a soft steel than for a hard one. A more realistic way for estimating β for an arresting crack would be to use an "effective yield strength", σ_e, which accounts for the elevation of yield stress associated with the decelerating crack. There appears to be no completely satisfactory way for doing this, however. Irwin[3-3] suggested that the yield strength of the running crack might be equivalent to the yield strength for a one millisecond loading time. Assuming that the yield strength is elevated 40 MPa (6 ksi) per order of loading rate, then five orders of loading rate would elevate the static yield strength by 200 MPa (30 ksi), making $\beta_a \leq 0.5$. Hence, if $\beta = 0.5$, the measured value of crack arrest toughness can be designated K_{Ia}. Of course, it may be that a plane strain condition is attained with even higher values of β. Some light might be shed on this by examining the data in Fig. 3-11. At room temperature, the thinner specimens did not crack in plane strain, and the average yield strength, given by the open and closed circles, is approximately 260 MPa (38 ksi). Elevating this for the running crack gives a value of 460 MPa (67 ksi), making $\beta_a = 4.4$ for the thinner plate. Hence, the limiting value of β_a for plane strain cracking

is between 0.5 and 4.0. Tests by Mager and Marschall[3-5] on A533, Class 1 steel suggest that β_a may be as high as one for plane strain cracking.

3.1.5.2 In-Plane Dimension Requirements

In addition to the requirement for sufficient thickness to encourage plane strain cracking, the specimen crack tip stresses should not be influenced by the boundaries of the specimen. Hence, the smallest in-plane dimension, the uncracked ligament length $(W - a_f)$, must be large compared with the plastic zone size (r_y). The latter can be calculated for the limiting cases of plane stress and plane strain:

$$r_y \text{ (plane stress)} = \frac{1}{2\pi}\left(\frac{K_a}{\sigma_e}\right)^2$$

$$r_y \text{ (plane strain)} = \frac{1}{2\pi}\left(\frac{K_a}{\sqrt{3}\,\sigma_e}\right)^2 \qquad (3\text{-}3)$$

where again σ_e is chosen as the value equivalent to a one millisecond loading time. Using this value of elevated yield strength, the ratio of uncracked ligament length $(W - a_f)$ to plastic zone size is shown in Fig. 3-12.

The minimum acceptable ratio of $(W - a_f)$ to r_y can only be established on the basis of extensive testing. In assessing the results obtained here, however, the requirement given in ASTM Standard E561[3-4], may be consulted. This requirement is: $(W - a) \geq 4/\pi\,(K/\sigma_{ys})^2$, which is equivalent to remaining ligament being at least equal to four plane stress plastic zones. As can be seen in Fig. 3-12, this condition was satisfied by most of the tests on the A36 steel. If the idea of four plastic zone sizes is retained while the plane strain rather than plane stress plastic zone is considered appropriate, all of the values satisfy the requirement.

A plasticity correction is commonly made by adding an amount r_y to the measured crack length. In the more usual case when K is calculated from a load, the K thus modified exceeds the uncorrected one. The K_a

calculation, however, is based on a displacement measurement, and the plasticity correction lowers the value of K_a. The data collected on A36 steel were not corrected for plasticity, but the effect of an r_y correction was investigated. The dashed curve in Fig. 3-8 shows the effect of making a crack length correction equal to the plane stress r_y value. At the higher temperatures where increased toughness and decreased yield strength lead to large crack tip plastic zones, an effect is noticeable. The magnitude of the lowering of K_a is, however, not significant in terms of the expected scatter in K_a measurements or with respect to conclusions which can be based on the results presented here. Moreover, a substantially smaller correction based on a plane strain rather than a plane stress r_y would probably be more appropriate for these tests. Consequently, K_a values based on the measured crack length without a plasticity correction have been used in this paper.

3.1.6 Conclusions Regarding the Use of A36 in the Round Robin Program

1. The test method developed for measuring K_{Ia} of reactor pressure vessel steels is satisfactory for A36 steel as well.

2. The scatter of crack arrest toughness in A36 is not so large as to prohibit its use in a Round Robin program. Indeed, the largest toughness variation appears to be through the plate thickness. This toughness variation shows itself in the shape of an arrested crack front.

3. A rigorous definition of thickness requirements for plane strain cracking has not as yet been developed, but it appears that a value of $\beta_a = (1/B)(K_{Ic}/\sigma_{ys})^2 = 1$ may be satisfactory if the one m-sec. loading time yield strength is used.

3.2 Test Program on A514 Steel

Far less testing was done on this steel than on the A36 steel. Again, two certified plates, one 25.4 mm (1 in.) and the other 50.8 mm (2 in.) thick were purchased from a local warehouse. The tensile properties and chemical composition supplied by the mill and the ASTM specification for these values are shown in Tables 3-III and 3-IV. Tensile properties were measured on the purchased plates, and these values are also added to Table 3-III.

Charpy V-notch tests were made on the plates, as a function of test temperature, Fig. 3-13. This martensitic steel is obviously tougher than the pearlitic A36 steel in spite of the fact that it is also stronger. Toughness tests were made at -60C (-75F), and K_a was found to be 103 and 134 MPa-m$^{\frac{1}{2}}$ (93 and 120 ksi-in$^{\frac{1}{2}}$) for the thinner and thicker plates, respectively. At 0C (32F) popping did not occur, so that crack arrest toughness could not be measured.

3.3 Use of Structural Steels in the Round Robin Program

The test results described above indicate that both A36 and A514 steels can be used in the Round Robin test program. The A514 has such a low transition temperature, however, that it would have to be tested at a very low temperature, e.g., -60C (-75F). The A36 could be satisfactorily tested in the vicinity of room temperature, particularly if a 50.8 mm (2 inch) plate were used. If it is necessary to assure plane strain cracking, a sub-ambient temperature may be required.

REFERENCES

3-1. P. B. Crosley and E. J. Ripling, "A Compact Specimen for Plane Strain Crack Arrest Toughness Testing, Jour. Testing and Evaluation, Vol. 8, No. 1, ASTM, 1980.

3-2. W. S. Pellini, "Principles of Structural Integrity Technology," Off. Nav. Research. Available through the U. S. Dept. of Commerce, National Technical Information Service, 5285 Port Royal Road, Springfield, VA 22161.

3-3. G. R. Irwin, private communication.

3-4. ASTM E561-78T, "Tentative Recommended Practice for R-Curve Determination," 1979 Annual Book of ASTM Standards, Part 10.

3-5. T. R. Mager and C. W. Marschall, "Development of a Crack Arrest Toughness Data Bank for Irradiated RPV Materials (EPRI RP 1326-1) March 1980.

Table 3-I

MECHANICAL PROPERTIES AND CHEMICAL ANALYSIS OF A36 STEEL

Plate Thickness mm	Plate Thickness (in.)	Yield Point MPa	Yield Point (ksi)	Tensile Strength MPa	Tensile Strength (ksi)	Elongation in 200 mm percent	Elongation in 50 mm percent	C percent	Mn percent	P percent	S percent	Si percent
						Supplied by Mill						
25.4	(1)	283	(41.1)	486	(70.5)	27	--	0.24	1.07	0.010	0.029	--
50.8	(2)	270	(39.1)	498	(72.2)	27	--	0.21	0.99	0.020	0.025	0.212
						ASTM Requirements						
25.4	(1)	250 min.	(36)	400-550	(58-80)	20	23	0.25 max.	0.80-1.20	0.04 max.	0.05 max.	--
50.8	(2)	250 min.	(36)	400-500	(58-80)	20	23	0.26 max.	0.80-1.20	0.04 max.	0.05 max.	0.15-0.40
						Measured on Plate						
25.4	(1)	243	(35.3)	465	(67.5)	--	31.6	0.23	1.06	0.011	0.021	< 0.05
50.8	(2)	251	(36.4)	498	(72.3)	--	32.2	0.24	0.95	0.016	0.026	0.21

Table 3-II

THROUGH THE THICKNESS TENSILE PROPERTIES OF 50.8 mm A36 PLATE

Specimen No.	Location	Yield Strength MPa	Yield Strength (ksi)	Tensile Strength MPa	Tensile Strength (ksi)	Elongation %	RofA %
A60	Surface	265	(38.4)	496	(71.9)	33.6	64.4
A61	Surface	264	(38.3)	492	(71.4)	31.8	66.4
	Avg.	265	(38.4)	494	(71.6)	32.7	65.4
A62	¼ plane	252	(36.6)	512	(74.3)	31.4	66.3
A63	¼ plane	253	(36.7)	508	(73.7)	32.9	65.7
T7	¼ plane	255	(37.0)	492	(71.4)	32.9	65.3
T8	¼ plane	240	(34.8)	472	(68.5)	33.6	64.7
T9	¼ plane	252	(36.5)	490	(71.1)	30.0	66.6
	Avg.	250	(36.3)	495	(71.8)	32.2	65.7
A64	Center	250	(36.3)	505	(73.2)	32.1	62.9
A65	Center	245	(35.5)	503	(73.0)	32.1	66.6
	Avg.	248	(36.0)	504	(73.1)	32.1	64.8

Materials Research Laboratory, Inc.

Table 3-III

MECHANICAL PROPERTIES OF ASTM A514, GRADE B AND H

Plate Thickness		Tensile Strength		Yield Strength		Elongation in 2 in.	Reduction in Area
mm	(in.)	MPa	(ksi)	MPa	(ksi)	Percent	Percent
			Supplied by Mill				
25.4	(1)	820	(119)	738	(107)	20	63
50.8	(2)	820	(119)	738	(107)	20	63
			ASTM Requirements				
25.4-50.8	(1-2)	760-895	(110-130)	690 min.	(100)	18 min	50 min.
			Measured on Plate				
25.4	(1)	820	(119)	745	(108)	17	56
50.8	(2)	772	(112)	683	(99)	20	66

Table 3-IV

CHEMICAL ANALYSIS OF ASTM A514

Plate Thickness mm	(in.)	Grade	C %	Mn %	P %	S %	Ti %	Si %	Ni %	Cr %	Mo %	V %	B %
						Supplied by Mill							
25.4	(1)	B	.20	.95	.010	.014	.020	.31	--	.58	.20	.060	.0008
50.8	(2)	H	.17	1.22	.013	.015	--	.30	.49	.52	.24	.070	.0012
						ASTM Requirement							
25.4	(1)	B	.12-.21	.070-1.00	.035 max	.04 max	.01-.03	.20-.35	--	.40-.65	.15-.25	.03-.08	.0005-.005
50.8	(2)	H	.12-21	.95-1.30	.035 max.	.04 max.	--	.20-.35	.30-.70	.40-.65	.20-.30	.03-.08	.0005-.005

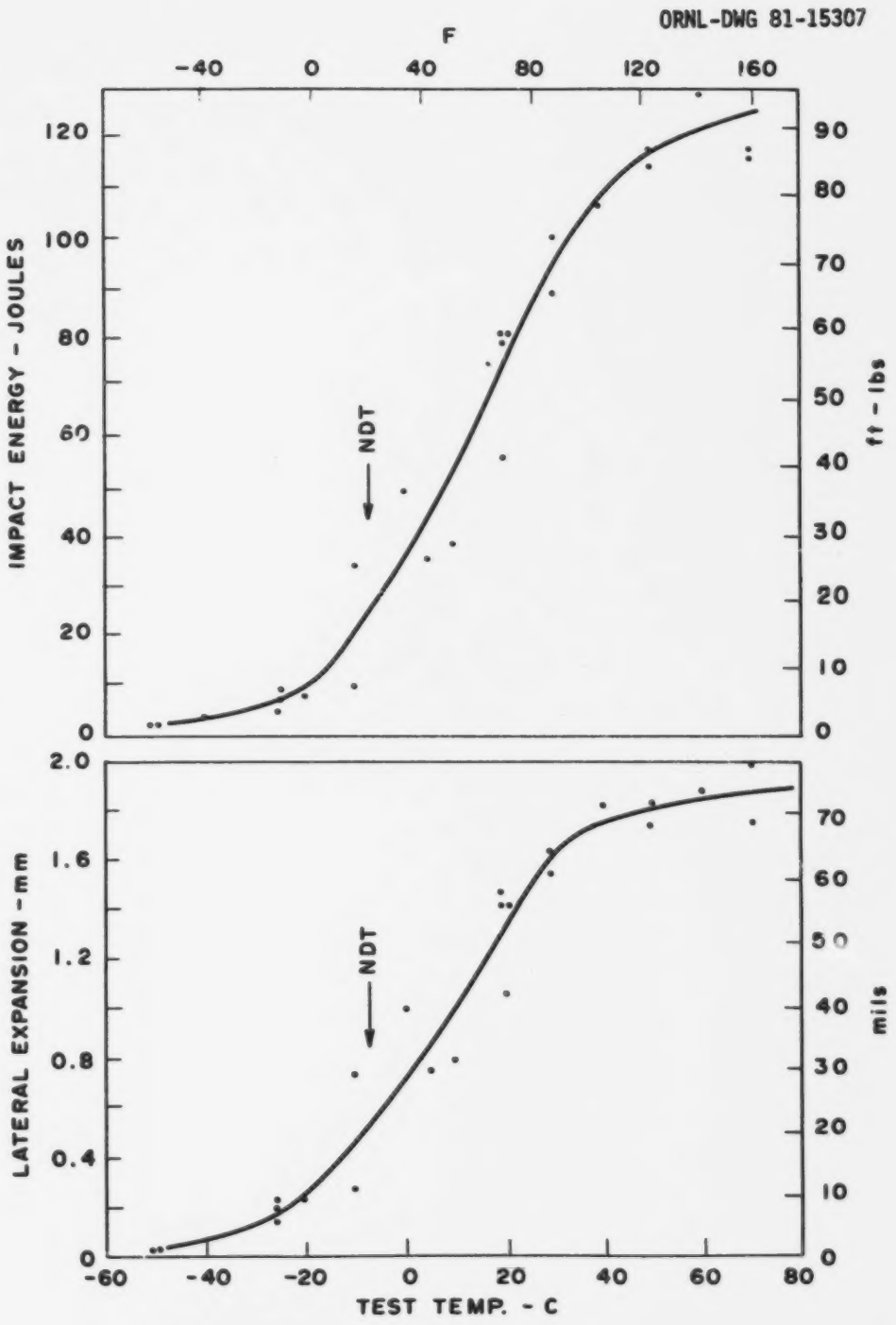

Fig. 3-1 CVN Impact and Lateral Expansion as a function of testing temperature for A36 steel [50.8 mm (2 in.) thick, L-T Direction].

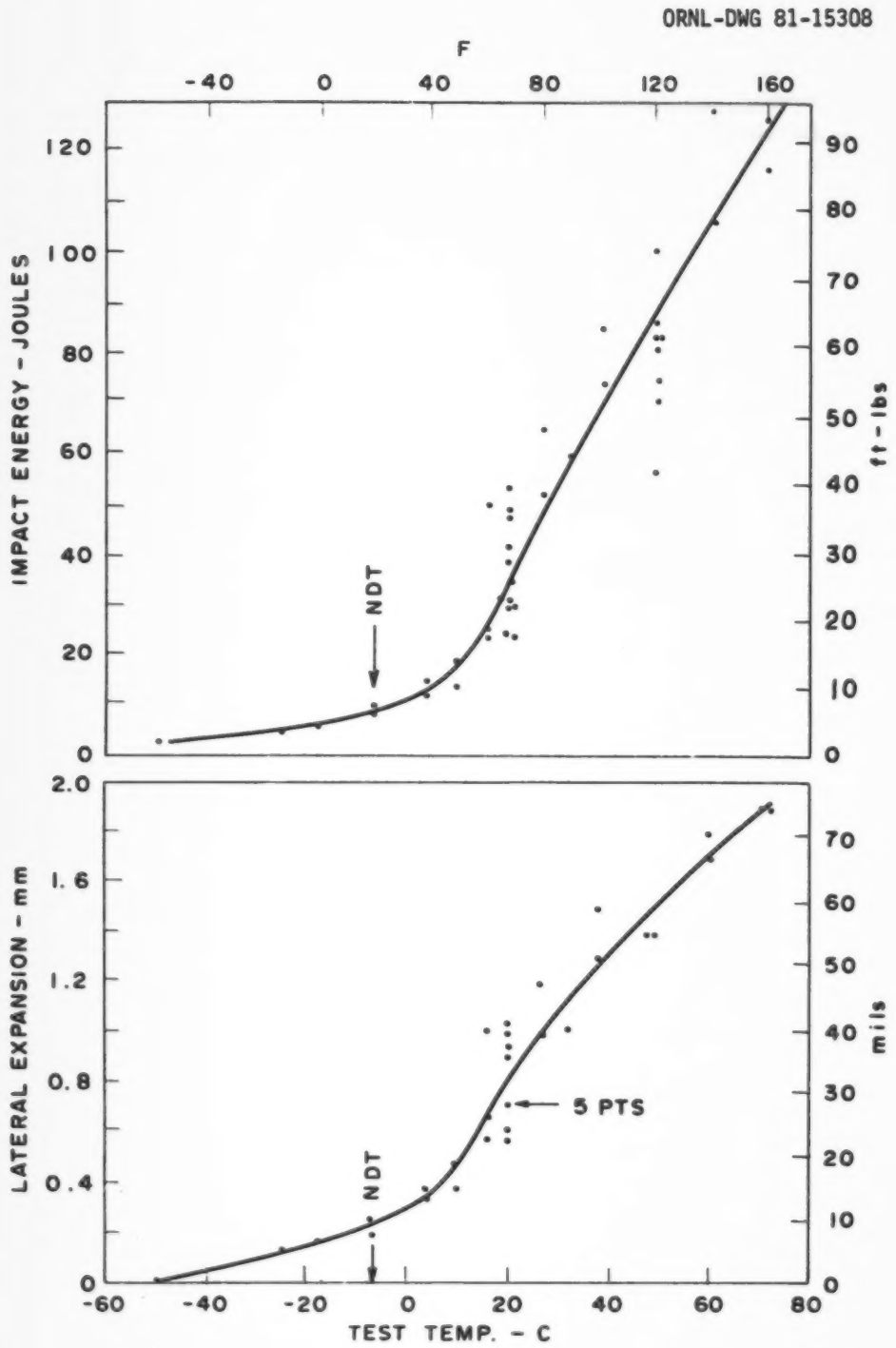

Fig. 3-2 CVN Impact Energy and Lateral Expansion as a function of testing temperature for A36 steel [25.4 mm (1 in.) thick, L-T direction].

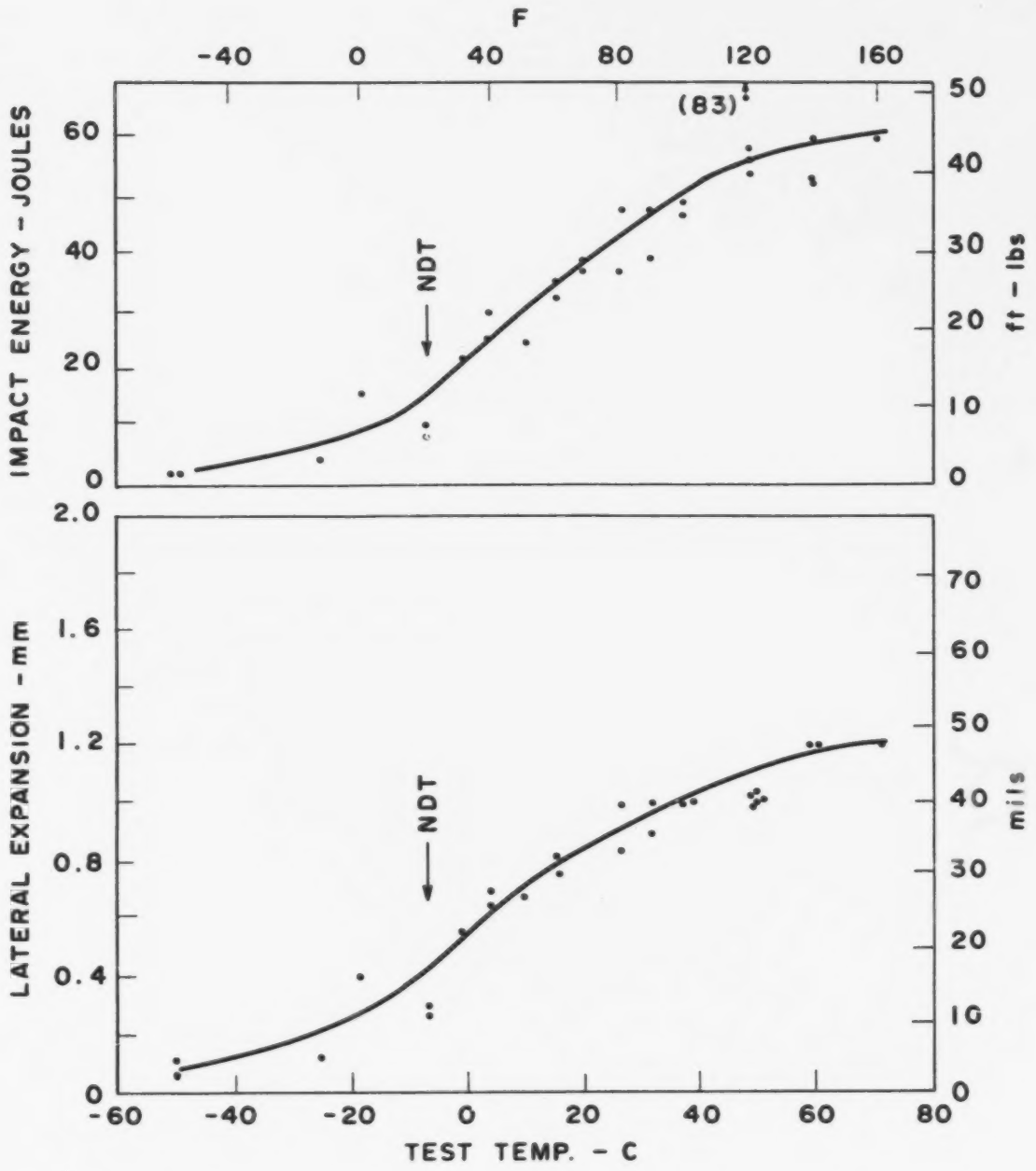

Fig. 3-3 CVN Impact Energy and Lateral Expansion as a function of testing temperature for A36 steel [25.4 mm (1 in.) thick, T-L Direction].

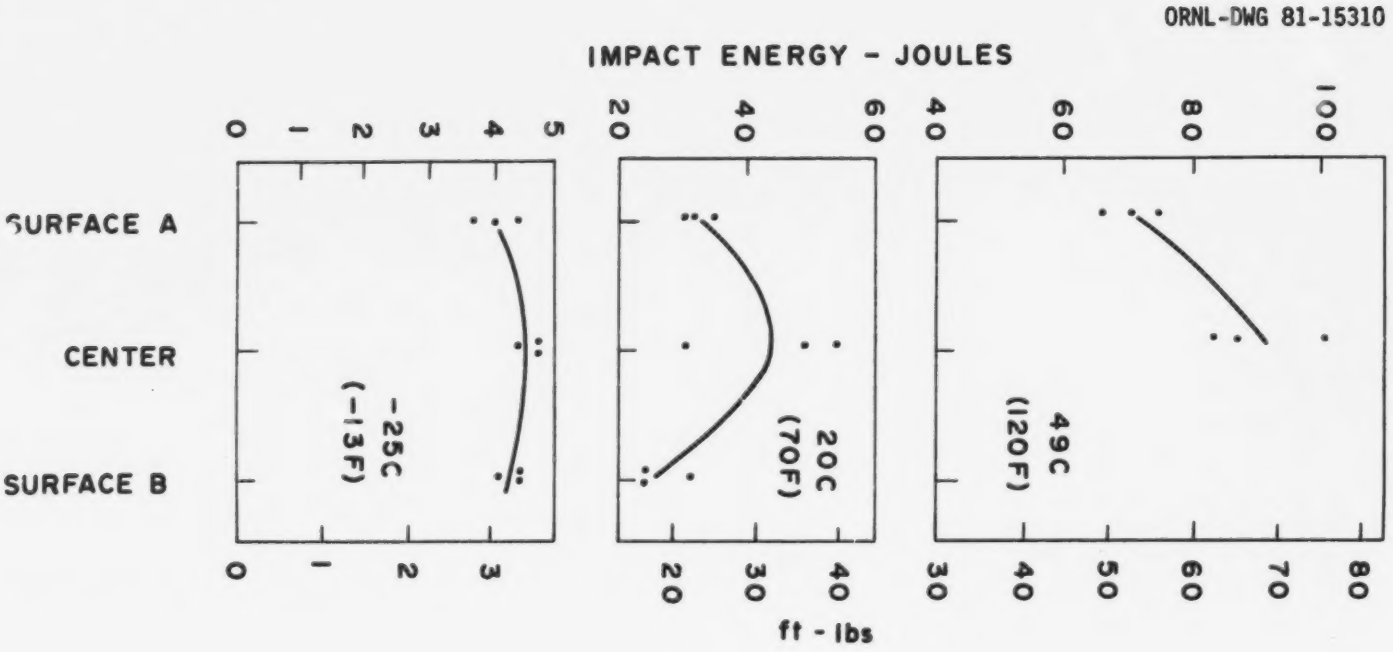

Fig. 3-4 Through-thickness variation of CVN toughness for 50.8 mm (2 in.) thick plate.

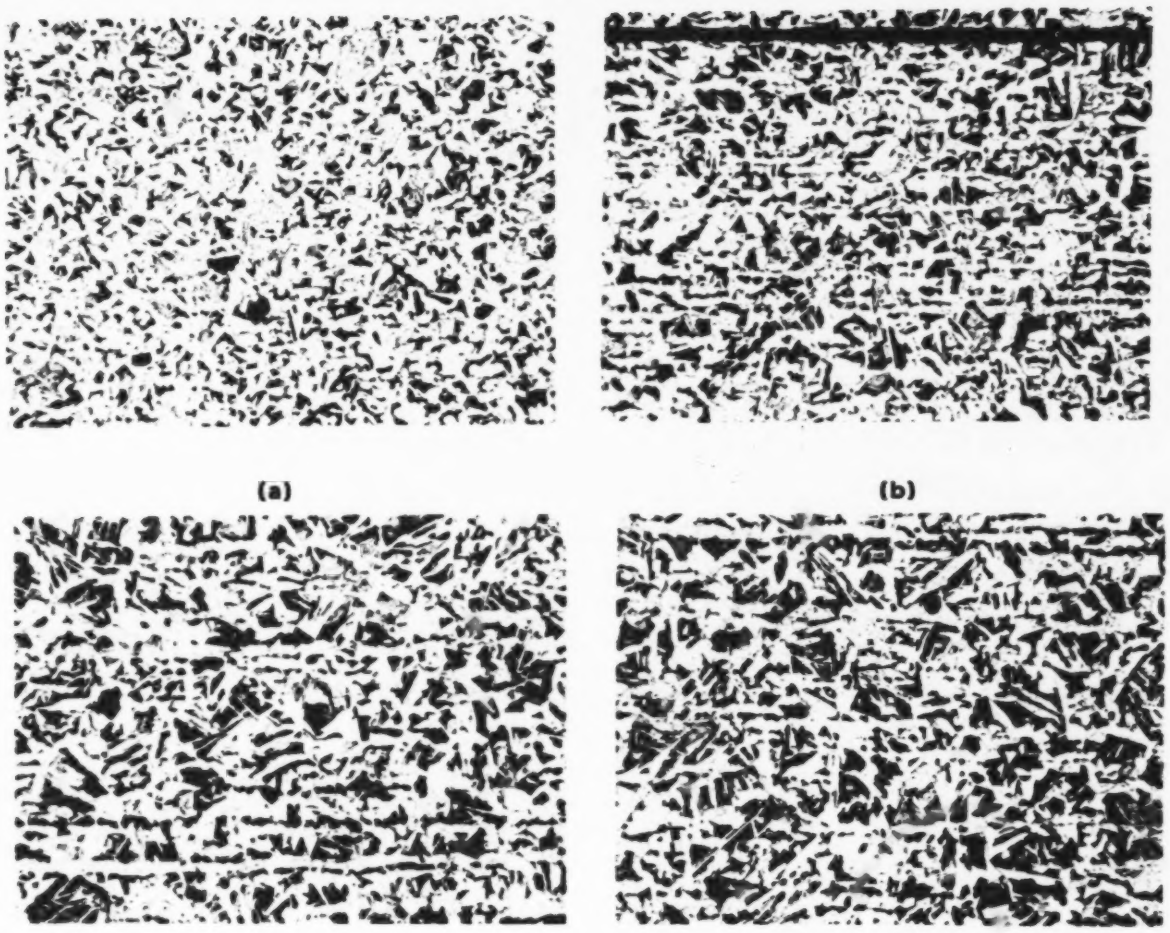

Fig. 3-5 Microstructure Through 50.8 mm (2 in.) Plate Thickness. (a) Surface. (b) 6 mm (0.24 in.) from surface (scratch shows edge of side groove plane). (c) 23 mm (0.47 in. from surface. (d) Center. (62X, Nital etch).

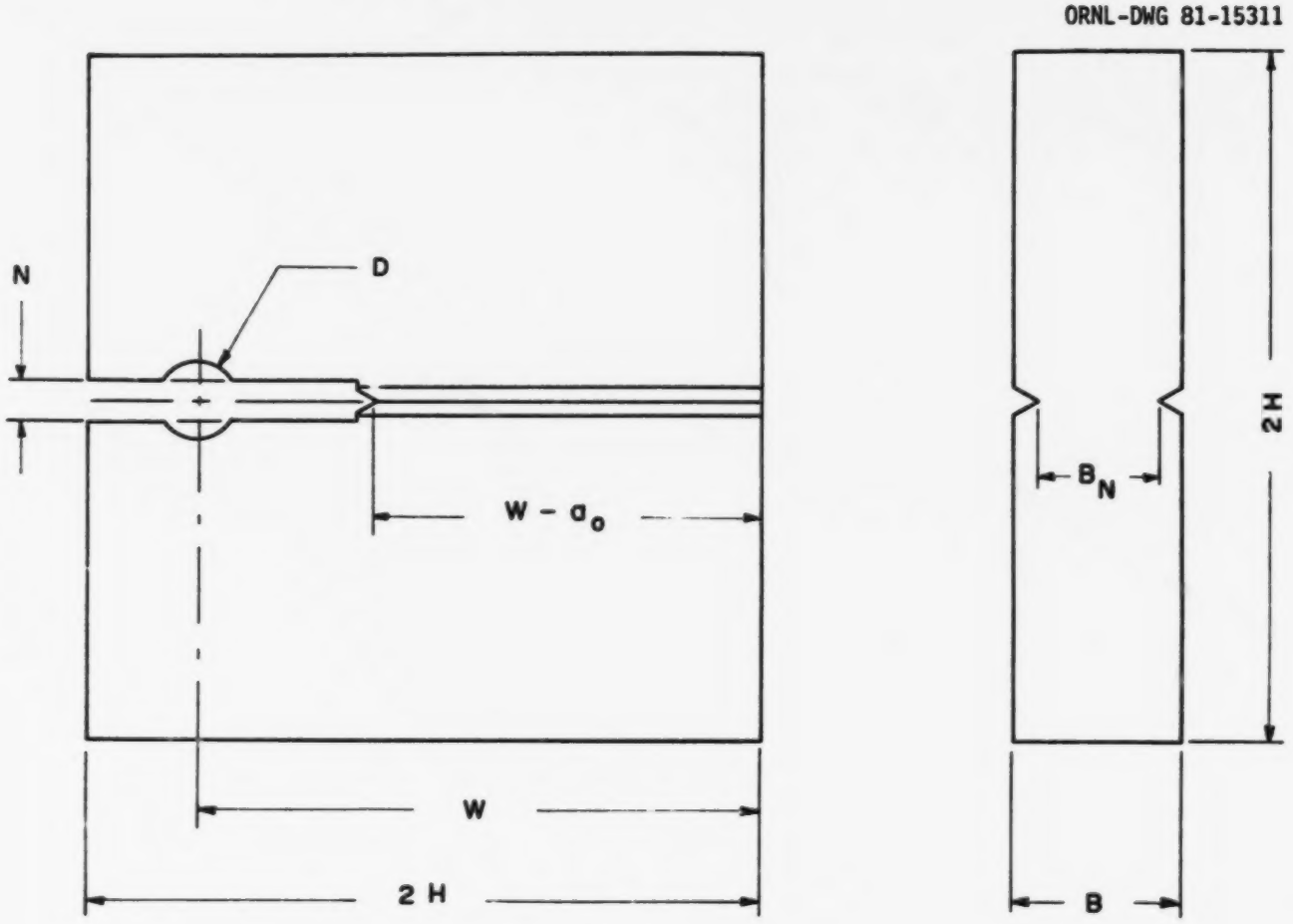

Fig. 3-6 Test Specimen Dimensions: W = 169.3 mm (6.67 in.), H = 101.6 mm (4.00 in.), B = plate thickness, B_N = 0.75 B, W - a_o = 110.1 mm (4.33 in.), D = 25.4 mm (1 in.), N = 12.7 mm (0.50 in.).

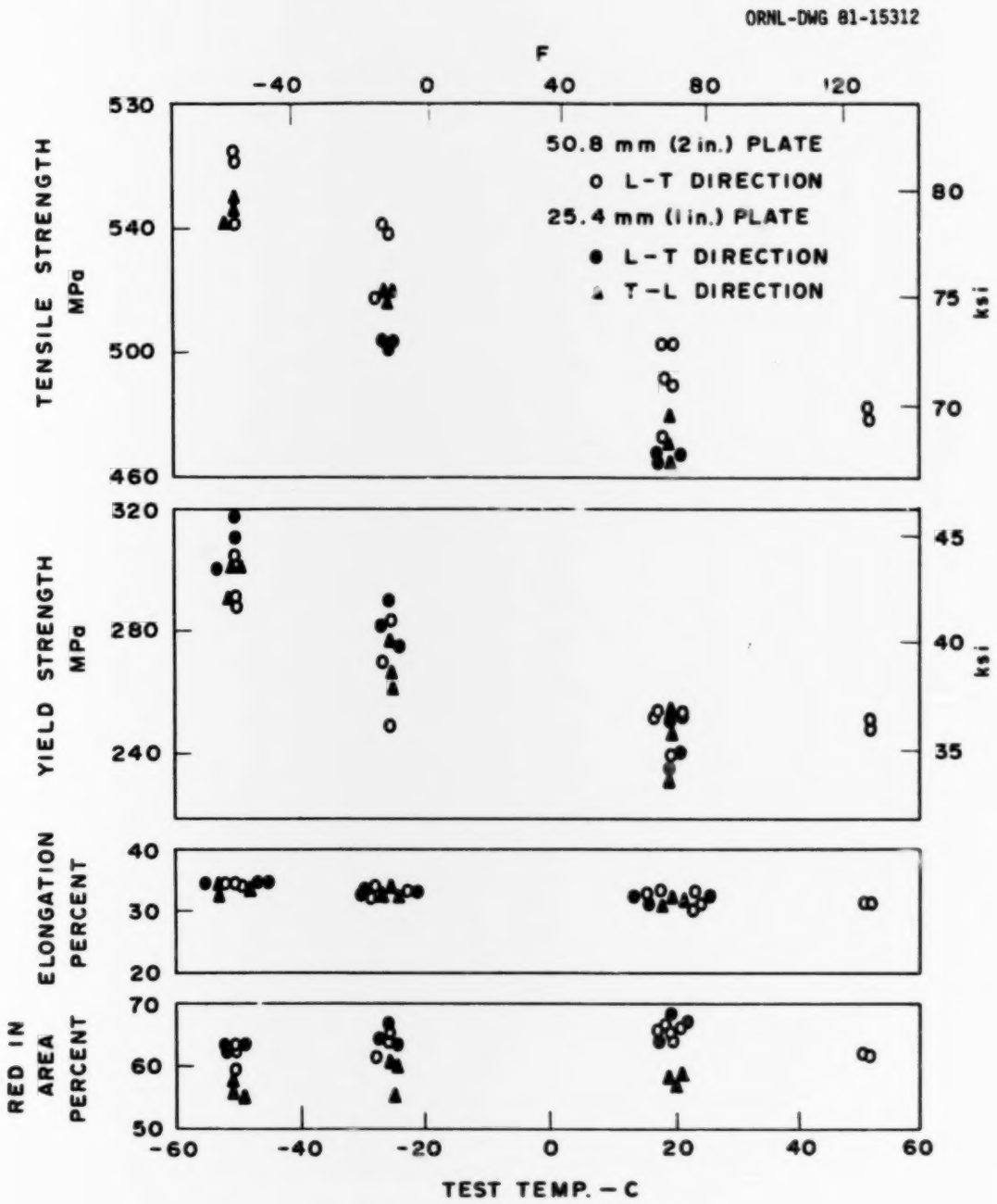

Fig. 3-7 Tensile properties of A36 steel plates.

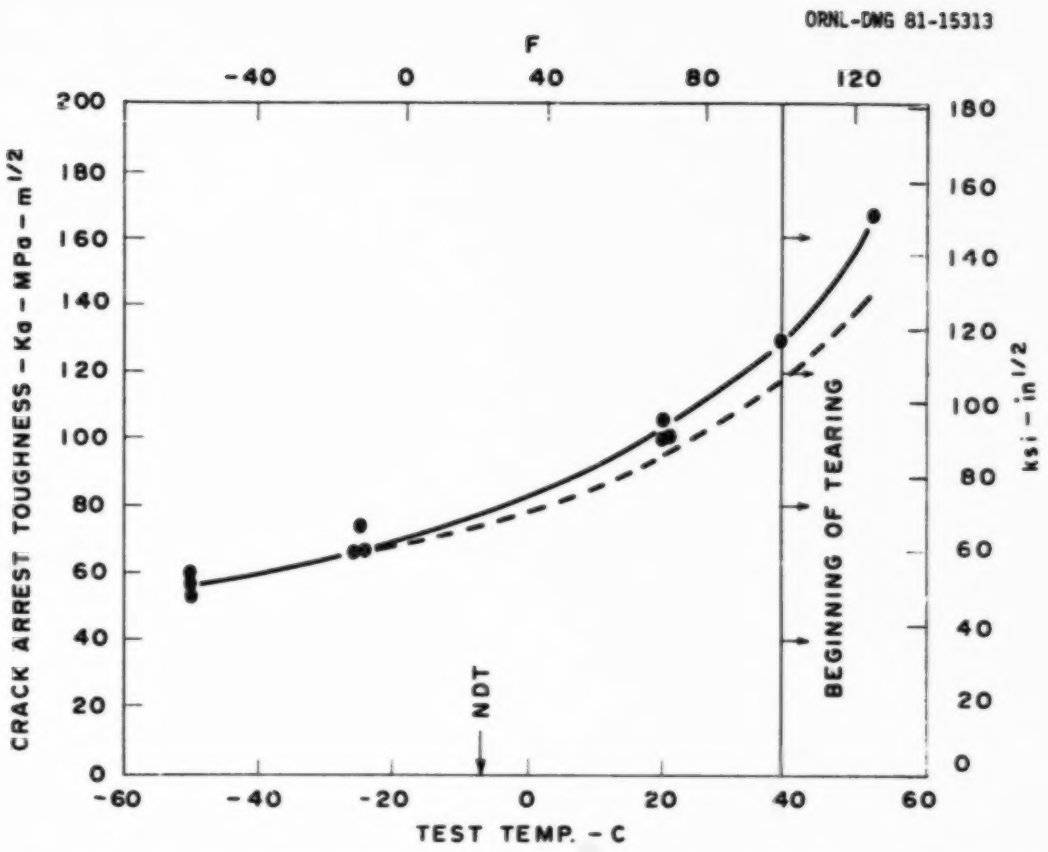

Fig. 3-8 Effect of test temperature on the crack arrest toughness of 50.8 mm (2 in.) thick A36 steel tested in the L-T direction.

ORNL-PHOTO 4719-81

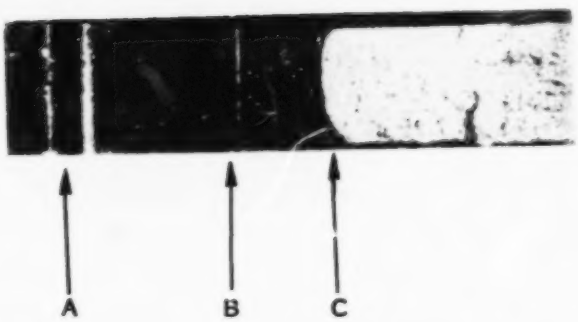

Fig. 3-9 Fracture Appearance of 50.8 mm (2 inch) thick specimen.

A. Loading Point

B. End of Machined Notch

C. End of Crack Jump, Marked by Heat Tinting.

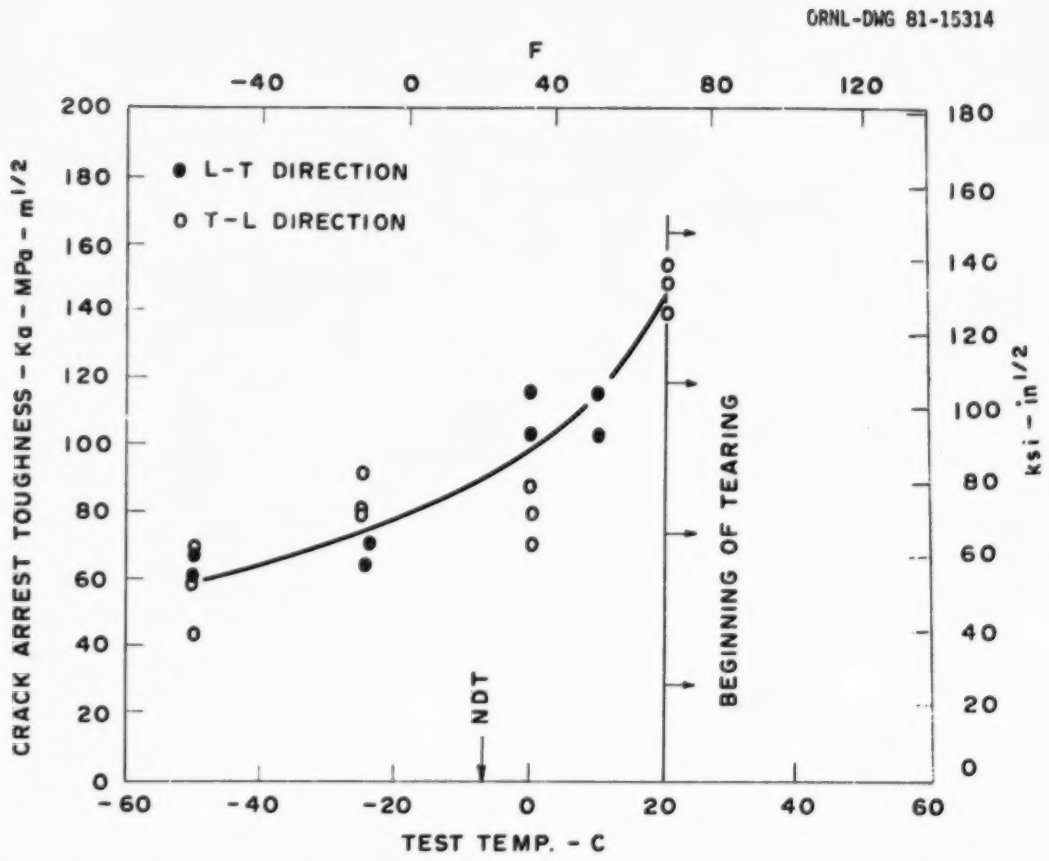

Fig. 3-10 Effect of test temperature on the crack arrest toughness of 25.4 mm (1 in.) thick A36 steel.

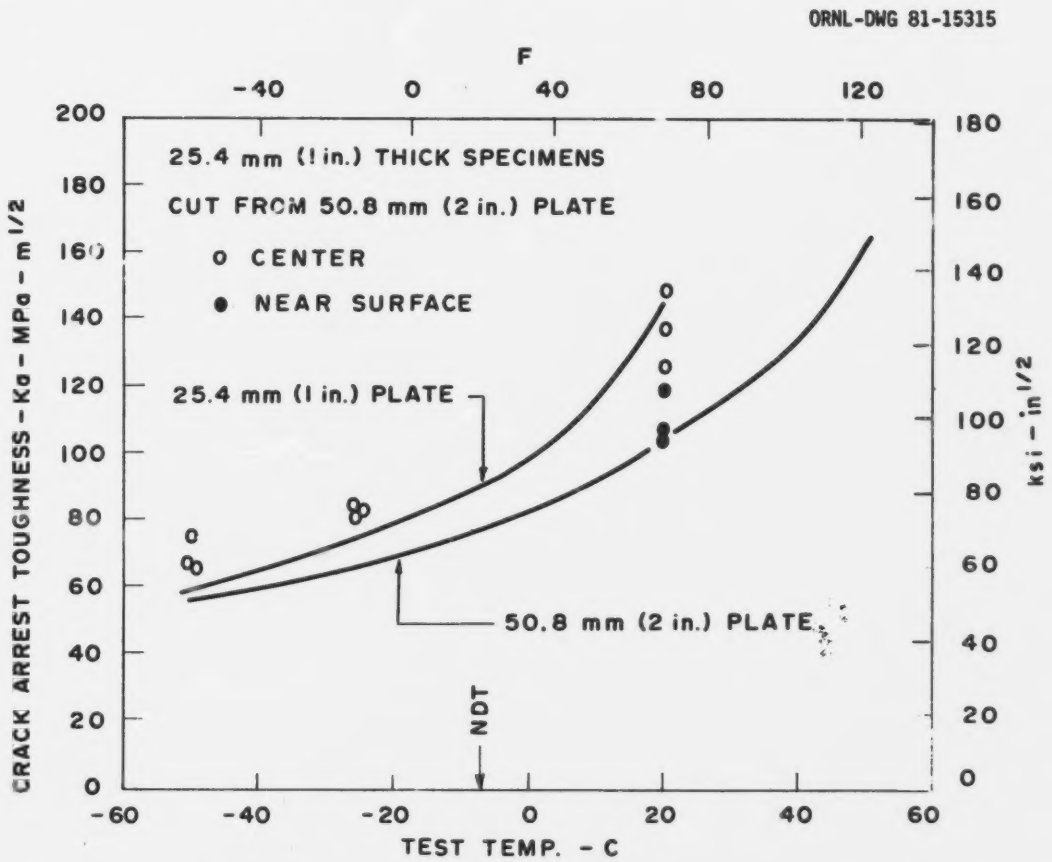

Fig. 3-11 Comparison of 25.4 mm (1 in.) and 50.8 (2 in.) plate toughness with toughness of 25.4 mm (1 in.) specimens cut from 50.8 mm (2 in.) plate, L-T direction.

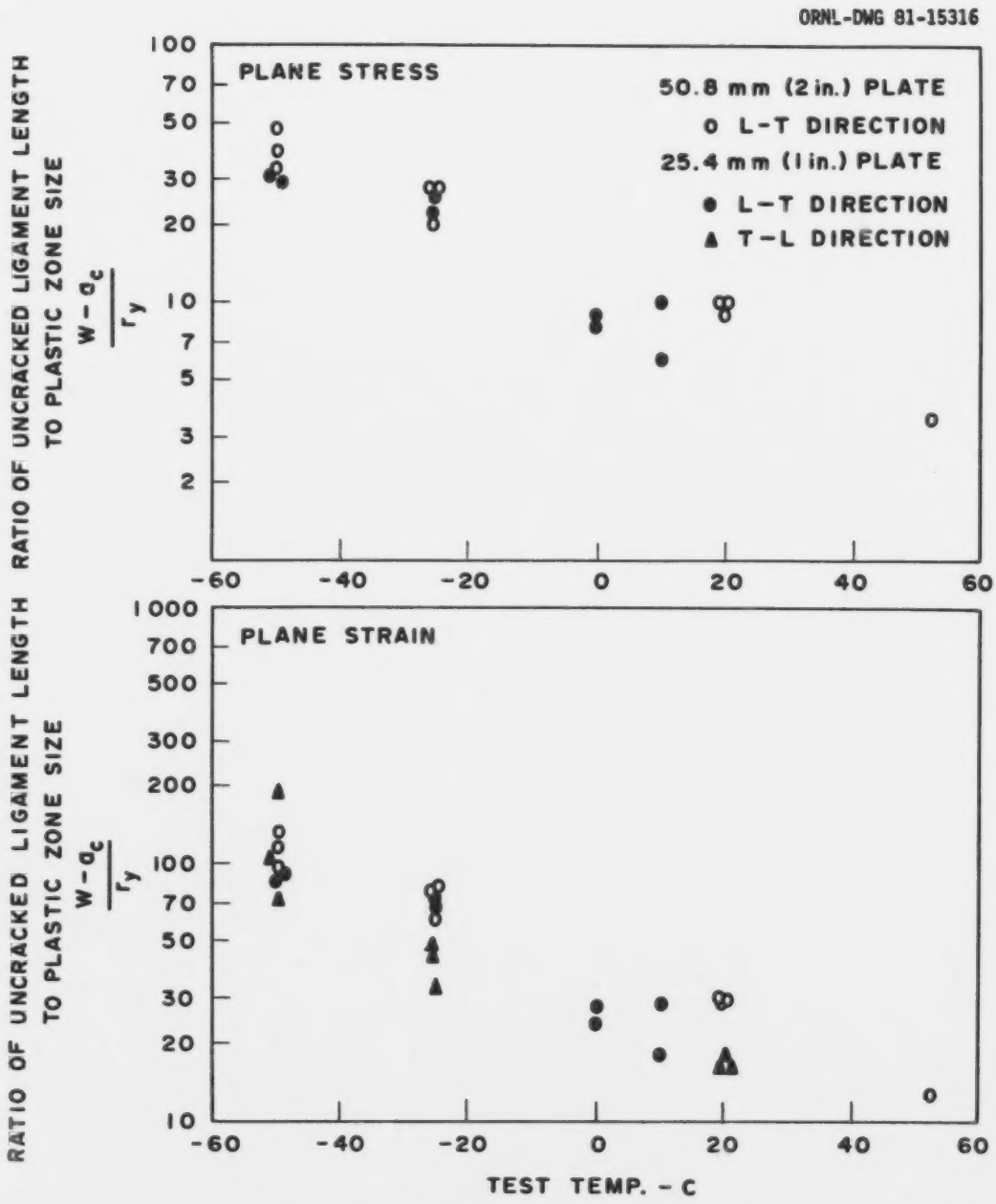

Fig. 3-12 Ratio of uncracked ligament length to plastic zone size for plane stress and plane strain cracking.

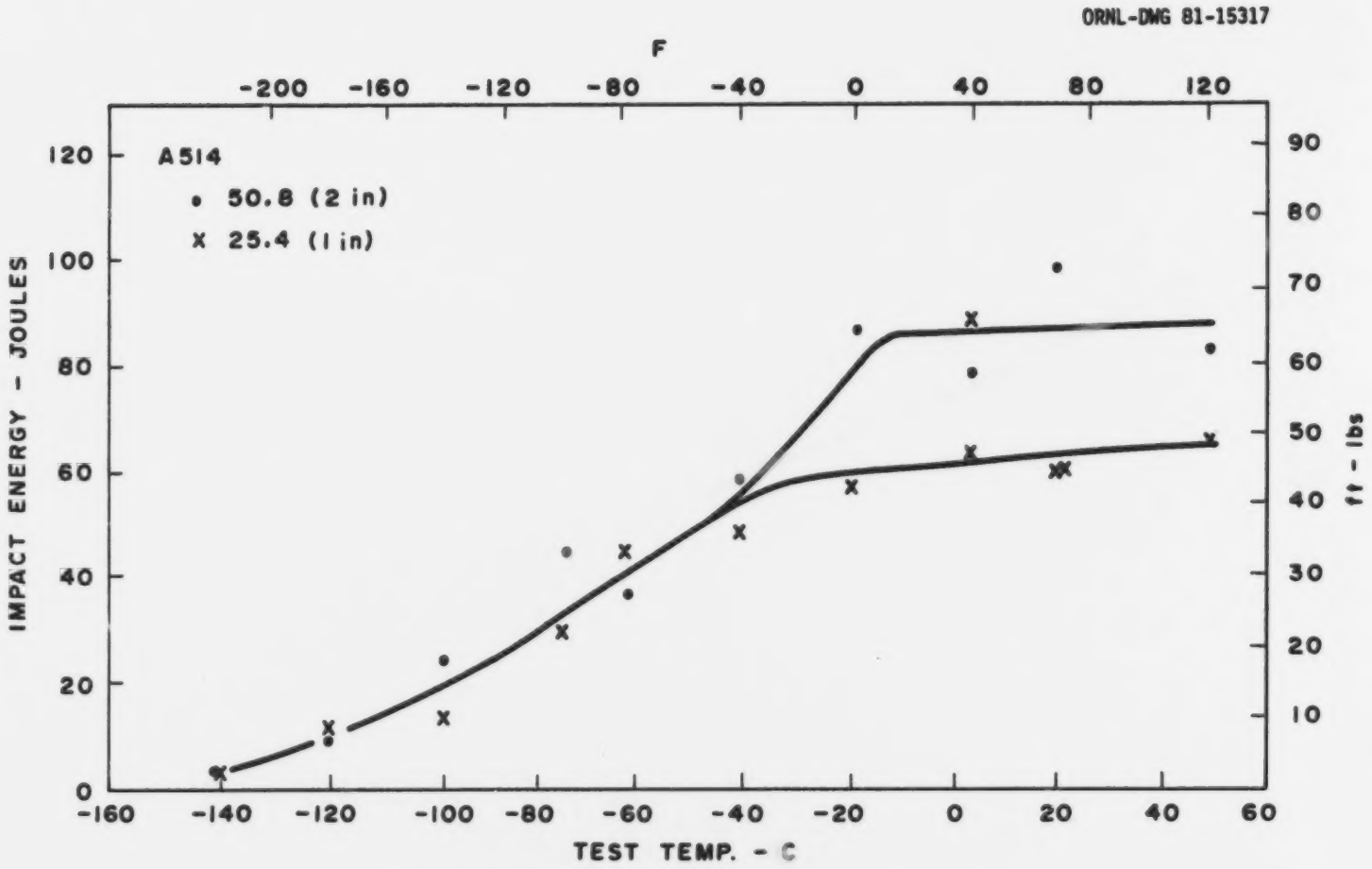

Fig. 3-13 Charpy impact results on A514 steel.

4. Round Robin Program

A Task Group was appointed by ASTM to carry out those steps necessary to develop a consensus method for crack arrest fracture toughness testing. (G. Irwin, University of Maryland; R. G. Hoagland, BCL; and E. J. Ripling, MRL, Chairman.) An important part of this group's activities consists of carrying out a Round Robin Test Program. The activities undertaken to initiate the Round Robin are described below.

4.1 Test Materials and Number of Tests

Three materials were selected for testing; one pressure vessel steel, A533, Grade B, Class 1, and two structural steels, A514 and A36. These were selected to represent a wide range of strength levels and microstructures as shown below:

Material	Yield Strength MPa	Tensile Strength MPa	Microstructure
A533B-1	345	550-690	Bainite
A514	690	760-895	Martensite
A36	≥ 250	400-550	Pearlite

A plate of A533B-1 was obtained from the Union Carbide Corporation, Nuclear Division, and it has been partially slabbed to test blanks. The two structural steels are to be supplied by the Department of Transportation, Federal Highway Administration. Lehigh University will characterize the steels.

It was tentatively agreed that each steel would be tested in triplicate at two temperatures. In order to stress the use of the reactor pressure vessel steel, all participants will be requested to test at least two materials, one of which must be the A533B-1 steel. The selection of either A36 and/or A514 is left to the participants.

4.2 Participants

Approximately 30 organizations have indicated an interest in participating in the Round Robin Test Program; one-third of these are American organizations, and the other two-thirds are overseas.

5.0 Conclusions and Recommendations

There are obviously a number of questions that still must be answered if a satisfactory test method is to be developed for crack arrest fracture toughness testing. The most important of these are:

1. Determination of specimen size requirements for plane strain crack arrest toughness testing.
2. Development of methods for initiating the run-arrest event for measuring higher toughnesses, say in excess of 150 MPa-$m^{\frac{1}{2}}$.
3. Determining the range of materials and applications for which crack arrest fracture toughness is useful.

NUREG/CR-
ORNL/Sub-81/7755/1
Dist. Category RF

Internal Distribution

1. R. G. Berggren
2. S. E. Bolt
3–7. R. H. Bryan
8. J. W. Bryson
9. D. A. Canonico
10. R. D. Cheverton
11. J. M. Corum
12. W. R. Corwin
13. W. B. Cottrell
14. J. R. Dougan
15. W. L. Greenstreet
16. R. C. Gwaltney
17. P. P. Holz
18. S. K. Iskander
19. K. K. Klindt
20. J. G. Merkle
21. C. A. Mills
22. S. E. Moore
23. F. R. Mynatt
24. D. J. Naus
25. F. H. Neill
26–27. J. L. Rich
28. G. C. Robinson
29. G. M. Slaughter
30. J. E. Smith
31. W. J. Stelzman
32. H. E. Trammell
33–37. G. D. Whitman
38. Patent Office
39. Central Research Library
40. Document Reference Section
41–42. Laboratory Records Department
43. Laboratory Records, RC

External Distribution

44. C. Z. Serpan, Reactor Safety Research, Nuclear Regulatory Commission, Washington, D.C. 20555
45. M. Vagins, Reactor Safety Research, Nuclear Regulatory Commission, Washington, D.C. 20555
46. Office of Assistant Manager for Energy Research and Development, DOE, ORO, Oak Ridge, TN 37830
47–48. Technical Information Center, DOE, Oak Ridge, TN 37830
49–388. Given distribution as shown in category RF (NTIS – 10)